NASA SP-3029

HANDBOOK OF THE PHYSICAL PROPERTIES OF THE PLANET VENUS

NATIONAL AERONAUTICS AND SPACE ADMINISTRATION

NASA SP-3029

HANDBOOK OF THE PHYSICAL PROPERTIES OF THE PLANET VENUS

by
L.R. Koenig, F.W. Murray,
C.M. Michaux, and H.A. Hyatt

Prepared under contract for NASA
by Douglas Aircraft Company, Inc.
Santa Monica, California

Scientific and Technical Information Division
OFFICE OF TECHNOLOGY UTILIZATION 1967
NATIONAL AERONAUTICS AND SPACE ADMINISTRATION
Washington, D.C.

For Sale by the Superintendent of Documents,
U.S. Government Printing Office, Washington, D.C. 20402
Price 60 cents
Library of Congress Catalog Card Number 66–61837

Foreword

A FUNDAMENTAL GOAL of the National Aeronautics and Space Administration is the systematic exploration of the solar system. Technological advances in the last decade have made it feasible to consider launching spacecraft to all the planets. To maximize the returns from ambitious planetary missions, however, it is important that we continually examine all information available. For this reason, the preparation of a series of handbooks was undertaken; this volume provides a survey of observational and theoretical studies of the planet Venus which should be of immediate value in preparations for forthcoming missions.

Although nearest to Earth and resembling it most closely in size and mass, Venus remains the "mystery" planet. An almost featureless veil of clouds completely obscures the surface from the observer. As a result, most early studies of Venus were theoretical in nature and not until recent developments in radio and radar astronomy and the successful flight of Mariner II has it been possible to obtain much-needed observational data.

Prepared in the Space Sciences Department of Douglas Aircraft Company, Missile and Space Systems Division, under contract with the National Aeronautics and Space Administration, this volume is a summary of data, theories, and scientific thought about Venus, current through December 1965.

ORAN W. NICKS, *Director*
Lunar and Planetary Programs

Acknowledgments

IN PREPARING THIS HANDBOOK, valuable assistance has been provided by J. H. Moore, S. T. Rollins, R. E. Santina, M. B. Baker, and V. Sirounian of the Douglas Aircraft Company, Inc.

Several portions of this material were reviewed by William E. Brunk of the National Aeronautics and Space Administration. His comments and suggestions for improving the text are appreciated.

Contents

		Page
1	ORBIT AND CONFIGURATIONS	1
2	MASS	11
3	DIAMETER	15
4	ROTATION	19
5	ACCELERATION OF GRAVITY	23
6	MEAN DENSITY	25
7	INTERNAL STRUCTURE	27
8	ELECTROMAGNETIC AND PARTICLE FIELDS	39
9	SURFACE TEMPERATURE	41
10	OPTICAL PROPERTIES	49
11	COMPOSITION OF ATMOSPHERE	61
12	ATMOSPHERIC STRUCTURE	69
13	ATMOSPHERIC CIRCULATION	81
14	CLOUDS	89
15	ASHEN LIGHT	99
16	MARINER II MISSION	101
17	SURFACE PROPERTIES	113
	REFERENCES	119
	GLOSSARY	129

1

Orbit and Configurations

ORBITAL ELEMENTS

THE FIVE ELEMENTS commonly employed to specify the size, shape, and orientation of a planet's orbit are:

(1) Mean distance from the sun, a
(2) Eccentricity of orbit, e
(3) Inclination of orbit to the ecliptic, i
(4) Longitude of ascending node, Ω
(5) Longitude of perihelion, $\bar{\omega}$

Additionally, to find the exact position of a planet at a given date, or epoch, it is necessary to specify the planet's mean longitude at epoch, L. Another value, often given for convenience, is the mean sidereal motion of the planet, either as daily motion, η, or yearly motion, η^*.

Mean values for the five elements of the orbit of Venus and the mean daily motion, η, at 400-day intervals from 1960 to 1966 are given in table 1–1. The formulas for calculating the secular, or very long-term, variation of each of these elements, plus η^* and L, are given in table 1–2 (refs. 1 and 2).

The value for eccentricity, $e = 0.0068$, indicates a nearly circular orbit for Venus, but the orbit is inclined at an angle, i, of $3\overset{\circ}{.}39$ to the ecliptic. Until Duncombe (refs. 2 and 3) corrected the secular variation formulas after locating large systematic errors in the older observations, the motion of the node was considered anomalous. Even though the orbital elements are derived from almost 24 000 meridian observations of Venus over 2 centuries, radar techniques now being used show great promise of refining the data. Since the 1961 inferior conjunction, great improvement in the accuracy of the astronomical unit (A. U.) has been made, and the value proposed by Muhleman (ref. 4) from radar data obtained at the 1962 inferior conjunction is $149\,598\,900 \pm 670$ kilometers. The remaining inaccuracy of the unit is caused largely by uncertainties in the ephemerides of Earth and Venus. Definitive corrections to the fundamental ephemerides will be possible when Venus can be followed by radar through most of its orbit.

TABLE 1-1.—*Mean Orbital Elements for Venus, 1960 to 1966*[a]

Epoch		Mean distance from Sun, a, A.U.	Mean motion, n, deg/sidereal day	Eccentricity of orbit, e	Inclination of orbit to ecliptic, i, deg	Ascending node longitude, Ω, deg	Perihelion longitude, $\bar{\omega}$, deg
Gregorian date	Julian day						
1960 Sept. 23.0	2437200.5	0.723332	1.602130	0.006792	3.39424	76.32625	131.01853
1961 Oct. 28.0	2437600.5	.723332	1.602130	.006791	3.39425	76.33611	131.03394
1962 Dec. 2.0	2438000.5	.723332	1.602130	.006791	3.39426	76.34597	131.04934
1964 Jan. 6.0	2438400.5	.723332	1.602130	.006790	3.39427	76.35583	131.06475
1965 Feb. 9.0	2438800.5	.723332	1.602130	.006789	3.39429	76.36569	131.08016
1966 Mar. 16.0	2439200.5	.723332	1.602130	.006789	3.39430	76.37555	131.09556

[a] Mean elements are taken from *The American Ephemeris and Nautical Almanac* and are referred to the mean equinox and ecliptic of date.

TABLE 1-2.—*Secular Variations of Mean Orbital Elements of Venus*

Element	Value in 1900	Formula for secular variation
Newcomb (ref. 1)		
Mean distance from Sun, a	0.7233316 A.U.	Constant
Mean motion, deg/sidereal year, η*	585°.17816200 (Julian yr)$^{-1}$	0°.0000000267T
Eccentricity of orbit, e	0.0068206938	$-0.000047740T+0.0000000907T^2$
Inclination of orbit to ecliptic, i	3°.39363	+0°.0010058T−0°.00000097223T^2
Longitude of ascending node, Ω	75°.77965	+0°.8999T +0°.00041000T^2
Longitude of perihelion, $\bar{\omega}$	130°.15885	+1°.40805T−0°.00097640T^2
Mean longitude of Venus, L	342°.76705	+58519°.21350T+0°.00030967T^2
Duncombe (ref. 2)		
Mean distance from Sun, a	0.723316 A.U.	Constant
Mean motion, deg/sidereal year, η*	585°.17816200 (Julian yr)$^{-1}$	+0°.0000000267T
Eccentricity of orbit, e	0.00682017	$-0.000047691T+0.0000000907T^2$
Inclination of orbit to ecliptic, i	3°.39365	+0°.0010003T −0°.00000097223T^2
Longitude of ascending node, Ω	75°.78063	+0°.9000T +0°.00041000T^2
Longitude of perihelion, $\bar{\omega}$	130°.16424	+1°.4064T −0°.00097640T^2
Mean longitude of Venus, L	324°.76708	+58519°.21365T+0°.00030967T^2

(1) Epoch is 1900 January 0.5 ephemeris time, or 1900 January 0 Greenwich mean time, or Julian date 241 5020.0
(2) Elements are referred to the mean equinox and ecliptic of date.
(3) Unit of time, T, is the Julian century of 36 525 mean solar days.

The motion of the Venus perihelion exceeds that predicted from Newtonian gravitational theory. This excess motion is 8″.4±4″.8 per century. The large probable error is caused by the difficulty in locating the perihelion of a nearly circular orbit. The observed excess is in fair agreement with the excess of 8″.63 predicted by the theory of general relativity (see refs. 5 and 6). Figure 1–1 shows the orbits of Venus and Earth and compares their orbital elements.

CONFIGURATIONS

Figure 1–2 represents the orbits of Venus and Earth with the positions of both planets at inferior conjunctions between 1962

TABLE 1–3.—*Inferior Conjunctions, Venus-Earth, 1959 to 1999*

Inferior conjunction date			Minimum distance			Venus	
Year	Day	Hour	A.U.	Km	Miles	Angular diam, sec of arc	Stellar magnitude
1959	Sept. 1	0617	0.28155	4.20929×10^7	2.61552×10^7	59	−3.2
1961	Apr. 10	2346	.28066	4.19591	2.60720	59	−3.2
1962	Nov. 12	2002	.26706	3.99262	2.48089	63	−3.1
1964	Jun. 19	2235	.28929	4.32495	2.68739	58	−2.8
1966	Jan. 26	0832	.26622	3.98015	2.47314	63	−3.2
1967	Aug. 29	2135	.28200	4.21596	2.61966	59	−3.2
1969	Apr. 8	1505	.28012	4.18796	2.60226	59	−3.3
1970	Nov. 10	0844	.26740	3.99779	2.48410	63	−3.1
1972	Jun. 17	1504	.28928	4.32487	2.68733	58	−2.8
1974	Jan. 23	2115	.26591	3.97548	2.47023	63	−3.2
1975	Aug. 27	1306	.28246	4.22297	2.62402	59	−3.2
1977	Apr. 6	0625	.27958	4.17982	2.59720	59	−3.3
1978	Nov. 7	2129	.26785	4.00450	2.48827	63	−3.1
1980	Jun. 15	0722	.28923	4.32415	2.68689	58	−2.8
1982	Jan. 21	1002	.26565	3.97157	2.46780	63	−3.1
1983	Aug. 25	0431	.28291	4.22969	2.62819	58	−3.2
1985	Apr. 3	2156	.27906	4.17209	2.59240	60	−3.4
1986	Nov. 5	1012	.26829	4.01099	2.49230	62	−3.1
1988	Jun. 12	2355	.28914	4.32279	2.68604	58	−2.8
1990	Jan. 18	2237	.26535	3.96716	2.46506	63	−3.1
1991	Aug. 22	2016	.28335	4.23613	2.63220	58	−3.2
1993	Apr. 1	1307	.27856	4.16453	2.58770	60	−3.4
1994	Nov. 2	2308	.26869	4.01702	2.39605	62	−3.1
1996	Jun. 10	1614	.28904	4.32126	2.68510	58	−2.7
1998	Jan. 16	1114	.26508	3.96310	2.46255	63	−3.1
1999	Aug. 20	1153	.28383	4.24332	2.63666	58	−3.2

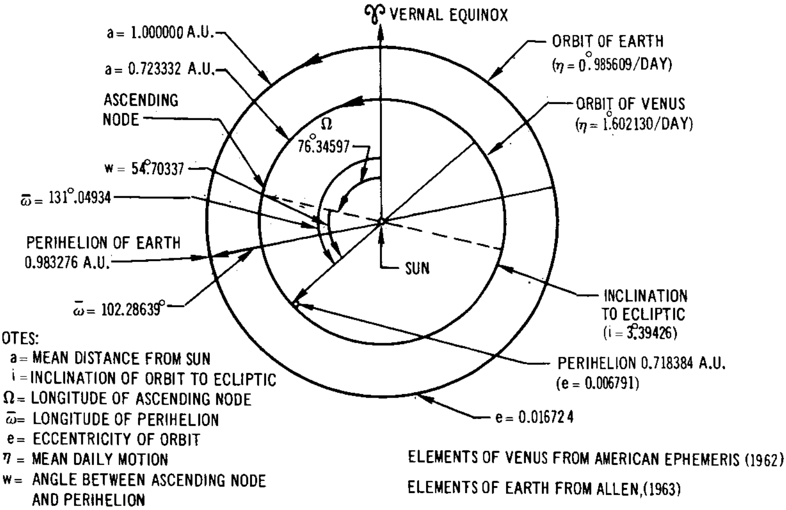

FIGURE 1–1.—Orbits of Venus and Earth.

and 1980. The synodic period, or mean interval between conjunctions, is 584 days. Because of the nearly circular shape of the two orbits, the distance separating the two planets at inferior conjunctions varies only slightly, and the actual time of closest approach almost coincides with the conjunction time. Table 1–3 lists the successive inferior conjunctions and the minimum distances of Earth and Venus from 1959 to 1999. They were calculated with

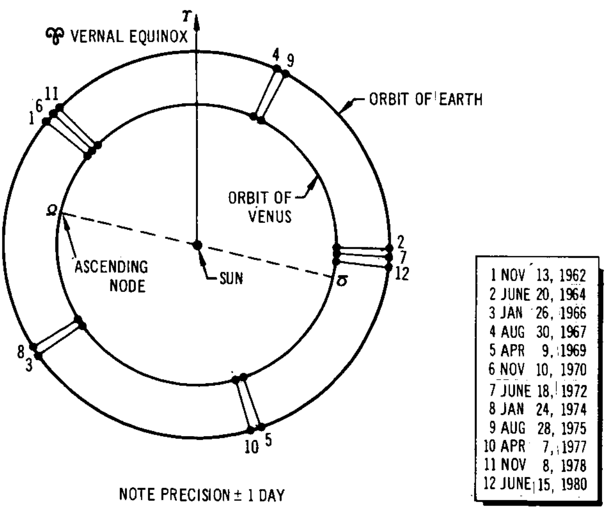

FIGURE 1–2.—Inferior conjunctions of Venus.

the aid of Herget's two modern tables (refs. 7 and 8). (These tables, based on Newcomb's work and instructions, were prepared by the U.S. Naval Observatory to provide precise coordinates homogeneously calculated at 4-day intervals over a 200-year period.) More accurate distances should be available in the future as a result of work being done with radar.

PHASE AND BRILLIANCE

Various relative configurations of Earth and Venus are shown schematically in figure 1–3. Elongations of Venus, an inner planet, never exceed 48°. For convenience, dates and values of greatest elongations are given in table 1–4, as calculated by Heath and quoted by Moore (ref. 9). The apparent angular diameter is then approximately 23″ to 25″. This variation is small because of the nearly circular orbits. Because of a combination of phase and distance from Earth, Venus shines brighter near greatest elongation than near inferior conjunction, when the Venus diameter is about 60″ (variation 58″ to 63″). It appears then as a very narrow, but brilliant, crescent with a magnitude of about −4.0. The dates of the greatest brilliancy of Venus (magnitude of −4.2 to −4.4) normally occur about 1 month after greatest elongation east and 1 month before greatest elongation west. In its eastern elongations, Venus sets after sunset and is called the evening star, and in its western elongations, after inferior conjunction, Venus becomes the morning star.

At superior conjunction, the diameter of Venus is only 10″ (smaller than Saturn's), but its brilliant, though small, disk, which is then full, maintains a −3.5 magnitude. Dichotomy, or half-phase, may occur at greatest elongation; however, the two phenomena generally do not coincide for Venus because of the slight eccentricity of its orbit and its inclination relative to Earth's orbit.

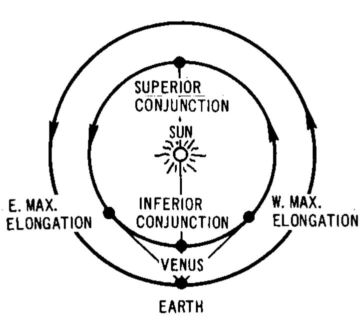

FIGURE 1–3.—Earth-Venus configurations.

TABLE 1-4.—*Greatest Elongations of Venus, East and West, 1959 to 1999*

Year	Greatest elongation east			Greatest elongation west		
	Date	Angle	Angular diam, sec of arc	Date	Angle	Angular diam, sec of arc
1959	Jun. 23	45°4′	24	Nov. 11	46°6′	24
1961	Jan. 29	46°9′	24	Jun. 20	45°8′	24
1962	Sept. 3	46°2′	25	....	....	....
1963	....	....	....	Jan. 23	47°0′	25
1964	Apr. 10	45°8′	24	Aug. 29	45°9′	24
1965	Nov. 15	47°2′	25	....	....	....
1966	....	....	....	Apr. 6	46°4′	25
1967	Jun. 20	45°4′	24	Nov. 9	46°6′	24
1969	Jan. 26	47°0′	24	Jun. 17	45°8′	24
1970	Sept. 1	46°2′	25	....	....	....
1971	....	....	....	Jan. 20	47°0′	25
1972	Apr. 8	45°8′	24	Aug. 27	45°9′	24
1973	Nov. 13	47°2′	25	....	....	....
1974	....	....	....	Apr. 4	46°4′	25
1975	Jun. 18	45°4′	24	Nov. 7	46°6′	24
1977	Jan. 24	47°0′	24	Jun. 15	45°8′	24
1978	Aug. 29	46°1′	25	....	....	....
1979	....	....	....	Jan. 18	47°0′	25
1980	Apr. 5	45°6′	24	Aug. 24	45°9′	24
1981	Nov. 11	47°2′	25	....	....	....
1982	....	....	....	Apr. 1	46°5′	25
1983	Jun. 16	45°4′	24	Nov. 4	46°6′	24
1985	Jan. 22	47°0′	23	Jun. 13	45°6′	24
1986	Aug. 27	46°1′	25	....	....	....
1987	....	....	....	Jan. 15	47°0′	25
1988	Apr. 3	45°9′	24	Aug. 22	45°8′	24
1989	Nov. 8	47°2′	25	....	....	....
1990	....	....	....	Mar. 30	46°5′	25
1991	Jun. 13	45°3′	24	Nov. 2	46°6′	25
1993	Jan. 19	47°1′	23	Jun. 10	45°8′	24
1994	Aug. 25	46°0′	25	....	....	....
1995	....	....	....	Jan. 13	47°0′	25
1996	Apr. 1	45°9′	24	Aug. 19	45°8′	24
1997	Nov. 6	47°2′	25	....	....	....
1998	....	....	....	Mar. 27	46°5′	25
1999	Jun. 11	45°3′	24	Oct. 30	46°5′	25

TRANSITS

Transits of Venus across the Sun's disk can occur only when both Earth and Venus are simultaneously close to the same node of the Venus orbit on the ecliptic. The inclination of the Venus orbit, the mean motions of the two planets, and the apparent diameter of the Sun are the determining factors. At present, transits are possible only in June and December and occur only four times in 243 years. Intervals between transits are 8, 121½, 8, 105½, 8, 121½ years, et seq. These events took place on December 4, 1639; June 6, 1761; June 3, 1769; December 9, 1874; and December 6, 1882. The next transits will occur on June 8, 2004, and eight years later, on June 6, 2012.

TABLE 1–5.—*Derived Orbital Constants for Venus*

Orbital time intervals

	Earth sidereal years	Earth tropical years	Earth sidereal days
Venus sidereal year	0.61519	0.61521	224.701
Mean synodic period	1.5987	1.5987	583.92

Distances from the Sun

	Astronomical unit	Kilometers	Miles
Mean solar distance	0.723332	108.210×10^6	67.238×10^6
Distance at perihelion	.718418	107.475	66.782
Distance at aphelion	.728246	108.945	67.695

Distances from Earth

	Astronomical unit	Kilometers	Miles
Minimum distance	0.267957	40.086×10^6	24.908×10^6
Maximum distance	1.735980	259.701	161.371

Orbital velocity

	Kilometers/sec	Miles/sec
Mean orbital velocity	35.05	21.78

ADDITIONAL CHARACTERISTICS

The sense of motion of Venus, which is the same as for all other planets, is counterclockwise when viewed from the north pole of the ecliptic. Derived orbital constants for Venus are given in table 1–5. It can be seen that the perihelion and aphelion distances of Venus are not greatly different, which is also true of Earth. Venus revolves around the Sun faster than does Earth, completing a circuit in 225 days at a mean orbital speed of 35 km/sec. The synodic period of revolution given is the mean. It should be noted that after one synodic period the planets generally do not meet in the same part of the sky; for this to take place, a long-period cycle is necessary. It can be calculated that 13 sidereal revolutions of Venus amount to almost exactly 8 tropical years (minus 1 day) of Earth, or 5 mean synodic periods will equal 8 calendar years (minus 2.4 days).

No satellite of Venus has ever been observed. The satellite survey made by Kuiper (ref. 10) placed a 5-kilometer upper limit to the diameter of a hypothetical Venus satellite, assuming its albedo to be the same as, or greater than, that of the Moon.

2

Mass

THE MASS OF VENUS usually is derived from analysis of perturbations caused by Venus in the orbital motion of Earth and Mercury. The effect on the orbit of Mars has been used, but a more satisfactory determination can be made by using the new theory of the motion of Mars by Clemence (ref. 11). Unfortunately, Venus has no known satellite whose orbit can be studied for a more accurate determination of mass. Rabe (ref. 12) has used close approaches of the minor planet Eros to obtain an independent check on the mass. Doppler shifts observed in the

TABLE 2–1.—*Mass of Venus Relative to the Sun*

Author	Reciprocal relative mass (with respect to Sun) m_s/m_p, with probable error	Method
Newcomb[a] (ref. 13)	408 000	Planetary perturbations
Ross (ref. 16)	403 490±2400	Mars orbit perturbations
Fotheringham (ref. 17)	406 358±723	Mercury, Earth, and Mars
Spencer-Jones (ref. 18)	404 700±800	Sun
De Sitter and Brouwer (ref. 19)	404 000±1000	Weighted mean
Morgan and Scott (ref. 20)	407 000±500	Earth
Clemence (ref. 21)	409 300±1400	Mercury
Rabe (ref. 12)	408 645±208	Eros
Brouwer (ref. 22)	408 000±800	Mercury
Makemson, Baker, and Westrom (ref. 23)	407 000±1000	Discussion
Brouwer and Clemence (ref. 14)	408 600±200	Weighted mean
Anderson, Null, and Thornton (ref. 15)	408 533±30	Mariner II

[a] Value adopted by *American Ephemeris and Nautical Almanac.*

frequency of the radio signals from Mariner II, when the spacecraft was in the vicinity of Venus, have been used to establish the deflection of the trajectory of the probe caused by the planet and, hence, to establish the mass of the planet.

Values calculated for the reciprocal relative mass (the ratio of the mass of the Sun to the mass of the planet) are listed in table 2–1 (refs. 13–23). The value conventionally used is that of Newcomb (ref. 13). On the basis of a weighted mean of four carefully selected values, Brouwer and Clemence (ref. 14) adopted the value $m^{-1} \pm 408\,600 \pm 200$. The value computed from Mariner II flyby data is $408\,533 \pm 30$ (ref. 15). These values are in agreement.

Figure 2–1 illustrates the dependence of the computed value of the absolute mass of Venus upon the values chosen for the absolute mass of the Sun and the ratio of the mass of the Sun to that of the planet. According to Allen (ref. 24), the mass of the Sun is $1.989(\pm 0.004) \times 10^{33}$ grams. Using this datum and the value 4.086

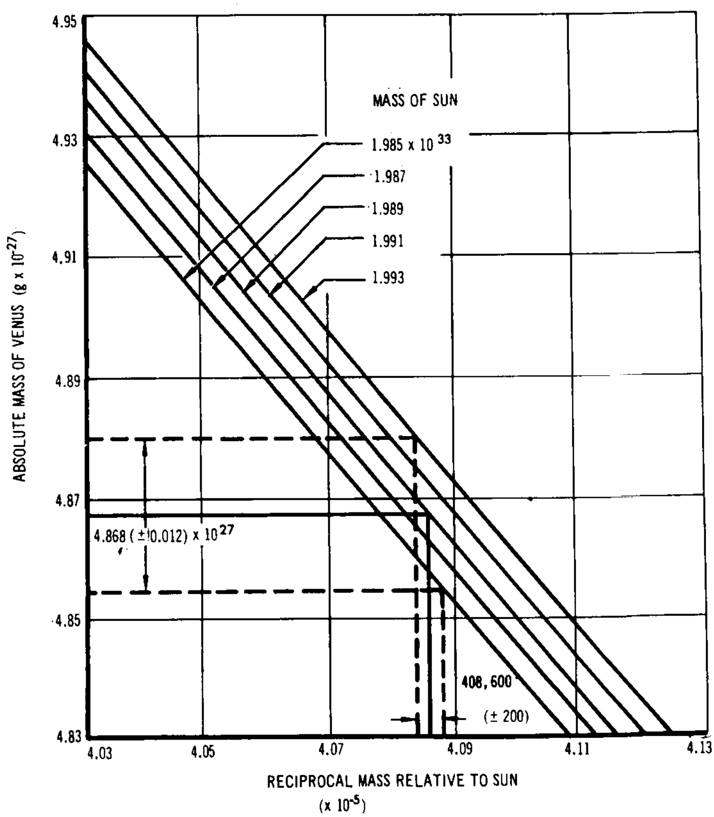

FIGURE 2–1.—Absolute mass of Venus.

$(\pm 0.002) \times 10^5$ grams (ref. 14) for the relative mass, the absolute mass of Venus is found to be $4.868(\pm 0.012) \times 10^{27}$ grams. If the value $4.08533(\pm 0.0003) \times 10^5$ grams (ref. 15) for the relative mass is used, the absolute mass is found to be $4.869(\pm 0.010) \times 10^{27}$ grams.

3

Diameter

THE DIAMETER OF THE SOLID GLOBE of Venus is not directly measurable because a thick cloud layer blankets the surface. Instead, what is commonly measured by astronomical instruments, such as the micrometer, is the optical diameter of Venus. Such measurement is limited to, or defined by, the visible surface of the planet, that is, the top of the opaque cloud layer. Optical diameter is designated as $2R_c$ to distinguish it from $2R_0$, the diameter of the solid globe. In the latest atmospheric models, the height of the opaque cloud layer is estimated as 30 kilometers or more (see ch. 14). At present, astronomers are limited to the techniques commonly used to measure planetary disks; in the future, however, it is expected that microwave experiments conducted onboard spacecraft will determine the diameter of the solid globe with great accuracy.

METHODS OF MEASURING DIAMETER

Since Venus is an inner planet, its disk, like that of the Moon, appears in all possible phases of illumination: dark, crescent, quarter, gibbous, and full (see fig. 3–1). Venus also transits the Sun on rare occasions and, at that time, appears as a large black disk against an intensely luminous background. Methods available for measuring the diameter of Venus under these conditions are outlined in the following text.

Direct Visual and Photographic Measurement.—Either the single-image micrometer (filar micrometer) or double-image micrometer is used for direct visual measurement. When using the filar micrometer, two wires are set tangentially to opposite limbs of the disk, and their separation is measured. When using the double-image micrometer, an identical image of the disk is moved into tangential contact on opposite limbs, and the displacement is measured. Large-scale, high-quality photographs are used in direct photographic measurement. Filar micrometer measurements on photographs are preferably made on the crescent tips. A scanning

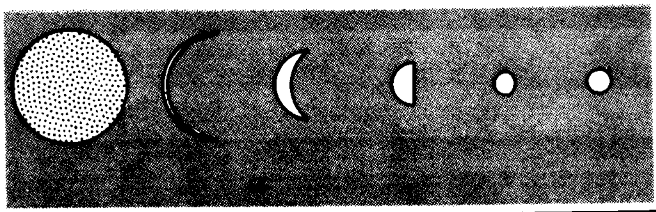

PHASE	NEW (DARK)	NARROW CRESCENT	LARGE CRESCENT (GREATEST BRILLIANCE)	HALF (DICHOTOMY)	GIBBOUS	FULL
CONFIGURATION	INFERIOR CONJUNCTION	WESTERN ELONGATION				SUPERIOR CONJUNCTION

FIGURE 3–1.—Phases of Venus and apparent diameters.

microphotometer can be used to measure luminance (brightness) diametrically across the disk.

Timing of Transits and Occultations.—During solar transits, the times of internal and external contacts of the limbs of the disk with the Sun's edge are recorded. When Venus occults a bright star, such as Regulus, the star's immersion and emersion times are recorded.

Photometric Method Applied to Solar Transits.—Photoelectric measurements of fluxes passing through a circular aperture are taken when the planet is in line with the center of the aperture and when it has moved away. A comparison of the measurements gives the fractional area of the Sun obscured by the transiting planet. This method has not been applied to Venus.

Radar-Range Determinations.—Radar-range determinations are made at inferior conjunctions of the planet with Earth.

RESULTS OF MEASUREMENTS

Several studies have been made of the methods and results of measuring the diameter of Venus. An average angular diameter of 16".88 at unit distance (1 A.U.) was determined by De Vaucouleurs (ref. 25) after a critical evaluation of micrometric measurements of the narrow crescent near inferior conjunction (when errors are minimized). (See table 3–1 for micrometric determinations.) Transit observations are considered to come closer to the lower limits for the optical diameter; De Vaucouleurs' weighted mean is 16".83 (see table 3–2). Values from the occultation of Regulus on July 7, 1959, apply to a low-density region of the atmosphere which is definitely above the opaque cloud layer. These occultation values provide a very precise upper

TABLE 3–1.—*Daytime Micrometric Measurements of the Optical Diameter of Venus at Unit Distance (1 A.U.)*

[After ref. 25]

Year observed	Author and year published	Method	Angular diameter, d_1, at— Superior conjunction, sec of arc	Dichotomy, sec of arc	Inferior conjunction, sec of arc
1862	Kaiser, 1872	Double-image micrometer	(16.20)	(17.12)	(17.07)
1865	Kaiser, 1872	Double-image micrometer	(16.31)	....	....
1898	Drew, 1901	Filar micrometer	16.59	17.07	16.95
1900	See, 1900	Filar micrometer	....	16.72	16.88
1903	Wirtz, 1912	Filar micrometer	16.79	16.97	....
1905	Wirtz, 1912	Filar micrometer	....	(17.27)	(17.07)
1912, 1914	Rabe, 1928	Filar micrometer	16.61	(17.18)	(17.36)
1921	Graff, 1922	Filar micrometer	....		
1924	Danjon, 1926	Filar micrometer	....	....	(17.22)
1938	Edson, 1960	Photographs	....	16.96	16.69
1939	Muller, 1949	Double-image micrometer	16.64	....	16.90
				....	....
1940	Richter, 1944	Filar micrometer	....	....	(17.17)
1962	Smith, 1963	Photographs	....	....	16.97
Mean of all values			16″52	17″04	17″03
Mean of selected values			16″66 ($d_1 > 16''5$)	16″88 ($d_1 < 17''0$)	16″88 ($d_1 < 17''0$)
Adopted mean value				16″88	

limit of 17″012 (refs. 26 and 27). Thus, the best optical methods indicate that the angular optical diameter, d_1, is between 16″8 and 17″0 at unit distance. De Vaucouleurs' critical examination of all optical determinations published between 1862 and 1962 led him to adopt a mean d_1 of 16″88 with a ±0.02 probable error. This corresponds to a linear optical diameter, $2R_c$, of 12 240 ± 15 kilometers.

TABLE 3–2.—*Solar Transit Measurements of the Optical Diameter of Venus at Unit Distance (1 A.U.)*

[After ref. 25]

Year of transit	Author and year published	Method	Angular diam, d_1, sec of arc	Weight
1761	Wurm, 1807	Filar micrometer	16.954	½
1761	Encke, 1824	Timing of contacts	16.611	½
1769	Wurm, 1807	Filar micrometer	16.810	½
1769	Ferrer, 1833	Timing of contacts	16.676	½
1761 1769	Powalky, 1871	General discussion	16.918	1
1874	Tennant, 1875	Double-image micrometer	16.903	½
1874	Auwers, 1891	Timing of contacts	16.85	1
1882	Auwers, 1894	Heliometer, corrected	16.820	1
Weighted mean of all values			16″830	

From the mean value for linear optical diameter, $2R_c$, and an assumed opaque cloud layer 35-kilometers thick, the diameter of the solid globe of Venus, $2R_o$ is found to be 12 170 ± 20 kilometers. This optical theoretical estimate is in agreement with the preliminary radar determinations which suggest a value for $2R_o$ of 12 200 ± 100 kilometers (ref. 28).

4

Rotation

DETERMINATION OF THE ROTATION PERIOD of Venus has been one of the most challenging problems for planetary astronomers. Radar astronomy has provided a new technique which has solved this mystery.

Figure 4–1 shows the widely divergent values proposed for the period of rotation before 1961. For the most part, either a day similar to that of Earth or a locked rotation period of approximately 225 days has been favored. These conclusions were based on uncertain methods such as observations of elusive and transient cloud markings and the measurement of Doppler shifts on spectrograms. Spectrographic Doppler shifts measured by Richardson (ref. 29) at Mt. Wilson in 1956 indicated the rotation period was definitely longer than 24 hours, the period often assumed from analogy with Earth. The principle of Doppler shift measurement is flawless; the approaching limb should produce a violet shift and the receding limb, a red shift. If the actual rotation period of Venus were similar to that of Earth, a measurable shift should have been detected long ago. The absence of such a shift may have

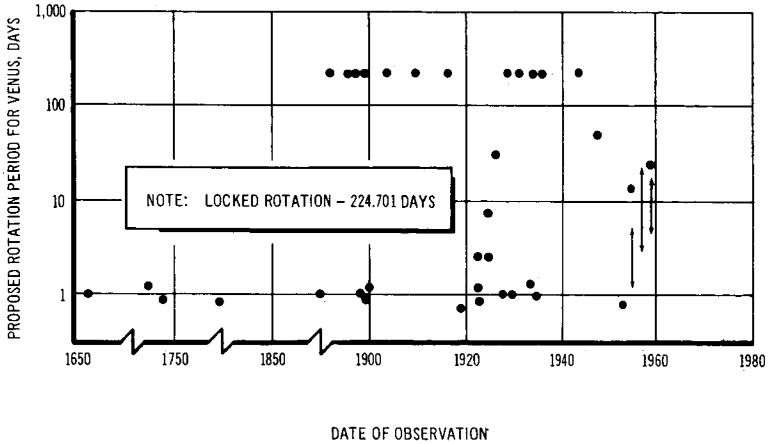

FIGURE 4–1.—Sampling of pre-1961 values for the rotation period of Venus.

TABLE 4–1.—*Radar Determinations of the Rotation of Venus*

Author	Year of inferior conjunction	Rotation sense	Rotation period, days	Axis inclination or coordinates
Carpenter (ref. 37)[a]	1962	Retrograde	~250	Approx ⊥ orbit
Goldstein (ref. 35)[a]	1962	Retrograde	~250±50	Approx ⊥ orbit
		Retrograde	248	[b]$\alpha=119°$, $\delta=-78°$
Klemperer et al. (ref. 38)	1962	Undetermined	180–280	Assumed ⊥ orbit
Muhleman (ref. 39)[a]	1962	Either direct or retrograde	570	Assumed ⊥ orbit
			250	Assumed ⊥ orbit
Drake (ref. 40)	1962	Retrograde	Undetermined	Approx ⊥ orbit
Rzhiga (U.S.S.R.) (ref. 41)	1962	Retrograde	~300	Assumed ⊥ orbit
Ponsonby et al. (ref. 42)	1964	Retrograde	100–300	Assumed ⊥ orbit
Shapiro (ref. 36)	1964	Retrograde	247±4	[c]$\alpha=272.°75$, $\delta=71.°50$
Carpenter[d]	1964	Retrograde	258±6	[c]$\alpha=258°\pm6°$, $\delta=68°\pm3°$

[a] These are based on the same series of observations made in the fall of 1962 using 12.5-centimeter radar.
[b] South Pole coordinates.
[c] North Pole coordinates.
[d] Private communication, August 1965.

impelled Slipher (ref. 30) and Lowell (ref. 31) to declare that Venus must be in synchronous rotation. The same conclusion was reached in 1890 by both Schiaparelli and Perrotin from visual observations and in 1955 by Dollfus who was aided by photography (refs. 32 to 34).

Radar astronomy techniques used since 1961 have revealed the startling fact that the rotation of Venus is retrograde, and its period is close to 250 days (see fig. 13–1). The Doppler effect is again the basis of measurement. A microwave pulse of known frequency is sent to Venus, and the signal received shows a spread of frequencies caused by the effective rotation of the planet which has two major parts: the relative motion between Venus and Earth, and the actual spin of Venus. Mathematically, the total rotation is the vector sum of its orbital component and its spin component expressed as $\omega_T = \omega_0 + \omega_s$. Power spectrum analysis of Venus spectrograms taken over a period of a few weeks and centered at inferior conjunction show a pronounced trend; the base bandwidth (the frequency spread corresponding to echoes from the limbs of Venus) is narrowed as conjunction is approached and widens afterward. This spectral narrowing indicates retrograde rotation because at conjunction the spin component of the total rotation is counterbalanced by the orbital component.

Goldstein's detailed analysis (ref. 35) of spectrograms obtained at the 1962 conjunction indicated a rotation period of approximately 248 days retrograde and a rotation axis nearly perpendicular to the orbit of Venus. The celestial coordinates derived for the South Pole of Venus were: right ascension $\alpha = 119°$ and declination $\delta = 78°$, with a probable error of $\pm 15°$. The accuracy of the period was given as ± 15 percent. Other radar determinations made by both the Americans and Soviets in 1962 confirmed the slow retrograde rotation, and the values differed slightly from those mentioned previously. Table 4–1 lists these results (refs. 35–42).

In 1964 Shapiro announced almost complete confirmation of the 1962 results (ref. 36). His conclusions were made possible by the large radio telescope (1000-foot dish) just completed at Arecibo, Puerto Rico. The retrograde period of rotation of Venus was found to be 247 ± 5 days, with an axis direction approximately 84° to the orbit, the North Pole coordinates being $\alpha = 18^h\ 11^m$ (or $272\overset{\circ}{.}75$) and $\delta = 71\overset{\circ}{.}5$ with a probable error of $\pm 4°$. The Venusian pole star would then be the fourth-magnitude star ϕ-Draconis.

5

Acceleration of Gravity

THE ACCELERATION OF GRAVITY at the surface of Venus cannot be accurately determined at this time because the values for the mass and radius of the planet are uncertain. At present, the gravity at the surface of Venus is calculated by the simple gravitational formula

$$\gamma = \frac{GM}{R^2}$$

where

M mass of the planet
R radius of the planet (mean radius)
G the universal gravitational constant 6.67×10^{-8} dyne cm^2 g^{-2}

This simple formula for the calculation of gravity on Venus, in contrast with Mars or Jupiter, is satisfactory because of the very slow rotation of Venus and its quasi-sphericity.

Indeed, the centrifugal force correction, $c = -R\omega^2 \cos^2\phi$ (where ω is rotation rate, and ϕ is latitude on the planet), becomes insignificant. At the equator, this correction is greatest ($\cos\phi = 1$), and is of the order of 10^{-5} cm sec^{-2} for the rotation rate of $\omega = 2.0 \times 10^{-7}$ rad sec^{-1}, which corresponds to a 250-day period. If Venus is spherical, as all astronomical observations indicate, radius length does not depend upon latitude on the planet. Polar and equatorial radii are the same, and no radius function of latitude, r_ϕ, enters into the calculation of gravity.

The surface gravity of Venus has been calculated here with the values of mass and radius of the solid globe adopted in chapters 2 and 3 with the probable errors giving upper and lower limits as follows:

(1) Mass, $M = 4.8678 \times 10^{27}$ grams, or 4.8558 to 4.8798×10^{27} grams
(2) Radius, $R_o = 6.085 \times 10^8$ centimeters, or 6.075 to 6.095×10^8 centimeters

Thus, the most probable value for the acceleration of gravity on the surface of Venus is 877.0 ± 5.0 cm sec^{-2}.

6

Mean Density

THE COMPUTED MEAN DENSITY of the solid globe of Venus is dependent upon the mass and radius values used in the calculation. The planet's mass is known to a fair degree of accuracy. The exact radius of the solid globe hidden beneath the thick cloud cover is highly uncertain. The values used here are those for the mass and the radius of the solid globe adopted in chapters 2 and 3. Upper and lower limits listed below express the adopted probable errors.

(1) Mass, $M = 4.868\ (\pm 0.012) \times 10^{27}$ grams

(2) Radius, $R = 6.085\ (\pm 0.01) \times 10^{8}$ centimeters

The mean density, $\bar{\rho}$, for Venus may be calculated by using the formula

$$\bar{\rho} = \frac{M}{\frac{4}{3}\pi R^3}$$

from which the value $\bar{\rho} = 5.158 \pm 0.010$ grams cm^{-3} is obtained. Figure 2–1 illustrates the dependence of the value of mass and, therefore, of the mean density of Venus on the accuracy to which the mass of the Sun is known. Allen (ref. 24) adopts 1.989×10^{33} grams as the mass of the Sun. A change in this adopted value by $+0.001 \times 10^{33}$ grams for the mass of the Sun would change the mean density of Venus by $+0.003$ g cm^{-3}.

7

Internal Structure

INFORMATION ABOUT THE SIZE, shape, mass, and rotation of Venus has been obtained through astronomical observations. Under certain assumptions (such as hydrostatic equilibrium and structural analogy with Earth) these data may be used to predict the physical structure of the planet's interior, that is, the variation with depth of pressure, temperature, density, and chemical composition. To obtain a representation of the internal constitution, hypothetical models for the planet's interior are computed. The mass, the principle radius, and the ellipticity are boundary conditions which must be satisfied.

The ellipticity of a planet is a result of the spin rate about its rotation axis and its internal constitution. For a fluid planet of a given chemical composition in hydrostatic equilibrium, the gravitational field and internal structure are both affected by the spin rate. However, no planetary interior completely resembles a fluid; rather, the strength of the material helps support some of the overlying strata. For this reason, three types of ellipticity have been introduced: dynamical, mechanical, and geometrical. Only geometrical ellipticity can be determined from Earth-based observation of Venus. Such observation shows no noticeable flattening, and, therefore, the geometrical ellipticity is assumed to be zero (ref. 43). This is in accord with observations which indicate that Venus rotates slowly (see ch. 4).

The generation and maintenance of planetary magnetic fields are poorly understood at present. The generation of the Earth's dipole magnetic field has been attributed by Cowling (ref. 44) and Jacobs (ref. 45) to a self-sustaining dynamo located in the fluid core. According to this theory, the convection currents in the core cause electric currents that produce the external dipole field; therefore, rapid changes in field strength are attributed to rapid changes of currents in the core, and field strength is expected to correlate with the period of rotation of the planet. The external magnetic field of Venus was sought during the 1962 Mariner II mission, but none was detected; the maximum value for the surface field, assuming it is dipole, has been set at 0.03 gauss (ref. 46). The slow spin rate, zero ellipticity, and low-strength magnetic field of Venus tend to support the dynamo theory. However, there remain mathematical difficulties in describing the circulation pattern and the generation of currents in the fluid core.

Venus has often been referred to as the twin of Earth because of its general similarity of radius, mass, and mean density (see table 7–1). The lack of oblateness and absence of satellites make it impossible to determine the internal constitution of Venus without knowledge of the chemical and mechanical properties of the interior regions. Hence, interior models are based upon the assumption of similarity between the interiors of Venus and Earth and upon the geophysical data adopted.

TABLE 7–1.—*Comparison of Earth and Venus*

Earth (ref. 24)	
Mass, M	$=(5.977\pm0.004)\times10^{27}$ g
Mean radius	=6371.03 km
Equatorial radius, a	$=(6378.17\pm0.04)$ km
Polar radius, c	=6356.79 km
Geometrical ellipticity, $(a-c)/a$	=1/298.26
Mean density, $\bar{\rho}$	$=5.517\pm0.004$ g cm^{-3}
Moment of inertia about spin axis, C	$=0.3306\ Ma^2$
Moment of inertia about equatorial axis, A	$=0.3295\ Ma^2$
Mechanical ellipticity, $(C-A)/A$	=1/305.29
Spin rate, ω	$=7.292\times10^{-5}$ rad sec^{-1} $=1$ rev day^{-1}
Venus	
Mass, M	$=4.86959\times10^{27}$ g (Mariner II)
Radius	$=6100\pm50$ km (values used for construction of models ranging from 61000 to 62000 km)
Radii, $a=c$	=6100 km
Geometrical ellipticity, $(a-c)/a$	=0
Mean density, $\bar{\rho}$	=5.1 g cm^{-3}
Moment of inertia about equatorial axis, unknown	
Mechanical ellipticity, unknown	
Spin rate, ω	=1 rev/247 days

In the construction of interior models, it is commonly assumed that the regions under consideration are in hydrostatic equilibrium. This assumption will hold true for most of the internal regions of a moderately large planet (such as Earth). If temperature effects such as nonadiabatic compressions are neglected, the internal structure of a planet can be determined by solving the following equation:

$$\frac{dP}{dr} = -\left[\gamma(r) - \frac{2}{3}\omega^2 r\right]\rho(P) \tag{7–1}$$

where

$$\gamma(r) = \frac{GM(r)}{r^2} = \frac{4\pi G}{r^2}\int_0^r \rho(x)x^2dx \tag{7–2}$$

where

P	the pressure
r	the distance from the center of mass to the spherical surface under consideration
γ	the acceleration of gravitation
$M(r)$	the mass interior to r
ω	the spin angular velocity
ρ	density
$\rho(P)$	the density/pressure relationship
x	the distance from the center of mass to the differential shells of integration interior to r
G	universal gravitational constant

Equations (7–1) and (7–2) are solved as though the planetary configuration had spherical symmetry; oblateness is allowed for in the definition of the parameter r.

The density/pressure relationship, $\rho(P)$, is obtained from the equation of state, which describes a functional relationship between the chemical composition, temperature, pressure, and density. Since neither the density/pressure relationship nor the chemical composition for the interior of Venus is known, the internal structure is based upon the assumption of similarity with the interior of Earth and the adoption of its $\rho(P)$ relation. This includes the adoption of some mean density-value characteristic of crust material. Seismological considerations yield data on the ratio of incompressibility to density and on the general zonal structure of the interior of Earth. These data and known boundary conditions allow the numerical integration of the above equations to obtain the density/pressure relationship for Earth. The known boundary conditions for Earth are mass, principal radius, moment of inertia, and ellipticity.

Discontinuities in the propagation of longitudinal and transverse earthquake waves have led to the division of Earth's interior structure into two principal zones: a dense liquidlike core at a depth of 2898 to 6371 kilometers surrounded by a lighter solidlike mantle at a depth of 33 to 2898 kilometers. The thin heterogeneous surface skin, or crust, of Earth is considered to be a third zone, 33 kilometers thick, with a mean density of 3.29 g cm^{-3}. Model structures for Venus will show the two-zone division because of the basic and necessary assumption of similarity to the interior of Earth. Figure 7–1 illustrates the two-zone features and the density/depth distribution for Venus models suggested by Jeffreys (ref. 47) and Bullen (ref. 48). Table 7–2 gives the internal constitution for the Jeffreys and Bullen models of Venus and table 7–3 gives a model interior for Earth (refs. 45, 49 and 50).

Construction of model interiors for other terrestrial planets is uncertain because the chemical composition of Earth's two zones is unknown and, especially, because it is not known whether the core is composed of a material chemically distinct from the mantle or a high-pressure phase modification of the same material (ref. 51). If the core is chemically distinct, the core radius can be taken as an independent parameter which permits considerable freedom in the computation of a planetary interior, particularly in meeting boundary conditions. If, however, the core material of Earth is a high-pressure modification of the mantle material, the formation of a core must be anticipated when a pressure is reached that corresponds to the interface pressure between the Earth's core and mantle.

The nature of the core is more uncertain because of the lack of knowledge about the exact thermal structures of Earth and Venus. Even if Venus has a two-zone structure similar to Earth's, differences in the thermal structures will affect the size of the core, because the density/pressure relationship of Earth may not coincide with Venus. The $\rho(P)$ relationship depends upon the internal temperature distribution. Undoubtedly, differences in the internal temperature distributions of Earth and Venus exist, and would be greater if the high surface temperatures are a result of internal heat escaping to the surface. The models shown in figure 7–1 neglect the differences in the thermal structures of the two planets.

The thermal history of a planet depends mainly upon the following factors:

(1) Initial amount and distribution of heat at formation

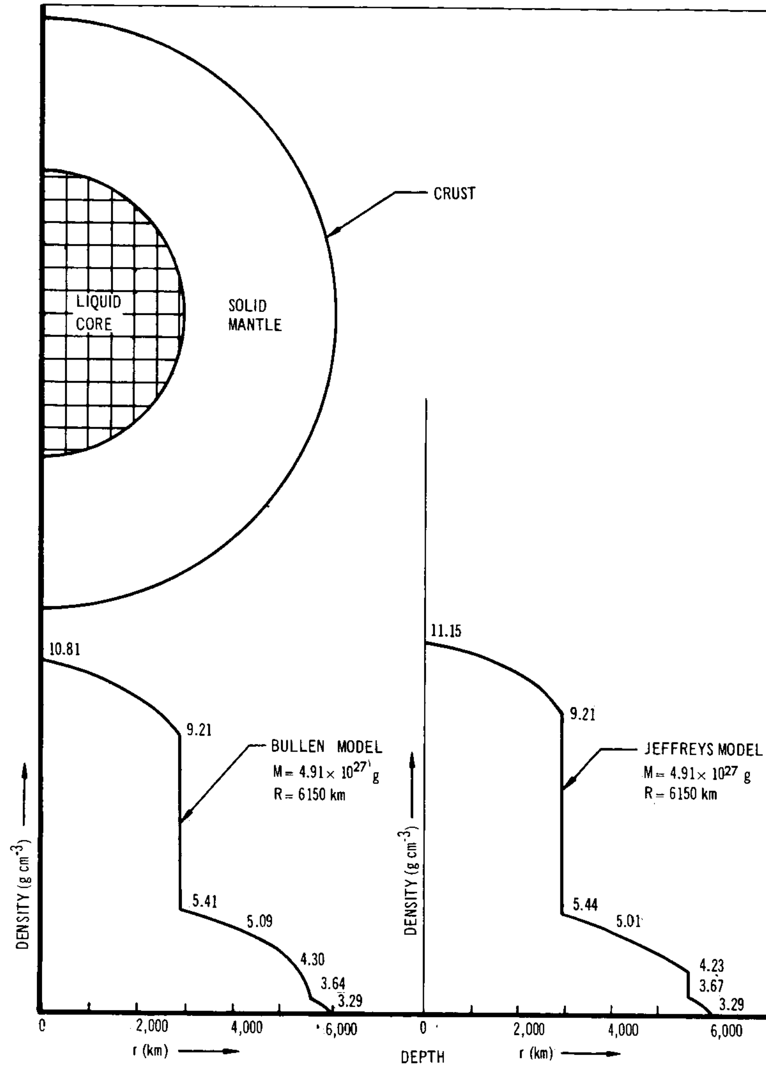

FIGURE 7–1.—Computed density distribution for interior of Venus.

(2) Initial and subsequent distribution of radioactivity
(3) Subsequent gravitational contraction which increases the internal energy of the planet
(4) Heat conductivity of the internal material at the prevailing temperatures and pressures

Because of the uncertainties in the various assumptions, the computed thermal models are rather speculative. MacDonald (refs. 52 and 53) has computed hypothetical temperature distributions

TABLE 7-2.—*Interior Models of Venus*

	Jeffreys (ref. 47)					Bullen (ref. 48)				
	Radius, r, km	Density, $\rho(r)$, g cm^{-3}	Pressure, $P(r)$, dynes cm^{-2}	Mass, $M(r)$, g		Depth, d, km	Radius, r, km	Density, $\rho(r)$, g cm^{-3}	Pressure, $P(r)$, dynes cm^{-2}	Mass, $M(r)$, g
Solid mantle, 78.5 percent by mass	6.15×10^3	3.29	0×10^{10}	4.910×10^{27}	Crust, 3 percent by mass	0	6150	3.29	0×10^{10}	4.91×10^{27}
	6.0	3.41	4.38	4.677		30	6120	3.32	0.7	4.76
	5.7	3.63	13.59	4.223		470	5680	3.64	14	4.20
	5.617	3.69	16.22	4.101	Solid mantle, 75.4 percent by mass	800	5350	4.30	25	3.70
	5.617	4.23	16.22	4.101		1200	4950	4.70	57	3.09
	5.0	4.48	39.38	3.138		2000	4150	5.09	73	2.07
	4.0	5.01	78.52	1.915		2800	3350	5.41	106	1.33
	2.911	5.44	124.4	1.057		3200	2950	5.57	124	1.06
Liquid core, 21.5 percent by mass	2.911×10^3	9.64	124.4×10^{10}	1.057×10^{27}	Liquid core, 21.6 percent by mass	3206	2944	9.21	124×10^{10}	1.06×10^{27}
	2.5	10.00	155.8	.686		3483	2667	9.50	145	.79
	1.5	10.74	217.8	.360		4000	2150	9.96	179	.43
	0.5	11.11	251.3	.006		5200	950	10.65	234	.04
	0	11.15	255.8	0		6150	0	10.81	249	

Astronomical data (Jeffreys):
- Mass of Venus = 0.817 ± 0.003 that of Earth or 4.91×10^{27} grams
- Radius of Venus = 0.9652 ± 0.0078 radius of Earth or 6150 ± 50 kilometers
- Density of Earth = 5.517 ± 0.004 g cm^{-3}
- Mass of Earth = $5.975\pm0.004\times10^{27}$ grams

Astronomical data (Bullen):
- Mass of Venus = 4.91×10^{27} grams
- Radius = 6150 ± 50 kilometers

TABLE 7–3.—*Model Interior for Earth*

[Density/pressure structure after Bullen's Earth model A (refs. 45 and 49); thermal structure after Gilvarry (ref. 50)]

	Depth, d, km	Radius, r, km	Density, $\rho(r)$, g cm^{-3}	Pressure, $P(r)$, dynes cm^{-2}	Percent of total mass	Temp., $T(r)$, °K	Velocity of seismic waves— Long., P, km sec^{-1}	Trans., S, km sec^{-1}
Crust, 0.8 percent by mass	0	6371	3.29	0×10^{10}	100	287	7.65	4.3
	33	6338	3.32	0.9	99.2	700	7.75	3.35
Solid mantle, 67.6 percent by mass	100	6271	3.38	3.1	97.2	1200	7.95	4.45
	400	5971	3.63	13.6	88.6	2200	8.92	4.95
	413	5958	3.64	14.1	87.5	2230	8.97	4.96
	500	5871	3.89	17.3	85.0	2370	9.75	5.33
	1000	5371	4.68	39.2	70.5	3000	11.42	6.36
	2000	4371	5.24	88.0	47.4	3800	12.70	6.93
	2898	3473	5.68	137	31.5	4300	13.64	7.30
Liquid core, 31.5 percent by mass	2898	3473	9.43	137	31.5	4300	8.1	0
	3500	2871	10.3	193	19.3	5000	8.9	0
	4000	2371	10.76	240	11.5	5500	9.51	0
	4892	1479	11.54	317	02.9	5960	10.44	0
	5121	1250	14.2	327	02.1	6070	9.7 (?)	0
	5121	1250	16.8	327	02.1	6070	11.16	0 (?)
	6371	0	17.2	364	0	6400	11.31	0 (?)

for Venus at various times after origin by assuming an initial temperature distribution, a distribution of heat sources, and a distribution with the depth of such parameters as the density, heat capacity, thermal conductivity, and opacity. Temperature at the outer surface of the planet is assumed to be constant with time.

Some of the computed thermal models for Venus are shown in figure 7–2; table 7–4 gives the various assumptions upon which these curves are drawn. MacDonald investigated the range of opacities from 10 to 1000 cm^{-1}, which covers the values observed in common silicate materials. (Silicate materials are believed to be the main chemical constituent of Earth's mantle.) MacDonald's calculations indicate that the temperatures encountered at depths of 200 kilometers are about 200° C higher for Venus than for a similar thermal Earth model. A liquid state is implied because the indicated temperatures at this depth are higher than the melting temperature of common silicates. The radioactive constituents of chondritic meteorites are as follows: potassium, 8.0×10^{-4} g g^{-1} (g of radioactive material/g of chondrite); thorium, 4.4×10^{-8} g g^{-1}; and uranium, 1.1×10^{-8} g g^{-1}. This composition is usually assumed because the observed average surface heat flow of 64 ergs cm^{-2} sec^{-1} from Earth is similar in magnitude to the computed value of 59.4 ergs cm^{-2} sec^{-1} that results from a uniform chondrite Earth model (ref. 52).

MacDonald (ref. 52) has mentioned the possibility that high temperatures observed near the surface of Venus are a possible

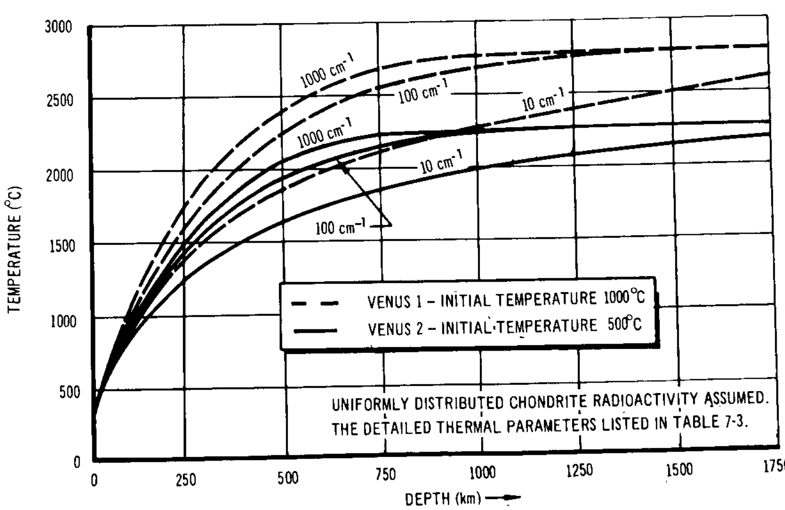

FIGURE 7–2.—Calculated temperature distribution in the outer portions of Venus.

TABLE 7–4.—*Thermal Parameters for Models of Venus*

[After ref. 52]

Initial temperature (uniformly distributed)	Venus 1=1000° C Venus 2=500° C
Surface temperature (constant in time)	300° C
Radioactivity concentration (uniformly distributed)	$U=1.1\times10^{-8}$ g g^{-1} $Th=4.4\times10^{-8}$ g g^{-1} $K=8.0\times10^{-4}$ g g^{-1}
Time of integration for model	4.51×10^{9} yr
Lattice conductivity	2.5×10^{5} ergs cm^{-1}–sec^{-1} – °C^{-1}
Uniform density	4 g cm^{-3}
Heat capacity	1.3×10^{7} ergs g^{-1} °C^{-1}
Final surface heat flow (ergs cm^{-2} sec^{-1}) for—	

	Venus 1	Venus 2
opacity=ϵ_0=10 cm^{-1}	17.2	14.4
ϵ_0=100 cm^{-1}	17.7	14.6
ϵ_0=1000 cm^{-1}	16.7	14.0

cause of the slow rotation rate. He speculates that the internal structure of Venus is similar to that of Earth, except that the high surface temperature indicates that the temperature depth distribution lies near, or above, the melting-point curve for the material in the outer regions of the mantle. This causes liquefaction of the material in the outer mantle regions and, consequently, introduces considerable body-tidal dissipation of energy from the solar-tidal interaction. The tidal forces decelerate the planet and account for the slow rotation rate of Venus. Also, the dissipated energy could help to heat the outer regions and keep the material liquefied.

If the initial angular velocity of Venus were of the same order of magnitude as that of Earth, and if the internal properties of the two planets were similar, MacDonald speculates that the present angular velocity should be greater than that of Earth. If the internal properties are still similar, Venus must have lost its angular velocity because of some torque exerted on it. Such a torque could arise from the body-tidal interaction with the Sun. The magnitude of this torque is proportional to the sixth power of the apparent diameter of the planet as seen from the Sun and to sin ϵ, where ϵ is the phase lag of the solar tide. According to MacDonald (ref. 52) the torque acting on Venus from solar-tidal interaction is approximately seven times greater than that acting on Earth, if the phase lag for Venus equals that for Earth.

However, because of the assumption of similarity, the mechanism for tidal dissipation on Venus is assumed to be similar to that of Earth. If the Earth's phase lag is used, the body tides of Venus would be incapable of decelerating it in 4.5 billion years (the estimated age of Earth). On Earth, tidal energy is dissipated mainly by solid friction. However, at temperatures near the melting point of the planetary material, other mechanisms, such as creep and elastoviscosity, come into play, and if there are large regions in the mantle of Venus near or at the melting point, the dominant tidal-dissipation mechanisms would be different and greater than those of Earth today. MacDonald argues that if this were the case, the body tides on Venus could decelerate it to the observed magnitude in less than 4.5 billion years.

Unfortunately, such concepts do not explain the retrograde rotation of Venus, unless it began in retrograde motion, nor do they account for the maintenance of high surface temperature. High surface temperature and low magnitude of rotation are compatible with the following hypotheses:

(1) The interiors of Earth and Venus are composed of similar material.

(2) A fraction of the outer regions of the mantle of Venus is at or near the melting point.

(3) The high surface temperature of Venus maintained over a long period of the planet's history has raised the temperature above the melting point of the common silicates near the surface of the planet but not necessarily at great depth.

(4) Earth and Venus have similar radioactive concentrations in their interiors.

(5) During the history of Venus, solar-tidal interaction has decelerated the planet to its present slow magnitude of rotation.

Lyttleton (ref. 54), with calculations concerning the course of evolution of Earth and Venus, has extended the Earth-Venus analogy. He computed a series of two-zone (mantle/core), all-solid models and a series of two-zone models with liquid cores for Earth and Venus. The different zones depict the pure-phase change of material (that is, from solid to liquid state). When the central regions of Earth and Venus undergo initial phase change to liquid form, the material becomes much more compressible, and the planet shrinks as the core increases in mass. This initial phase change is assumed to be caused by radioactive heating. The greater compressibility of the liquid form implies that the initial liquefaction extends almost instantaneously through a substantial fraction (5 percent) of the entire mass and results in a rapid collapse of approximately 60 kilometers of the outer surface. Subsequent contraction occurs gradually in the interior, and the indicated gravitational energy release during contraction considerably exceeds that from an Earth composed of chondritic radioactive sources (ref. 55). The amount of contraction between the initial all-solid Earth and the present two-zone Earth with a liquid core accounts for the several periods of mountain building. Because of the similarities between the two planets, the theory predicts the existence of mountains on the surface of Venus.

Most calculations of the internal constitution of Venus are based on assumptions of similarity with the Earth's interior and the consequent adoption of available geophysical data. The general assumption of similarity is based on two important hypotheses:

(1) Earth and Venus had similar origins with respect to time of formation, method of formation, and chemical composition.

(2) The evolutions of the two planets have been similar.

But if the first hypothesis is correct, the lack of external magnetic field, low retrograde rotation, and apparent high surface temperatures show that the evolution has been different for each planet.

8

Electromagnetic and Particle Fields

MAGNETIC FIELD OF VENUS

BEFORE THE MEASUREMENTS made by Mariner II in 1962, correlations of geomagnetic activity, the position of Venus, and various assumptions were used to estimate the magnetic moment of Venus (refs. 56 and 57). Houtgast and Van Sluiters (ref. 57) gave a value of the magnetic moment of Venus, assuming a dipole field, 5000 times greater than that of Earth. These results were only tentative, and have been changed radically as a result of the magnetic field and solar wind measurements made by Mariner II (see ch. 16). Analysis of the Mariner II measurements placed an upper limit on the dipole magnetic moment of Venus of $M_V = 0.05 M_E$, where M_E is the magnetic moment of Earth (ref. 58). The maximum-sized magnetosphere and shock front and the Mariner trajectory are shown in figure 8–1 (ref. 59).

It is not known how far the field of Venus extends in the antisolar direction (the same is true of Earth's field). For this estimate, it was assumed that the dipole axis is normal to the solar

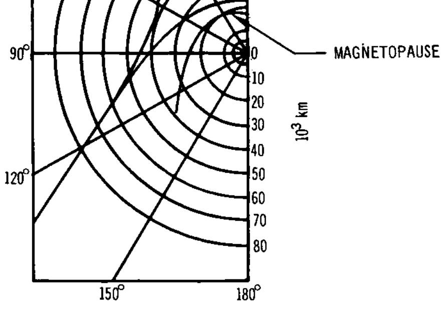

FIGURE 8–1.—Polar plot of probe-Venus distance as a function of probe-Venus-Sun angle. (After ref. 59.)

wind velocity. If other dipole orientations are considered, the estimate may change by a factor of two (ref. 58). As far as can be judged from the Mariner II observations, the magnetic moment of Venus could be zero, or the field could be multipolar and, though strong at spots on the surface, could decrease rapidly with distance from the planet.

Dynamo theory predicts that if Venus rotates slowly the magnetic field produced by currents in the planet's core will be small. Recent measurements indicate a rotation period of 247 ± 5 days for Venus (see ch. 4). Thus, the negative results of Mariner II measurements are consistent with a field produced by a slowly rotating core; from dynamo theory, the magnetic moment is expected to be much less than the upper limit of $0.05 M_E$ (ref. 58).

TRAPPED RADIATION NEAR VENUS

A radiation zone similar to that about Earth is possible for Venus under the following conditions: if $M_V = 0.05 M_E$ (the upper limit), if suitable acceleration and injection mechanisms are acting, and if the geometry of the field is such that charged particles can remain trapped. The radial extent of the trapping region can only be on the order of about 3 R_V (R_V = radius of Venus) compared with 8–10 R_E for Earth. The intensity of the trapped particles around Venus (assuming a dipole field) will be much less than in Earth's belt for to have durable trapping by a magnetic field, the energy density of the magnetic field must be greater than that of the particles. In addition to distribution and intensity differences, the maximum kinetic energy of a trapped particle would also be less since the first adiabatic invariant must be conserved. The maximum kinetic energy of a proton trapped in Earth's field is approximately 700 million electron volts. In the field of Venus, the maximum is lower by a factor difficult to estimate but which should be approximately 10.

If M_V is less than $1/20\ M_E$ but greater than $1/750\ M_E$, there still may be some particles trapped in the Venusian magnetosphere. If $M_V = 1/750\ M_E$, the radial extent of the Venusian magnetosphere on the sun side is lowered to the top of the atmosphere. If M_V is less than $1/750\ M_E$, solar wind interacts directly with the atmosphere of Venus.

9

Surface Temperature

INFERENCES CONCERNING SURFACE CONDITIONS on Venus cannot be based on optical observation because the planet is perpetually shrouded by clouds that are opaque to the visible wavelengths. Millimeter and centimeter wavelengths can penetrate the clouds, however, and such emissions from Venus have been detected. If it is assumed that these signals are the result of blackbody radiation, a brightness temperature can be derived from the Planck distribution. Results of such computations are given in table 9–1 which is based largely on compilations by Deirmendjian and Pollack and Sagan with some additional values listed by Barrett and Staelin (refs. 60–82).

When the data in table 9–1 are transcribed to figure 9–1, the following three natural groupings are obtained:

(1) Brightness temperatures at millimeter wavelengths are clustered at approximately 380° K

(2) Brightness temperatures at centimeter wavelengths are clustered at approximately 550° K

(3) Brightness temperatures at decimeter wavelengths are clustered at approximately 680° K

Observations made by Mariner II at 1.35 centimeters and from Earth at 40 centimeters are exceptions to these three generalizations. These observations, however, are uncertain because of conditions under which measurements were obtained. However, it is fairly well established that in the centimeter and lower decimeter range, the brightness temperature is approximately 580° to 600° K and it is somewhat cooler in the millimeter range. According to Drake (ref. 82), the Venus wavelength spectrum between 1.35 and 40 centimeters approximates a blackbody spectrum.

There are several possible explanations for the microwave emissions. If the emissions are thermal, they could represent the temperature of the surface of the planet, that of some layer of the lower atmosphere, or that of a hot, dense ionosphere.

The ionospheric theory would require electron density of the order of 10^9 electrons cm^{-3} to explain the observed emission

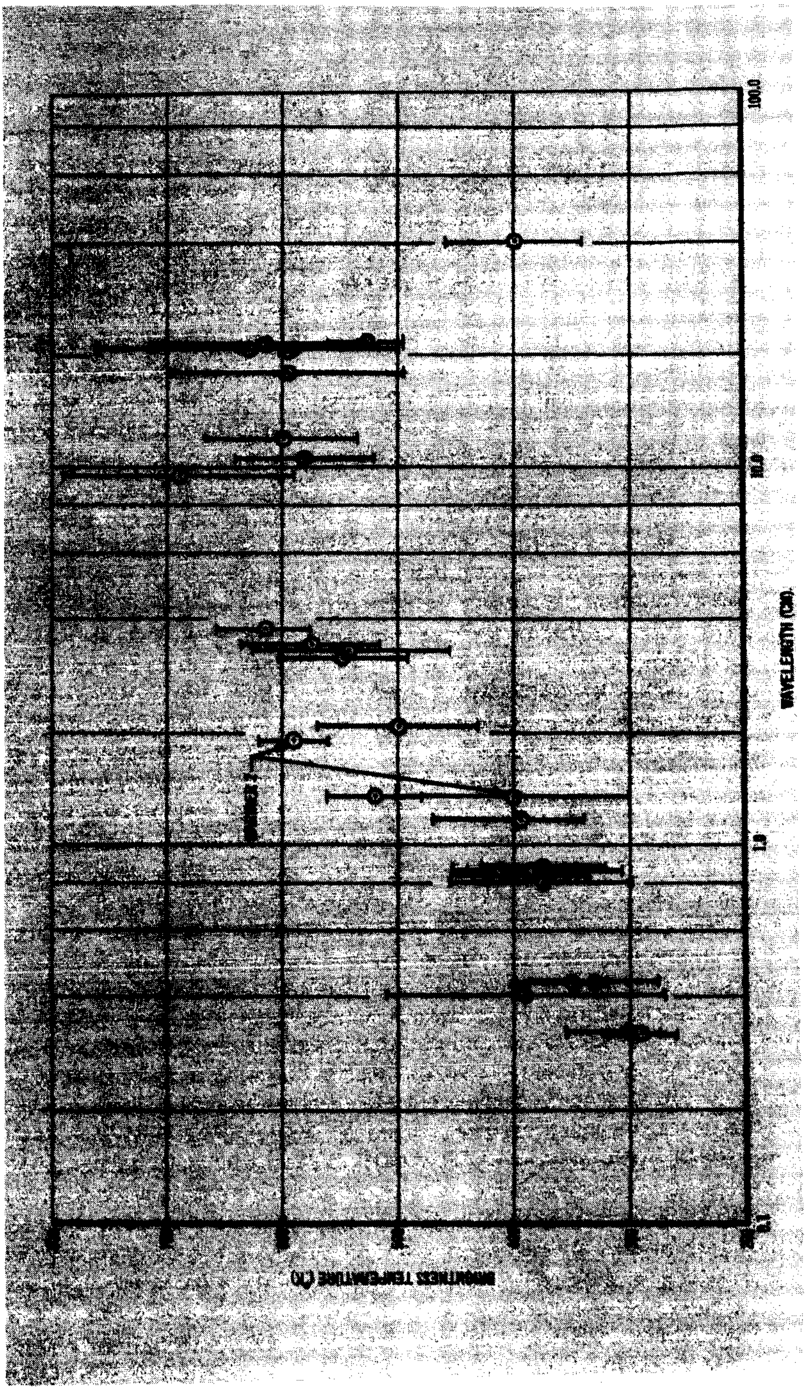

FIGURE 9–1.—Microwave brightness temperature of Venus at inferior conjunction.

TABLE 9-1.—*Microwave Brightness Temperatures of Venus*

[Whole disk near inferior conjunction, except as noted]

Author	Wavelength, cm	Equivalent blackbody brightness temperature, °K
Epstein[a]	0.32	290±30
Tolbert and Straiton (ref. 63)	.32	300+57/−27
Kislyakov, Kuz'min, and Salomonovich (ref. 64)	.40	390±120
Tolbert and Straiton (ref. 63)	.43	330+56/−36
Grant, Corbett, and Gibson (ref. 65)	.43	350+50/−30
Kuz'min and Salomonovich (ref. 66)	.80	374±75
Thornton and Welch (ref. 67)	.835	395±60
Lynn, Meeks, and Sohigian (ref. 68)	.85	380+72/−34
Copeland and Tyler (ref. 69)	.86	353±10
Tolbert and Straiton (ref. 63)	.86	375±52
Gibson (ref. 70)	.86	410+30/−20
Staelin, Barrett, and Kusse (ref. 71)	1.18	395+75/−55
Gibson and Corbett (ref. 72)	1.35	[b]520±40
Barath et al. (ref. 73)	1.35	[c]400±100
Barath et al. (ref. 73)	1.90	[c]590±30
McCullough and Boland (ref. 74)	2.07	500±70
Mayer, McCullough, and Sloanaker (ref. 75)	3.15	548±55
Babinova et al. (ref. 76)	3.30	542±85
Mayer (ref. 77)	3.40	575±60
Haddock and Dickel[a]	3.75	616±40
Kuz'min and Salomonovich (ref. 78)	9.60	[b]690±100
Mayer, McCullough, and Sloanaker (ref. 79)	10.2	600±65
Clark and Spencer (ref. 80)	10.7	580±60
Clark and Spencer (ref. 80)	18.0	596±100
Clark and Spencer (ref. 80)	21.0	616±100
Lilley (ref. 81)	21.0	630±130
Davies[a]	21.0	595±6
Drake (ref. 82)	21.4	528±33
Drake (ref. 82)	40.0	400±60

[a] Quoted by Pollack and Sagan (ref. 61).
[b] Mean value for several phases.
[c] Mariner II; near terminator and disk center.

(ref. 83). This is two or three orders of magnitude larger than the known electron density of any layer in the terrestrial ionosphere and is higher than would be expected from normal ionization and recombination processes in the atmosphere of Venus (see ch. 11). Further, Mariner II did not observe the microwave limb brightening that should occur with a hot ionosphere, but, on the contrary, observed limb darkening (ref. 73).

A hot lower atmosphere has been suggested by Öpik (ref. 84) in his aeolosphere theory. For a number of reasons, which are outlined in chapter 12, the aeolosphere theory is not generally favored. Among the reasons is the determination by Barrett and Staelin (ref. 62) that this model is not consistent with the observed microwave spectrum.

Finally, if the microwave emissions are thermal and represent the temperature of the surface of Venus, the deduced temperature must be reconciled with other observations. The spectrum of the microwave emissions suggests that the centimeter and decimeter radiation represents a hot surface, while the millimeter radiation represents some cooler layer higher in the atmosphere. According to this theory the atmosphere would be transparent to centimeter emissions, but partly opaque—perhaps because of some cloud layer—to millimeter emissions (ref. 83).

The brightness temperature is not equivalent to the actual temperature, for the emissivity, as indicated by radar measurements, is less than unity. Owen (ref. 85) and Sagan (ref. 86) use a value of 0.9 for emissivity, implying a surface temperature 11 percent higher than the brightness temperature, or about 700° K. Such a high temperature requires an explanation, for the radiative equilibrium temperature of Venus is only 250° K. (If rotation were synchronous, the radiative equilibrium temperature on the bright side would still be only 350° K.) The most widely accepted theory is that the high temperatures are produced by a strong greenhouse effect. This and other models are discussed more fully in chapter 12.

There is the possibility that the microwave emissions are not thermal, permitting the temperatures to be much more moderate. Harteck, Reeves, and Thompson (ref. 87), suggest a chemical origin of the microwave emissions. They have shown experimentally that certain reactions which might be expected on Venus produce microwave emissions that correspond to unreasonably high blackbody temperatures. They have not, however, shown that likely or possible reactions would lead to the observed spectrum.

The hypothesis of Tolbert and Straiton (ref. 88) suggests that electrical discharges associated with charged particles in the atmosphere could be a possible source of the microwave emission. They point out that on Earth higher cloud and rain emission temperatures have been measured than those which would be associated with the temperature and opacity of the medium. They state that given the same distribution of particle density, rate of fall, and particle size over Venus that is associated with a medium rainfall on Earth, and given a radiation efficiency 1/10 of that associated with high-conductivity particles, a major part of the Venus radiation that has been observed can be explained by the radiation from the fluctuation of electrical charges on particles in the Venusian atmosphere. They do not attempt to identify the chemical composition of the particles, but point out that with water the possible radiation is attenuated and absorbed.

If it is assumed that the microwave emission is thermal, some inferences concerning temperature variations can be taken from the relatively few observations made at times other than inferior conjunction. Mayer, McCullough, and Sloanaker (ref. 75) found that, for 3.15-centimeter emissions,

$$T_{BB} = 621 + 73 \cos(\alpha - 11.7)$$

where T_{BB} is the brightness temperature in degrees Kelvin and α is the planet's phase angle, with $\alpha = 180°$ representing inferior conjunction. Their findings are shown in figure 9–2. Drake, (ref. 82) whose findings are shown in figure 9–3 (ref. 82), using 10-centimeter emissions found that

$$T_{BB} = 622 + 39 \cos(\alpha - 17)$$

and later

$$T_{BB} = 622 + 41 \cos(\alpha - 21)$$

These illustrations show that little change occurs from one year to the next. Further, the remarkable agreement between the values of the constant term in the equations for both wave-

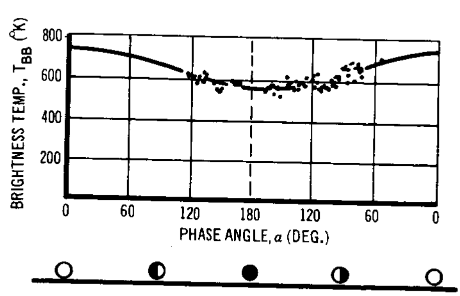

FIGURE 9–2. — Variation of equivalent blackbody disk temperature of Venus with phase, from 3.15-centimeter radiation intensity. (After ref. 75.)

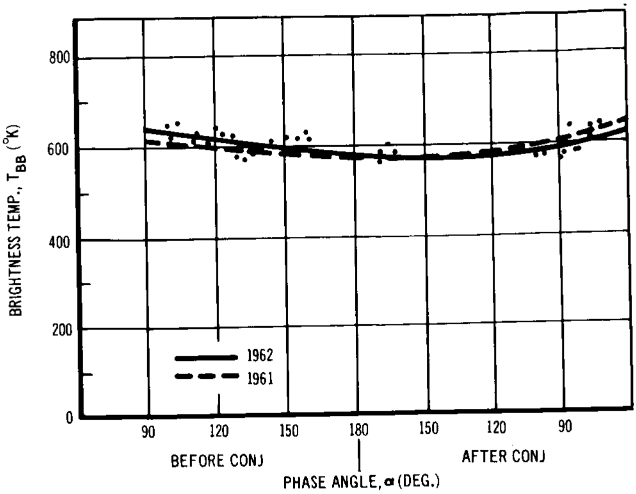

FIGURE 9–3.—Variation of equivalent blackbody disk temperature of Venus with phase, from 10-centimeter radiation intensity. (After ref. 82.)

lengths strengthens the indication that the emissions come from a solid surface and do not vary. The amplitude of the variable term changes with wavelength, implying that Venus is not in synchronous rotation. If the planet were in synchronous rotation, the same temperature would be established to great depths and would be observed at all wavelengths. The minimum temperature for each of the three sets of data occurs after the inferior conjunction. If it can be assumed that on Venus, as on Earth, the minimum temperature occurs after local midnight and the maximum temperature occurs after local noon, it is evident that Venus has retrograde rotation. By extrapolation, these results

TABLE 9–2.—*Estimated Surface Temperatures on Venus*

[After ref. 61]

Temperature measurement	Value, °K
Mean for entire disk	700±20
Mean for dark side	600±35
Mean for bright side	800±35
Subsolar point	1000±125
Antisolar point	610±125
Pole	470±95
Difference between subsolar and antisolar points	390±90
Difference between subsolar point and pole	530±165

indicate that the bright side of Venus is from 78° to 146° K warmer than the dark side. Kuz'min and Salomonovich (ref. 78) suggest a difference of 150° to 200° K.

Pollack and Sagan (ref. 61) have estimated the surface temperatures on Venus (see table 9–2), basing their estimates on a theoretical examination of phase effect and emissivity measurements, together with the assumption of plausible surface materials (see ch. 17).

10

Optical Properties

OBSERVERS HAVE NOTED that Venus has a slight lemon-yellow coloration when viewed through a telescope. The two explanations most frequently offered for this phenomenon are absorption by particles in the cloud layer and Rayleigh scattering.

Among the absorbing particles that have been proposed as an explanation are sulfur dioxide from volcanic activity, carbon suboxide, ammonium nitrate, and nitrogen dioxide. However, none of these particles has been detected in the atmosphere of Venus, and their abundance is likely to be low, if not nil (see ch. 11 and 14).

The explanation based on Rayleigh scattering has been proposed by several authors and has been discussed in some detail by Sagan (ref. 86). Coulson (ref. 89) has shown that, as the air mass increases, the ultraviolet and violet peaks in the spectrum of the emerging light are suppressed and a blue peak appears. For large solar zenith angles, the blue peak is also suppressed, leaving mainly green, yellow, and orange. Since the atmosphere of Venus is massive, Sagan concluded that this effect could explain the yellow color of the planet. If this hypothesis is true, Venus should be bluer at large phase angles. This is in accordance with the observations of a rapid decrease in color index for phase angles greater than 120°. These observations are discussed later in this chapter.

MAGNITUDE OR BRIGHTNESS

The traditional system of stellar magnitude has been employed to measure the brightness of planets. In practice, relative magnitudes are determined, and the difference between the magnitude of the planet in question and the chosen standard of reference is reported (the definition of the zero point of reference has been revised through the years). The scale is defined so that the relative magnitude is equal to 2.5 log L_s/L_p, where L_s is the mean brightness of the standard reference stars and L_p is the brightness of the planet. Thus, one unit of magnitude corresponds to a brightness difference factor of approximately 2.5, and the smaller the magnitude, the brighter the body. Discrete frequencies or selected regions of the spectrum may be used to describe magnitudes. Magnitude differences measured at discrete frequencies are independent of the detector used. However, this is not the case where magnitude difference measurements are made for an extended spectral region. If the spectral energy distribution is not the same in the two sources, then the spectral sensitivity of the detector plays a role. Detectors of specific selectivities, such as the eye, photographic plate, or photoelectric cell, will not give the same magnitude difference. Only nonselective detectors (such as bolometers) measure the true ratio of luminous energy. Hence, each selective detector has a corresponding particular magnitude system and in each of these the zero point is fixed by special convention.

The magnitude system was devised primarily for stellar astronomy and, because of the temporal variation of the position of the planets with respect to Earth and Sun, the observed magnitudes of planets are commonly reduced to a standard distance for purposes of comparison. The distance of the planet from the Sun is represented by R, and the distance from Earth by Δ. When magnitude is reduced, it is assumed that both R and Δ equal one astronomical unit, or $R\ \Delta = 1$.

The light reaching Earth from Venus is solar radiation that is reflected from the planet. The total intensity of the radiation from each point on the planetary disk is made up of light scattered by molecules (Rayleigh scattering), dust particles and clouds (Mie scattering), and ground reflection (over oceans, Fresnel reflection). In principle, it is possible to fit measurements of variations in brightness and polarization of the radiation across the planetary disk to theoretical models. Once agreement between theory and observation is made, a great deal will be learned about the atmosphere of Venus. This approach has been given impetus by Sekera and Viezee (ref. 90) who computed the expected intensity and polarization of the light from a planet at several phase angles, taking into account all orders of scattering for various hypothetical molecular atmospheres (no clouds) of various depths and planetary albedos. A plane-parallel atmosphere was assumed. Observational data are lacking to supplement theoretical studies which, in the case of Venus, should include consideration of clouds.

The visual, reduced magnitude of Venus as a function of phase

TABLE 10–1.—*Reduced Visual Magnitudes at Phase Angles 0° and 50° and Phase Integrals*

[After ref. 43]

Author	Type of observation	Year	$V_1(0°)$	$V_1(50°)$	Phase integral, q_v
Müller	visual	1893	−4.16	−3.44	1.194
Müller	visual	1926	...	...	1.078
King	photovisual	1919	...	−3.50	...
Danjon	visual	1949	−4.27	−3.71	1.296
Knuckles et al.	photoelectric	1961	−4.76	−3.69	0.888
Mean adopted by De Vaucouleurs			−4.40	−3.58	1.087

angle, and the related phase integral, q_v, are shown in table 10–1. The variation of the apparent visual, reduced magnitude with phase angle, based on data of Danjon that is discussed by Harris (ref. 91), is

$$V\ (\alpha) = -4.29 + 0.09\left(\frac{\alpha}{100°}\right)^1 + 2.39\left(\frac{\alpha}{100°}\right)^2 - 0.65\left(\frac{\alpha}{100°}\right)^3$$

where α is the phase angle in degrees. On the right side of the equation, the first term is the reduced magnitude at zero phase angle and the remaining terms represent the phase variations, (Δm). De Vaucouleurs (ref. 43) suggested the use of the mean of the phase variations (visual phase curves) plotted in figure 10–1. These data (mean Δm) are tabulated in table 10–2 together with the resulting phase function, which is the ratio of normalized flux density at phase angle α to that at zero phase angle. The marked phase effect is a result of variations in the amount of sunlit hemisphere that is seen from Earth and the fact that at different phase angles the predominant radiation originates from different regions of the planetary disk. Thus, a crude mapping of the radiation field across the disk is achieved.

Harris (ref. 91) compared the observed and theoretical variation of the brightness of Venus with phase angle. Some of his findings are included in table 10–3. Observations and calculations based on Rayleigh scattering are in good agreement between phase angles from 0° to approximately 120°, if particle albedo is less than unity. These calculations, which were intended only as approximations, were based on the Rayleigh phase function and did not take into account polarization.

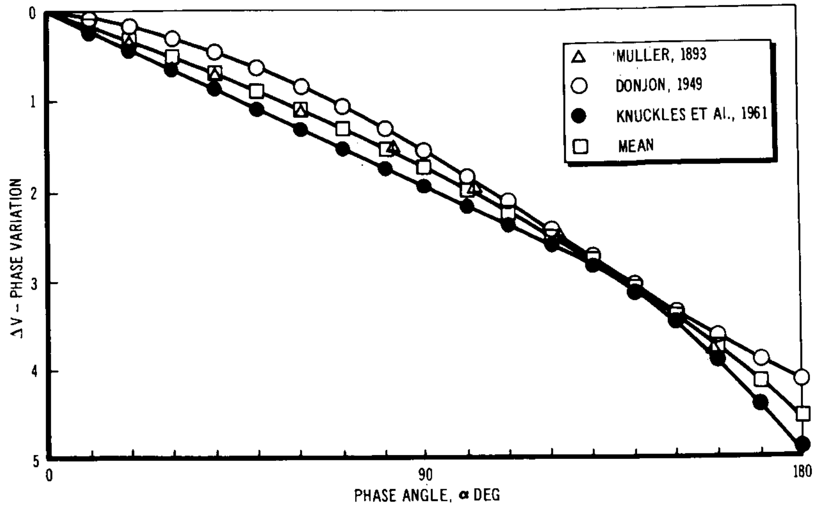

FIGURE 10–1.—Visual phase curves for Venus. (After ref. 43.)

TABLE 10–2.—*Venus Mean Phase Function*

[After ref. 43]

Phase angle, α, deg	Phase variation, Δm	Phase function, $\Phi(\alpha)$
0	0.00	1.000
10	0.14	0.880
20	0.29	.765
30	0.45	.660
40	0.63	.560
50	0.82	.470
60	1.03	.387
70	1.25	.316
80	1.48	.256
90	1.72	.205
100	1.97	.163
110	2.22	.129
120	2.48	.102
130	2.77	.078
140	3.06	.060
150	3.39	.044
160	3.72	.032
170	4.11	.022
180	4.50	.016

TABLE 10–3.—*Comparison of Measured and Theoretical Phase Functions* [a]

[After ref. 91]

Phase angle, deg	Venus observations	Rayleigh (optically thick atmosphere)	Approx Rayleigh (particle albedo less than 1.0)	Lambert
0	1.00	1.00	1.00	1.00
20	0.91	0.91	0.92	0.944
40	.71	.71	.73	.800
50	....	.59	....	.708
60	.49	.48	.52	.609
80	.31	.31	.33	.410
100	.18	.18	.20	.236
120	.107	.091	.102	.109
140	.062	.037	.042	.034
160	.036	.009	.009	.006
180	.023	0.000	0.000	0.000
Geometric albedo	.540	.798	.52	
Phase integral	1.296	1.33	1.32	
Bond albedo	.71	1.00	.69	

[a] Ratio of flux density at phase angle to that at zero phase angle, both normalized to unity at full phase.

Van de Hulst (ref. 92) pointed out that, if polarization is neglected as in Harris' work, systematic errors in intensity result. His findings, showing limb darkening according to two different laws of scattering and varying albedo of single scattering, are shown in figure 10–2.

ALBEDO

The brightness of Venus is a result of its high albedo—the ratio of reflected to incident electromagnetic radiation. The albedo can be described in various ways. The geometric albedo, p, is the ratio of the average luminance of the planet at full phase to the luminance of a perfectly diffusing, flat surface at the same distance from the Sun and normal to the incident radiation. The spherical albedo, or Bond albedo, A, is the ratio of the total luminous flux reflected by the planet in all directions to the total flux incident upon it in a beam of parallel light. The Bond albedo is most suitable when discussing the planets; it is equal to the geometric albedo multiplied by the phase integral, q. This integral can be obtained from data on the variation in brightness of Venus

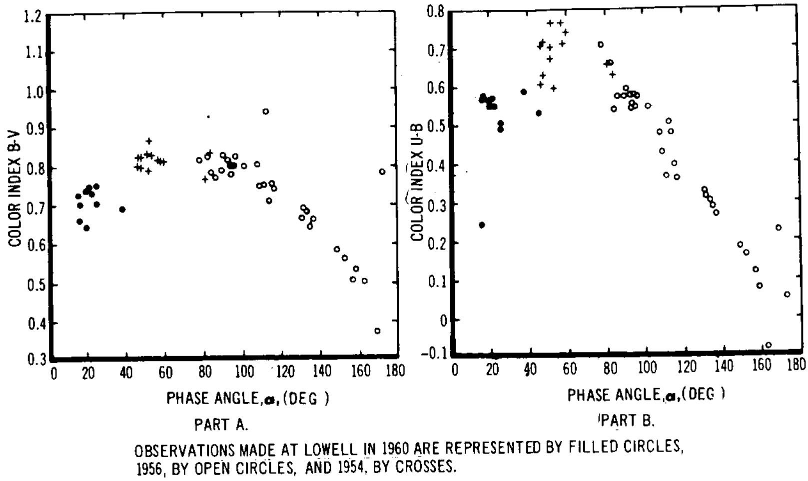

FIGURE 10–2.—Limb darkening for a planet with semi-infinite atmosphere. Observations made at Lowell in 1960 are represented by filled circles, 1956, by open circles, and 1954, by crosses. (After ref. 92.)

with solar phase angle. Either albedo may refer to a restricted spectral region. The radiometric albedo (or integral spherical albedo), A^*, refers to the spectral region of solar radiation.

Thus, $1-A^*$ is that portion of the incident solar energy absorbed by the planet and provides a measure of the use of solar energy within the planet (to heat the planet and its atmosphere, to enter into photochemical reaction, etc.). Table 10–3 shows the value of the Bond albedo for Venus.

COLOR INDEXES

The color index of a body is the difference in the magnitudes in two different spectral regions. The index was first devised to describe the approximate spectral distribution of light from stars that were too faint to provide detailed spectrograms.

Various systems have been used to specify the color index. The most common is the difference between the photographic (blue-sensitive) and photovisual magnitudes (the B–V color index). In planetary work, the U, B, V, R, and I systems have been used. These systems are defined by combinations of light filters and sensors such that U, B, V, R, and I indicate predominant sensitivity in the ultraviolet, blue, visible, red, and infrared regions of the spectrum, respectively (see ref. 91).

Color index nomenclature has been adapted in planetary astronomy to provide a rough indication of the color of the planet and a measure of the selectivity of its reflectivity. If a planet has the same color index as the source of its illumination (the Sun), the planet is a grey (nonselective) reflector; if, however, there is a difference in color indexes, selective reflectivity is indicated.

Table 10–4 gives some values for the color indexes of Venus and the Sun for comparison. The variation of color indexes with phase angle (fig. 10–3) has been determined by Knuckles et al. (ref. 93). De Vaucouleurs (ref. 43) attributes the decrease in color indexes (apparent blueing of the planet) when α is greater than 120° to the increased influence of forward molecular scattering in the light from the planet that reaches the observer as the planet comes between the Sun and Earth. He questions the reality of the decrease in color index when α is less than 40°.

TABLE 10–4.—*Mean Color Indexes and Color Differences for Venus and the Sun*

[After ref. 91]

Body	Color indexes from differences between magnitudes		Differences between Venus and Sun for each wavelength region	
	U–B	B–V	U	B
Venus	0.50	0.82	....	....
Sun	.14	.63	+0.55	+0.19

POLARIZATION

As the solar phase angle varies, solar radiation scattered from Venus that is observed on Earth must travel different paths within the atmosphere of Venus to achieve the required equivalent angle of reflection. Hence, the light penetrates different amounts of atmosphere and undergoes different amounts and angles of reflection and refraction with phase angle. The degree of polarization produced by cloud particles is a function of particle size and chemical composition and the path taken by the light when it penetrates or reflects from the particle. Hence, polarization varies with both material and phase angle, and, in principle, it should be possible to match the observed polarization with that produced by different materials in the laboratory in order to identify the cloud composition. Scattering in a pure molecular atmosphere causes strong polarization of light; however, scattering in clouds generally will decrease polarization.

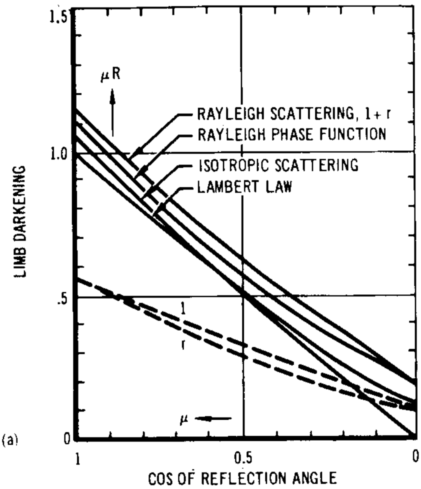

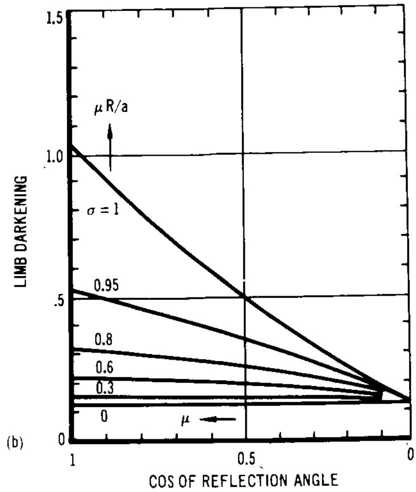

FIGURE 10–3.—Venus color indexes as a function of phase angle. (a) Different scattering functions with albedo of single scattering equals 1. Separate intensities of polarized components in Rayleigh scattering are denoted by l and r, where l and r represent the components parallel and perpendicular to the scattering plane, respectively; (b) Isotropic scattering for different values of albedo of single scattering. (After refs. 92 and 93.)

Studies of the weak polarization of light from Venus were made by Lyot and Dollfus (ref. 94). The variation of polarization with phase angle, as obtained by Lyot, is shown in figure 10–4 together with a curve obtained in the laboratory that is representative of small water droplets. Of those materials investigated, the small water droplets provided the best fit to the observed curve from Venus, and, on the basis of these findings it was suspected that water is present in the atmosphere of the planet although spectrographic evidence was negative (however, the polarization data are not conclusive). Based on the assumption of a water-droplet cloud and the known effect of molecular scattering on increasing polarization, Dollfus concluded that the effective height of the atmosphere above the clouds was 800 meters (STP) and, therefore, the cloud summit was at a pressure of approximately 90 millibars.

Dollfus also obtained mappings of the distribution of polarization across the disk of Venus at different phase angles. The patches of equal polarization on the planetary disk do not correspond to visual markings. More detailed mappings of polarization and intensity combined with theoretical investigations, such as those initiated by Sekera and Viezee (ref. 90), would be useful in resolving some of the unknown factors of Venus.

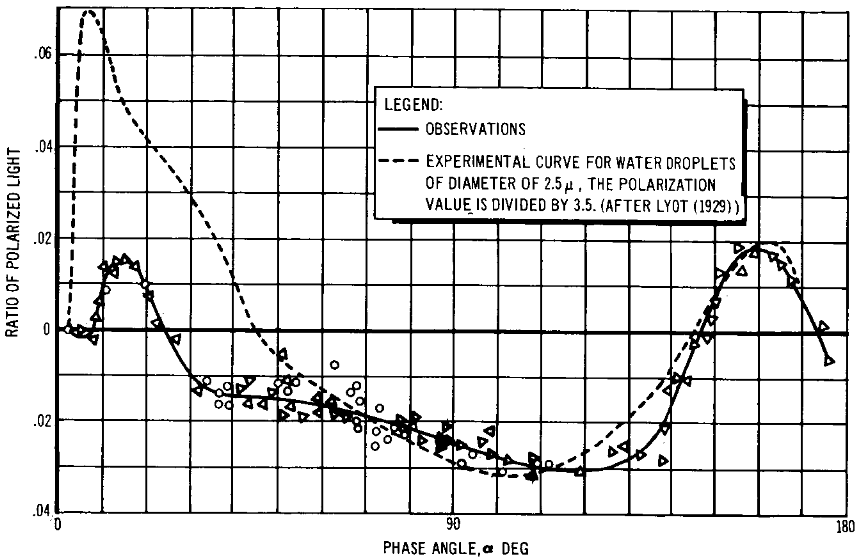

FIGURE 10–4.—Polarization of diffuse reflected light from Venus as a function of phase angle as determined by Lyot. (From ref. 94.)

OPTICAL THICKNESS

Coulson and Lotman (ref. 95) computed the volume-scattering coefficients and optical thicknesses related to four model atmospheres for Venus, then used these data and scattering tables by Coulson et al. (ref. 96) for a molecular atmosphere to approximate the absolute intensity of both the direct and scattered solar radiation as a function of height above the surface and the distribution of scattered radiation in the atmosphere.

PHOTOGRAPHIC PHOTOMETRY OF VENUS

Photographs of Venus taken in ultraviolet light disclose details over the planet's disk. Photographs taken in longer wavelengths show weak details. Red or infrared photographs are featureless.

Figures 10–5 and 10–6 represent the variation of intensity obtained by Ross (ref. 97) from extensive photographic study of Venus. Figure 10–5 shows an intensity curve in ultraviolet parallel to the terminator at a distance of one-third radius. Figure 10–6 shows the intensity curves in ultraviolet and red along a section perpendicular to the terminator. The disk of Venus shows a large decrease in intensity near the terminator. This decrease has been interpreted as indicating the presence of cirrus clouds

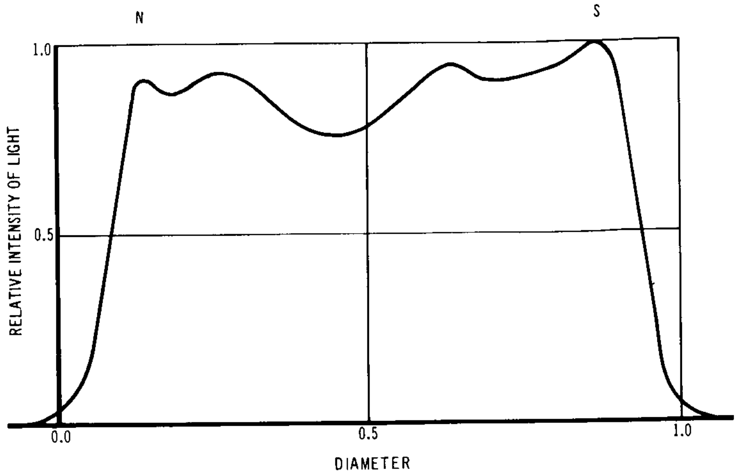

FIGURE 10–5.—Disk of Venus—intensity curve parallel to terminator; ultraviolet, June 26. (After ref. 97.)

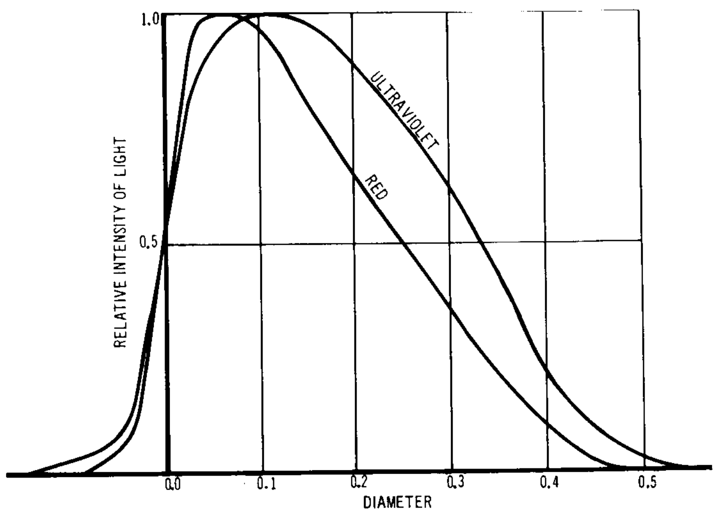

FIGURE 10–6.—Disk of Venus—intensity curve perpendicular to terminator. (After ref. 97.)

at high levels or an upper surface of billowy clouds. Maximum intensities are observed over the cusps. The maximum variation amounts to 24 percent.

Figure 10–6 shows that the intensity curve in red falls faster than that in ultraviolet as the terminator is approached. This is considered to be caused by scattering effects which are more pronounced for shorter wavelengths. The photographic studies of

Yezerskii (ref. 98) disclose a maximum intensity on a region of the Venus disk where the angles of incidence and reflectance are equal. This leads to the assumption that, in addition to diffuse scattering by molecules and aerosols present in the atmosphere of Venus, there is also a specular reflection of light which could indicate the presence of a thick atmosphere.

11

Composition of Atmosphere

THE COMPOSITION OF THE ATMOSPHERE of a planet is a function of geological time and depends on the extent to which gases escape, the degree of gas replenishment by exhalation from the crust (slowly or through volcanic activity), gas removal or addition by chemical reactions either at the crust or in the atmosphere, and the capture of gaseous materials from interplanetary medium or meteors.

According to Brown (ref. 99), the Earth's atmosphere is almost entirely of secondary origin, having evolved subsequent to the formation of the planet. By analogy, it is reasonably certain that the atmosphere of Venus is also a result of processes active after the formation of the solid planet. This, however, is questioned by Suess (ref. 100), who suggests that Venus has retained gases from its primary atmosphere and that neon, rather than nitrogen, comprises most of its atmosphere. The cosmic abundance of the elements should provide some indication of the most probable gas in any planetary atmosphere. Molecular hydrogen and helium, although of great cosmic abundance, rapidly escape from Venus and the smaller planets because of low gravity. Accordingly, carbon, oxygen, nitrogen, and their reaction products have been sought in the atmosphere of Venus, principally by analysis of details in the spectra of reflected and attenuated sunlight from the planet. Different atmospheric constituents will introduce different absorption lines in the spectrograms, therefore, the presence or absence of various substances can be learned by the analysis of the spectrograms.

LOWER ATMOSPHERE

Among gases that might be expected in significant quantities in the atmosphere of Venus are nitrogen, water, oxygen, and carbon dioxide; however, only carbon dioxide, first identified by Adams and Dunham (ref. 101), has been verified. Doppler shift spectral analysis provides some evidence of oxygen (refs. 102 and 103).

The presence of water has long been suspected, and now its presence is reasonably certain on the basis of the polarization data by Bottema et al. (ref. 104) and by balloon-borne spectroscopy (refs. 105 to 107). Sinton (ref. 108) reported some very marginal evidence of carbon monoxide, but Kuiper (ref. 109) could not detect it and placed an upper limit of 3 cm-atm on this component.

Based on the assumption of an atmosphere composed of large quantities of carbon dioxide, but unknown amounts of nitrogen (it is difficult to detect by Earth-based spectroscopic means), various models have been proposed, ranging in composition from mostly carbon dioxide, as proposed by De Vaucouleurs and Menzel (ref. 110), to the more recent estimate of Spinrad (ref. 111) of 4 ± 2 percent by mass carbon dioxide and the remainder considered to be principally nitrogen.

In the absence of direct evidence, consideration of chemical reactivity and the geological cycle of gases can provide estimates of the presence or absence of atmospheric constituents, and known limitations of measuring techniques that give negative results provide upper limits to quantities (see ref. 112).

Table 11–1 summarizes the present state of knowledge of the chemical composition of the atmosphere of Venus (refs. 103, 104, 107, 113, and 114). Because of mechanical mixing, the gaseous composition of the lower atmosphere of Venus should be invariant with height, except for possible condensable vapors; however, in the upper atmosphere, photochemical reactions and the escape of lighter chemical species should result in chemical stratification.

UPPER ATMOSPHERE

If a particular composition of the lower atmosphere is assumed, an estimate of the chemical structure and stratification of the upper atmosphere can be made on the basis of photochemical equilibrium. Table 11–2 lists some expected reactions in the upper atmosphere of Venus, and figure 11–1 is a model of the dissociated region of Venus obtained by calculations based on conditions shown (after ref. 115). Photochemical equilibrium may also be used as a basis for computation at ionospheric electron concentrations by stipulating a balance between the production and destruction of free electrons as follows:

$$\frac{dn_e}{dt} = V_{\text{ion}} - \alpha n^2_e = 0$$

The rate of ionization, V_{ion}, may be estimated to be, at most,

TABLE 11-1.—*Venusian Atmosphere—Summary of Chemical Composition*

Constituent	Method of determination	Cm–atm, standard condition	Spectral region, μ	Author of identification or estimate	Remarks	Content in Earth's atmosphere
Constituents identified with some assurance						
Carbon dioxide gas, $C^{12}O_2^{16}$	In absorption	10^5	0.8–1.0	Adams and Dunham (ref. 101)		3.2×10^2 cm
$C^{13}O_2^{16}$				Kuiper[a]		
CO_2		10^3	2.10	Moroz[a]		
		2×10^5 ($4\pm2\%$ by mass)	0.782	Spinrad (ref. 111)		
				Kuiper (ref. 109)	$O^{16}/O^{18}=500$ (same as Earth) $C^{12}/C^{13}=89$ (same as Earth)	
Ionization and dissociation products of $CO_2(CO^+_2, CO^+, O^+)$, formed by bombardment of CO_2 with fast protons	In emission	....	Photographic	Polyakova, Fogel, and Ch'iu[a]	Identified from Kozyrev's spectrum of the radiation of Venus' night sky. Laboratory spectrum obtained by irradiating CO_2 with beam of 40-keV protons. Proposed identification with nitrogen is apparently wrong.	

TABLE 11–1.—*Venusian Atmosphere—Summary of Chemical Composition*—Concluded

Constituent	Method of determination	Cm–atm, standard condition	Spectral region, μ	Author of identification or estimate	Remarks	Content in Earth's atmosphere
Constituents identified with some assurance—Continued						
Water vapor, H_2O	In absorption	0.020–0.123[b]	1.13	Bottema et al. (ref. 104)	Balloon observations	10[b] 1×10^3 to 1×104 cm
		0.28[b]	1.4	Dollfus (ref. 107)		
		0.05±0.04[b]	1.13	Strong[a]		
Molecular oxygen, O_2	In absorption	?	Red	Prokofyev,[a]	Balloon observations	1.7×10^5 cm
		57 (Upper limit)	Red	Spinrad, and Richardson (ref. 113)		
		Negligible	0.630	Prokofyev (ref. 103)		
Carbon monoxide, CO	In absorption	15	2.35	Sinton[a]	Tentatively identified, but there are no quantitative estimates.	0 to trace
		5	2.35	Moroz[a]		
Unidentified constituents having upper bounds						
Nitrous oxide, N_2O	In absorption	<4	2.26	Moroz[a]		0.4 ppm
		<100	2.15(?)	Kuiper[a]		0 to trace
Ammonia, NH_3	In absorption	<3	2.26–2.32	Moroz[a]		
		<4	1.51	Kuiper[a]		

Carbon suboxide, C_3O_2		<2	2.25	Moroz[a]		nil
		<2	2.32–2.37	Moroz[a]		
Methane, CH_4	In absorption	<20	1.16–1.71	Kuiper[a]		1.2 cm
						2 ppm
Ethylene, CH_2CH_2	In absorption	<3	2.32	Moroz[a]		nil
		<3	1.68	Kuiper[a]		nil
		<2	2.35	Moroz[a]		nil
Ethane, CH_3CH_3	In absorption	<1	1.20–1.73	Kuiper[a]		nil
Formaldehyde, HCHO	In absorption	<0.3	Ultraviolet	Wildt[a]		
Hydrogen sulfide, H_2S		....	Ultraviolet	(no data)		Variable
Sulfur dioxide, SO_2		....	Ultraviolet	(no data)		0–0.5 ppm
Ozone, O_3		....	Ultraviolet	(no data)		1.5–4.5 mm
Argon, Ar		....		(no data)	Expected in analogy with Earth to be about 1% by volume.	0.93%
Neon, Ne		....		(no data)		18 ppm

[a] As listed by Moroz (ref. 114).

[b] Content shown as millimeters of precipitable water (total water in column of air expressed as its height if condensed as liquid).

3×10^5 electrons cm^{-3} sec^{-1} (ref. 116). The recombination coefficient depends on molecular species present. For Venus, the most likely constituents in the ionosphere are CO_2^+, CO^+, N^+, N_2^+, O^+, and O_2^+. The recombination mechanisms will be as follows:

(1) Radiative recombination (for atomic ions):

$$e^- + X^+ \rightarrow X + h\nu \quad (\alpha = 10^{-12}\ cm^3\ sec^{-1})$$

(2) Dissociative recombination (for molecular ions):

$$e^- + Xy^+ \rightarrow X^* + y^{**} \quad (\alpha = 10^{-8} \text{ to } 10^{-6}\ cm^3\ sec^{-1})$$

(3) Three-body recombination:

$$e^- + X^+ + M \rightarrow X + M' \text{ (negligibly slow)}$$

Table 11–3 contains an ionospheric model computed by Danilov (ref. 117) on the basis of an atmosphere composed entirely of carbon dioxide. Danilov assumed that ionization resulted solely from solar ultraviolet light. He found a maximum electron density on the order of 10^6 cm^{-3}. This is similar to concentrations in the most dense portions of the Earth's ionosphere and militates against the ionospheric atmospheric model (see ch. 9). Danilov and Yatsenko (ref. 118) pointed out the possibility that, because of the low magnetic field of Venus, the flux of corpuscular energy from the Sun in addition to ultraviolet light could contribute to ionization in the upper atmosphere. They attempted to show that the microwave emission spectrum of Venus could be explained on the basis of a two-layer ionospheric model with the upper (colder)

TABLE 11–2.—*Possible Photochemical Reactions in the Atmosphere of Venus*

$$CO_2 + h\nu \rightarrow CO + O$$
$$CO + O + M \rightarrow CO_2 + M$$
$$O + O + M \rightarrow O_2 + M$$
$$CO + C + M \rightarrow C_2O + M$$
$$C_2O + CO + M \rightarrow C_3O_2 + M$$
$$C_3O_2 + O \rightarrow CO_2 + C_2O$$
$$O_2 + h\nu \rightarrow O + O$$
$$O + O_2 + M \rightarrow O_3 + M$$
$$O_3 + h \rightarrow O_2 + O$$
$$O_3 + O \rightarrow 2O_2$$
$$CO_2 + h\nu \rightarrow CO_2^+ + e^-$$
$$CO_2 + h\nu \rightarrow CO + O^+ + e^-$$
$$O^+ + e^- \rightarrow O + h\nu$$
$$CO_2^+ + e^- \rightarrow CO + O$$
$$O^+ + CO_2 \rightarrow CO^+ + O_2$$
$$CO^+ + e^- \rightarrow C + O$$

TABLE 11–3.—*Possible Ionospheric Structure of Venus*

[After ref. 117]

Height, km	Temp., °K	$[CO_2]$, cm^{-3}	V_{ion}, $cm^{-3}\ sec^{-1}$	V_{form}, $cm^{-3}\ sec^{-1}$	$[O^+)$, cm^{-3}	n_e, cm^{-3}	$[CO^+]$, cm^{-3}	$[CO_2^+]$, cm^{-3}
10	...	1.0×10^{12}	5.7×10^{-2}	1.9×10^{-2}	10^1	2.4×10^2	8.0×10^1	1.6×10^2
100	270	2.4×10^{11}	6.9×10^3	2.3×10^3	1.0×10^2	8.3×10^4	2.8×10^4	5.6×10^4
120	...	7.9×10^9	2.4×10^5	8.0×10^4	1.0×10^5	5.4×10^5	1.5×10^5	3.0×10^5
140	...	2.5×10^8	1.0×10^4	3.3×10^3	1.3×10^5	1.8×10^5	1.8×10^4	3.6×10^4
160	...	1.2×10^7	4.8×10^2	1.6×10^2	1.3×10^5	1.3×10^5	1.2×10^3	2.4×10^3
180	...	5.0×10^5	1.9×10^1	6.7	1.3×10^5	1.3×10^5	5.1×10^1	1.0×10^2
200	305	3.2×10^4	1.3	4.3×10^{-4}	1.3×10^5	1.3×10^4	$<10^1$	$<10^1$
250	...	2.0×10^1	7.8×10^{-4}	2.6×10^{-4}	1.6×10^4	5.5×10^2	...	...
300	340	2.3×10^{-2}	9.0×10^{-7}	3.0×10^{-7}	5.5×10^2	...	...	...

V_{ion} total ionization rate, $V_{form}\ CO_2^+ + V_{form}\ O^+$
V_{form} formation rate of O^+ ions
[X] concentration of species

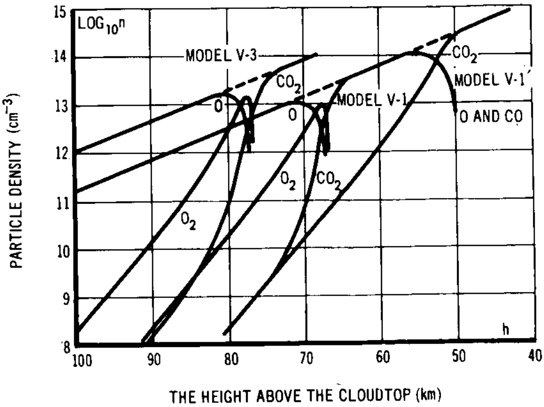

Model	Parts CO_2–N_2	CO_2, cm STP	CO or O, cm STP	O_2, cm STP	Height of layer above the cloud-top, km	Depth of layers, km
V–1	0.15; 0.85	10 000	4	0.1	70	10
V–1′	.15; .85	10 000	30	.1	50	10
V–2	.50; .50	33 333	6	....	75	8
V–3	.90; .10	60 000	7	.1	80	5

Average temperature: 215° K. Scale height: 6 to 8 kilometers.
Total pressure at the cloudtop: 90 millibars.

FIGURE 11–1.—**Concentration of neutral gases on Venus in photochemical equilibrium. (After ref. 115.)**

region partially transparent to radiation from the lower (hot) layer. The required high electron concentrations (10^9 cm^{-3}) were explained mainly on the basis of expectations of atomic, rather than molecular, constituents in the upper atmosphere and the consequent low recombination coefficient for atomic ions in comparison with the recombination coefficient of molecular ions. According to this view, Danilov's model pertains to the lowest level of the ionosphere, and more dense layers are above it. However, as shown in chapters 9 and 12, the ionospheric model as discussed by Danilov and Yatsenko generally is rejected on other grounds.

12

Atmospheric Structure

THE STRUCTURE of the atmosphere of Venus is a subject of controversy because it is difficult to directly observe the major part of it. By combining the evidence obtained by various means, it is possible to develop more or less self-consistent models. However, because details of these models are frequently contradictory, the choice among them may depend upon data derived later. The additional data may also spur the development of newer models.

PRINCIPAL OBSERVATIONS TO BE EXPLAINED

Any proposed model of the Venus atmospheric structure must account for the principal observations outlined in the following text.

PERMANENT CLOUD COVER

A permanent cloud layer covers the entire planet. Its blackbody equivalent temperature is approximately 234° K on both the light and dark sides of the planet. This cloudtop temperature, which is determined by infrared bolometry in the 8- to 12-micron window, is well established (ref. 119). Some geographical and day-to-day variations have been reported, but the temperature is remarkably uniform. Considerable limb darkening indicates a decrease of temperature with height, but the decrease is slight.

MICROWAVE BRIGHTNESS TEMPERATURES

Microwave brightness temperatures of approximately 380° K in millimeter wavelengths and 600° K in centimeter wavelengths have been determined (see ch. 9). The spectrum of the microwave emissions rules out synchrotron or cyclotron radiation from a Van Allen belt, and the Mariner II probe showed no evidence of such a belt (ref. 120).

Attempts have been made to explain the high brightness temperatures on the basis of a hot ionosphere (for example, ref. 118);

however, this model has proved untenable. Spectroscopic evidence produced by Spinrad (ref. 111) indicated that the high temperatures were in a region of high pressure, and Mariner II investigations showed that there was limb darkening in the microwave emissions, indicating a source at the surface or in the lower atmosphere (ref. 73). The microwave emissions might conceivably be of nonthermal origin (see ch. 9). If, however, they are thermal, the surface temperature is about 700° K. High surface temperatures rule out not only the ionospheric theory of the atmosphere's structure, but also several of the earlier theories about the nature of the surface of Venus such as the carboniferous swamp, the planetary oil field, and the global-seltzer ocean theories, all of which require that there be large amounts of liquid water at the surface. The planetary-oil-field theory presupposes a large aqueous ocean on which hydrocarbons of unspecified depth float. The global-seltzer theory requires that an aqueous ocean, with large quantities of carbon dioxide dissolved in it, cover the planet.

PRESSURE AT THE CLOUDTOP

Dollfus (ref. 94) determined a pressure of 90 millibars at the cloudtop by means of polarimetry (see ch. 10). Sagan (ref. 86), working downward from the level of the occultation of Regulus, found the cloudtop pressure to be between 1200 and 2 millibars and, more probably, between 280 and 31 millibars on the dark side. He adopted Dollfus' value of 90 millibars for the dark side, but suggested approximately 600 millibars for the bright side. Kaplan (ref. 121) used a similar method but obtained only 7 millibars as the cloudtop pressure.

PRESSURE AND TEMPERATURE ABOVE THE CLOUDTOP

A pressure of 2.6 (± 0.13) $\times 10^{-6}$ atmospheres at the level of the occultation of Regulus was determined by De Vaucouleurs and Menzel (ref. 110). They originally estimated this level to be 70 kilometers above the cloudtop, but later revised it to 55 ± 8 kilometers (ref. 121). Observations of the occultation of Regulus produced the following value for scale height, H:

$$H = \frac{RT}{m\gamma} = 6.8 \pm 0.2 \text{ km}$$

and its derivative

$$\left(\frac{1}{H}\right)\left(\frac{dH}{dz}\right) = 0.01 \text{ km}^{-1}$$

where R is the universal gas constant, T is the temperature, m

the molecular weight, and γ the acceleration of gravity. Assuming an atmosphere of 95 percent nitrogen and 5 percent carbon dioxide, Rasool (ref. 122) found an occultation-level temperature of 203° K, indications of a minimum mesopause temperature of about 200° K, and a mean stratospheric temperature of 207° K.

THE GREENHOUSE THEORY

All investigators who have proposed models of the Venus atmosphere face a major difficulty in accounting for the high surface temperature indicated by microwave emissions, assuming these emissions to be of thermal origin. Such conditions are usually attributed to the greenhouse effect. If the atmosphere is transparent to visible radiation, the ground surface will be heated by insolation; it then radiates in the infrared (IR). If the atmosphere is opaque to these wavelengths, the radiation is trapped, producing relatively high temperatures at low levels. The usual atmospheric constituents for absorbing IR radiation are carbon dioxide and water vapor. Barrett and Staelin (ref. 62) have shown that an atmosphere consisting only of nitrogen and carbon dioxide is not compatible with the observed microwave spectrum.

Although only a small amount of water has been detected above the cloud, the assumption of substantial amounts of water at lower levels is not excluded. Considering both water vapor and carbon dioxide, the lower atmosphere may be sufficiently opaque to IR radiation to make the greenhouse model feasible. Sagan (ref. 83) estimated that a total water content of 1 to 10 g cm^{-2} and a carbon dioxide content of 18 km-atm with a surface pressure of approximately 4 atmospheres would give the atmosphere sufficient opacity in the IR spectrum for a greenhouse effect of the required magnitude. In Sagan's model, the cloud layer would be thin cirrus, through which the sun would be visible. Features of this model are illustrated in figure 12–1. The clouds shown schematically near the tropopause are actually much thinner than represented, according to Sagan. The altitude scale at the far left and the temperature profile illustrate the now-discarded ionospheric model. As indicated, the ionospheric model would have a relatively low pressure at the surface, contrary to the spectroscopic evidence of Spinrad (ref. 111). A greenhouse model differing from that of Sagan (ref. 83) has been described by Owen (ref. 85), the properties of which are listed in table 12–1.

Although opinion favors the greenhouse theory, there are objections to it. Some writers question whether an atmosphere opaque

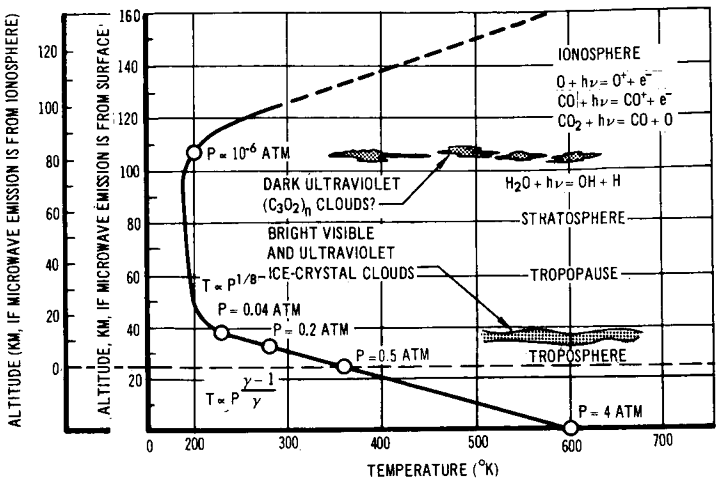

FIGURE 12–1.—A temperature profile of Venus. (Slope of ionospheric temperature is schematic only and not consistent with recent observations.) (After ref. 83.)

enough in the IR to maintain surface temperatures in excess of 600° K with a radiative planetary temperature of only 250° to 350° K would also be transparent enough in the other wavelengths to allow solar radiation to reach the surface. This problem is magnified if the surface pressure is large. Spinrad (ref. 111), on spectrographic evidence, has set a minimum of 10 atmospheres, as compared with the 4 atmospheres of Sagan, and some estimates are higher.

Another objection, stated by Mintz (ref. 123), is that differential heating by incoming radiation on a slowly rotating planet should set up a large-scale meridional circulation which, together with smaller scale thermal convection, should transport heat vertically and thus severely limit the greenhouse effect.

THE AEOLOSPHERE THEORY

Öpik (ref. 84), who assumed that there is little or no water on Venus, maintains that the greenhouse effect is not adequate to explain the high microwave temperatures. Instead, he proposed the existence of an aeolosphere, a region between the surface and the clouds in which winds raise and maintain large quantities of dust. Solar radiation cannot penetrate the dust blanket; hence, the heating is ascribed to wind friction. Above the aeolosphere is the visible cloud at 340° K, and above this, a haze layer at 234° K. The lapse rate is adiabatic between the surface and the haze layer.

The visible cloud is about 30 kilometers above the surface. Surface pressure ranges from 4.3 atmospheres for 80 percent carbon dioxide to 7.0 atmospheres for 20 percent carbon dioxide. Winds in the aeolosphere are driven from above by differential heating at the visible cloud layer. Although Öpik assumed the microwave emissions to be of thermal origin, his aeolosphere model could provide particles to generate nonthermal emissions in accordance with the mechanism proposed by Tolbert and Straiton (ref. 88).

There are a number of objections to the aeolosphere model. There is evidence that the visible cloud is composed of water, not dust (see chs. 11 and 14). For its microwave spectrum to agree with observations, the dust density would have to be 10 g cm^{-3},

TABLE 12–1.—*Properties of Greenhouse Model of Venus*

[After ref. 85]

Measurement	Minimum	Maximum	Most probable
Surface temperature (dark side), °K	540 (at pole)	640	610–640
Surface temperature (light side), °K	700	800	750
Cloudtop temperature, °K	...	...	234
Albedo	0.6	0.76	0.76
Cloudtop height, km	60	100	80
Water content, g cm^{-3}	0	22.2×10^{-3}	Insignificant
Surface pressure, atm.	30	Several hundred	50
Cloudtop pressure, mb.	90 (dark side)	608 (light side)	Dependent on hemisphere
Surface wind speed, km hr^{-1}	0.3218	0.4827	Very light
Height of occultation, km	107	163	135
Occultation temp., °K	195	216	203
Occultation pressure, mb	2.4×10^{-3}	2.9×10^{-3}	2.6×10^{-3}
Density, g cm^{-3}	1.325×10^{-3} (cloudtop)	2.607×10^{-2} (surface)	6.5476×10^{-3} (in cloud layer)
Molecular weight	29.6	29.6	29.6
Specific heat ratio	1.347 (surface)	1.4 (cloudtop)	1.389 (in cloud layer)
Speed of sound, km sec^{-1}	0.3056 (cloudtop)	0.5278 (surface)	0.4166 (in cloud layer)
Volume mixing ratio of CO_2 to N_2	0.05	0.20	0.15

according to Barrett and Staelin (ref. 62). The aeolosphere model is also in disagreement with phase effect observations. Since the surface temperature would be indirectly controlled by solar heating, it should respond sluggishly to phase change, but observations show that there is a variation on the order of 100° K with phase change (see ch. 9). Further, the strong phase effect implies a subadiabatic lapse rate from surface to cloudtop on the dark side, but an adiabatic lapse rate is required to raise and suspend the large quantity of dust. Finally, Öpik neither described the general circulation of his aeolosphere nor showed that a wind pattern sufficient for the model is dynamically possible.

THE AIRBORNE HYDROSPHERE THEORY

Some investigators still doubt the presence of sufficient water in the atmosphere of Venus to provide a greenhouse effect adequate to produce high surface temperature. Spinrad (ref. 124) determined that, at least down to a pressure of 8 atmospheres, the mixing ratio of water to total atmosphere is less than 10^{-5}. Deirmendjian (ref. 60), however, postulates sufficient water for a thick precipitating cloud. He dismisses Spinrad's results primarily because Spinrad disregarded scattering. Deirmendjian's airborne hydrosphere model is an attempt to explain the observed spectrum of microwave emission (see ch. 9) as a result of attenuation by water drops. Deirmendjian finds that a 10-kilometer-thick cloud with 100 drops cm^{-3} and 0.5 kilometer of water yields the proper attenuation. If drop concentration is 500 drops cm^{-3}, the cloud need only be 2-kilometers thick. The presence of such a thick water cloud was suggested earlier by Anderson and Evans (ref. 125) on the basis of albedo measurements, and Mariner II indicated a thickness of at least 2 to 3 kilometers for the Venus cloud layer (ref. 126). Both Deirmendjian and Anderson and Evans noted that such a cloud would not admit solar radiation to the surface, so there could be no greenhouse effect. Either the microwave brightness temperature of around 700° K would come from some form of release of heat from the interior of the planet, or it would be nonthermal in origin. Assumption of a thick precipitating cloud leads to conjecture of low-level electrical discharges producing microwave emissions (ref. 88) and the possibility of a relatively cool surface.

On Earth, the analogous emissions arise from lightning discharges and from micro discharges between charged particles within strongly convective clouds. The airborne hydrosphere model leads to a total mass of only 4.8×10^{19} grams of water in the atmosphere of Venus, as compared with 1.4×10^{24} grams in the Earth's oceans. Barrett and Staelin (ref. 62) point out that while this model (assuming the emissions are of thermal origin) in general agrees with the microwave spectrum, there is direct conflict at 1.35 centimeters.

KAPLAN'S MODELS

It is apparent that there are few check points in the atmosphere of Venus where any of the prime variables of pressure, temperature, and height are known accurately, and none where all three are known. Furthermore, there is no agreement on the atmosphere's molecular weight, which must be known for a temperature-pressure relationship. Kaplan (ref. 121) has produced three model atmospheres (standard, minimum, and maximum) that make use of what he considers the most probable values of these variables. Although his models were presented as tentative and were constructed without benefit of data from Mariner II, they have not yet been superseded. Values for significant levels (for example, the surface, the top of the cloud, and the occultation level) are shown in table 12–2. The values were calculated on the basis of the following assumptions:

(1) Molecular weight is 29.62.
(2) Volume concentration is 10 percent carbon dioxide and 90 percent nitrogen.
(3) Surface gravity is 9 m sec^{-2}.
(4) Carbon dioxide dissociation occurs between 3×10^{-6} and 3×10^{-7} atmospheres.
(5) Pressure-temperature relationship is

$$\frac{T_1}{T_2} = \left(\frac{p_1}{p_2}\right)^k$$

where

$$k = \left(\frac{dH}{dz} - \frac{1}{\gamma} \cdot \frac{d\gamma}{dz}\right)^{-1}$$

(6) Exponent k is constant throughout a layer.
(7) Extremes of temperature are approximately 20 percent higher and lower than standard temperatures.

Thus, in Kaplan's models, the pressure at the cloudtop (for example, 0.007 atm at $T = 230°$ K in the standard model) is an order of magnitude lower than the most probable value adopted by Sagan (ref. 86) and widely accepted by other investigators.

TABLE 12-2.—*Significant Levels for Model Atmospheres of Venus*

[After ref. 121]

Atmospheric model	Pressure, atm	Temp., °K	k	Height, km	Density, g cm^{-3}
Standard	10 0.007 3×10^{-6} 3×10^{-7} 10^{-7}	700 230 200 230 270	0.1532 0.0180 −0.0607 −0.1459	0 97.21 151.28 168.29 178.24	5.089×10^{-3} 1.084×10^{-5} 5.344×10^{-9} 4.233×10^{-10} 1.199×10^{-10}
Minimum	12.5 0.025 3×10^{-6} 3×10^{-7} 10^{-7}	560 160 160 184 216	0.2016 0 −0.0607 −0.1459	0 62.53 108.86 122.28 130.21	7.952×10^{-3} 5.566×10^{-5} 6.680×10^{-9} 5.279×10^{-10} 1.499×10^{-10}
Maximum	7.5 0.002 3×10^{-6} 3×10^{-7} 10^{-7}	840 250 240 276 324	0.1473 0.0063 −0.0607 −0.1459	0 127.58 179.81 200.42 212.63	3.181×10^{-3} 2.850×10^{-6} 4.453×10^{-9} 3.519×10^{-10} 9.993×10^{-11}

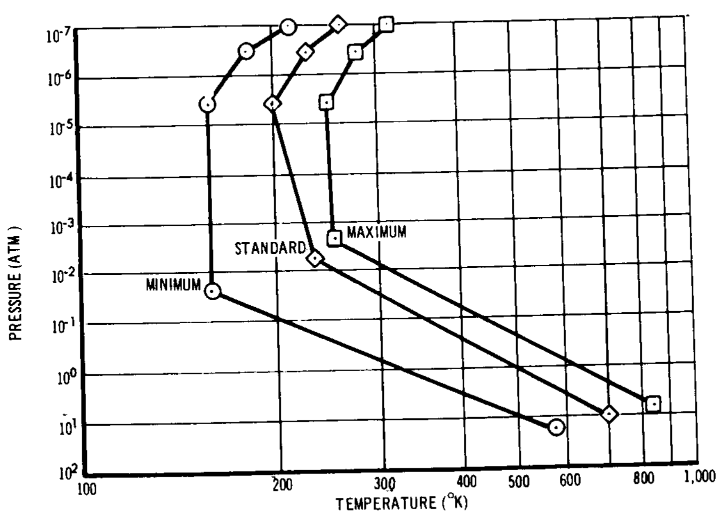

FIGURE 12-2.—Temperature as a function of pressure, model atmospheres of Venus. (After ref. 121.)

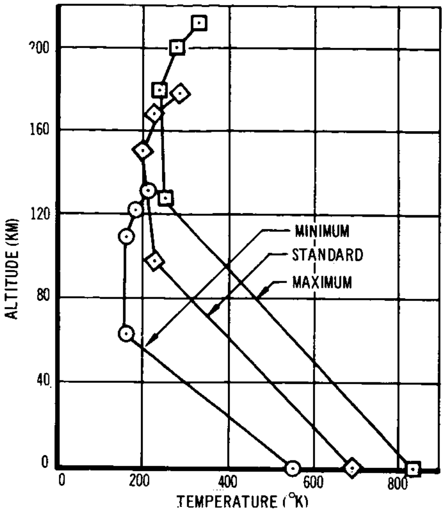

FIGURE 12–3.—Temperature as a function of height, model atmospheres of Venus. (After ref. 121.)

The graphs of temperature as a function of pressure, and temperature as a function of height shown in figures 12–2 and 12–3, respectively, correspond to table 12–2.

TEMPERATURE-PRESSURE RELATIONSHIPS

Sagan (ref. 86), taking a dark-side cloudtop pressure of 90 millibars and temperature of 234° K, calculated the structure of the lower atmosphere for several lapse rates. With the actual lapse rate of $1/\eta$ times the adiabatic lapse rate, figure 12–4 shows the pressure-temperature curves for $\eta = 1.00$, 1.25, 1.50, 1.75, and 2.00.

FIGURE 12–4.—Structure of lower atmosphere of Venus for assumed values of subadiabatic index. (After ref. 86.)

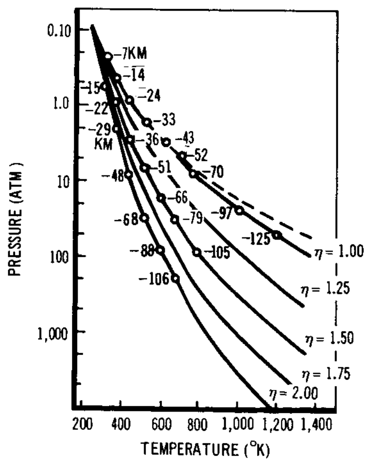

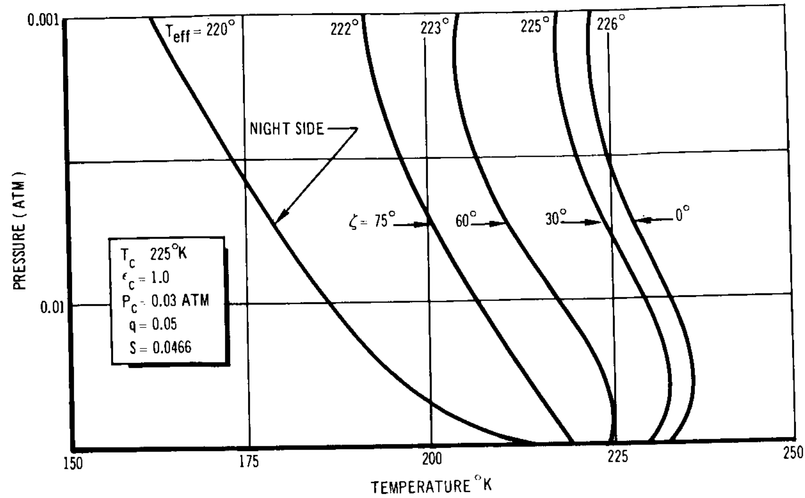

FIGURE 12–5.—Radiative equilibrium temperature distribution in atmosphere of Venus, I. (After ref. 127. Effects of various solar zenith angles.)

T_c	atmospheric temperature at cloudtop level
ξ	solar zenith angle
P_c	pressure at cloudtop level
q	carbon dioxide volume concentration
ϵ_c	spectral emissivity of cloud surface at cloudtop level
S	solar constant in W cm^{-2}

The numbered points on the curves show distances below the cloudtop in kilometers. No lower limit is assumed; a vertical line through the adopted surface temperature will yield surface pressure and cloudtop height. Thus, if the surface temperature is 600° K and the lapse rate is adiabatic ($\eta = 1$), the cloudtop height is approximately 40 kilometers and the surface pressure is approximately 2.5 atmospheres. Higher surface temperature or a subadiabatic lapse rate would lead to a thicker subcloudtop layer and a greater surface pressure.

The variation of temperature with pressure in the layer above the cloudtop has been studied in detail by Hanel and Bartko (ref. 127), who assumed radiative equilibrium. Solar heating can cause a difference of about 30° between day and night at some small distance above the cloud layer (as shown in fig. 12–5), although the temperature of the cloud itself is known to change only a few degrees. In this and the following figures, T is the atmospheric temperature, ζ the solar zenith angle, P the pressure, q the carbon dioxide volume concentration, ϵ the spectral emissivity of the cloud surface, and S the solar constant in W cm^{-2}. The subscript c

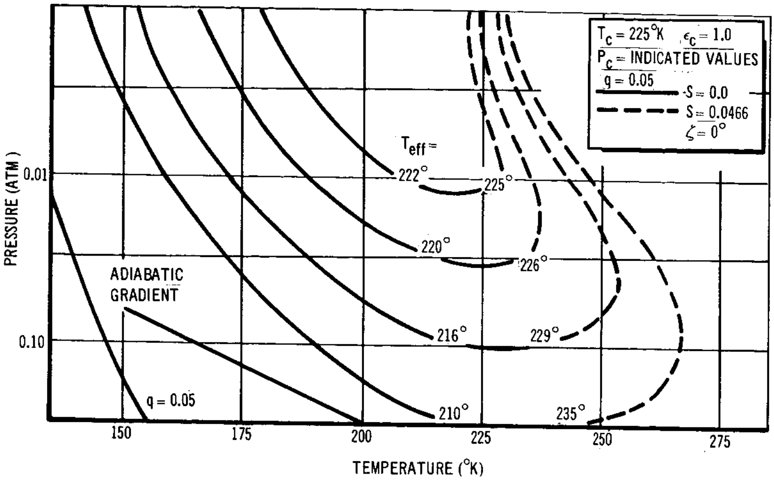

FIGURE 12–6.—Radiative equilibrium temperature distribution in atmosphere of Venus, II. (After ref. 127. Function of cloudtop pressure level for dark and sunlit hemispheres.)

T_c	atmospheric temperature at cloudtop level
P_c	pressure at cloudtop level
q	carbon dioxide volume concentration
ϵ_c	spectral emissivity of cloud surface at cloudtop level
S	solar constant in W cm^{-2}
ξ	solar zenith angle

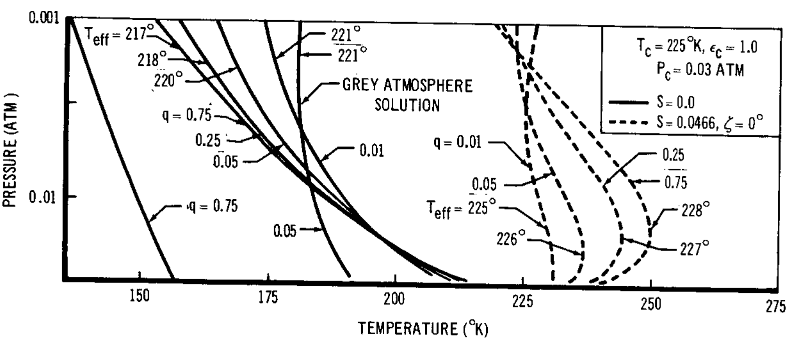

FIGURE 12–7.—Radiative equilibrium temperature distribution in atmosphere of Venus, III. (After ref. 127. Effects of various carbon dioxide concentrations for dark and sunlit hemispheres.)

T_c	atmospheric temperature at cloudtop level
P_c	pressure at cloudtop level
S	solar constant in W cm^{-2}
ξ	solar zenith angle
q	carbon dioxide volume concentration

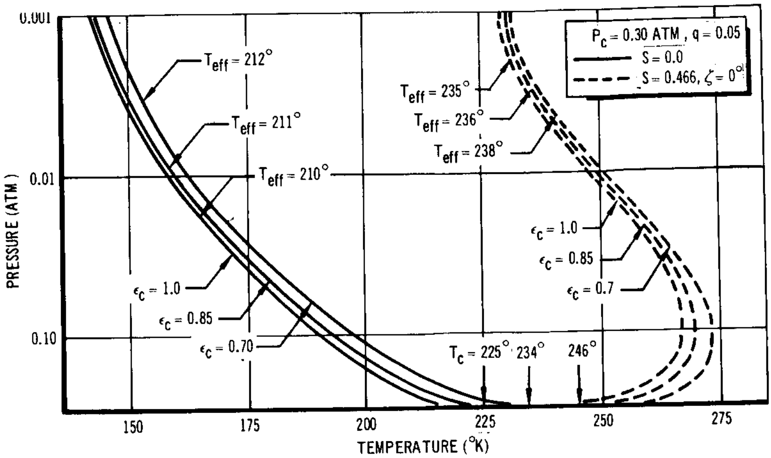

FIGURE 12–8.—Radiative equilibrium temperature distribution in atmosphere of Venus, IV. (After ref. 127. Effect of cloudtop emissivity and temperature for an almost constant net flux, for dark and sunlit hemispheres.)

T_c	atmospheric temperature at cloudtop level
P_c	pressure at cloudtop level
q	carbon dioxide volume concentration
ϵ_c	spectral emissivity of cloud surface at cloudtop level
S	solar constant in W cm^{-2}

indicates cloudtop level. The temperature distribution for various cloudtop pressures is shown in figure 12–6. This model exhibits a discontinuity at the cloudtop and superadiabatic gradients just above the cloudtop; these discrepancies could be eliminated by more elaborate computation. Carbon dioxide clouds could not occur unless the actual temperature curve approached the carbon dioxide condensation curve shown in figure 12–6. The effect of concentrations of carbon dioxide from 5 to 75 percent is shown in figure 12–7. On the dark side, little effect occurs in the lower levels. The effect of varying emissivity of the cloudtop is shown in figure 12–8.

13

Atmospheric Circulation

THE CIRCULATION OF THE ATMOSPHERE of Venus, which is not directly observable, must be inferred from theoretical principles and observations of other properties. The planet's cloud layer implies a circulation of some vigor, because there must be a mechanism for suspending cloud particles, whatever they may be, against the force of gravity. Furthermore, the strong differential heating that the atmosphere of Venus receives from the Sun must create some sort of planetary circulation. The nature of the circulation, however, is dependent upon other properties, such as planetary rotation rate, radiative properties of the atmosphere, and composition of clouds. Although it is not possible to describe the general circulation of the atmosphere of Venus with any degree of certainty, it is possible to deduce some necessary features of the circulation corresponding to a given atmospheric model. In many instances, considerations of atmospheric circulation will tend to support or refute a particular model (see ch. 12).

The basic premise of the aeolosphere model of Öpik (ref. 84) is that the high microwave temperatures are the result of wind friction in the dust-laden lower layer of the atmosphere. Appreciable wind speed (for example, 10 m sec^{-1}) is necessary to raise such quantities of dust to a height of 20 to 30 kilometers, to keep the dust suspended, and to provide frictional heating to maintain the high temperature. The dust particles, however, could produce nonthermal emissions according to the mechanism proposed by Tolbert and Straiton (ref. 88). This "cool" model might require less suspended dust and, consequently, a less vigorous circulation. In any case, the momentum must be imparted to the aeolosphere by the wind above the visible cloud; this wind, in turn, would be driven by differential heating from solar radiation.

In addition to the problem of whether thin air aloft could drive the massive aeolosphere, there is the more fundamental question of whether differential heating at the visible cloud surface is sufficient to produce a strong enough upper-level circulation. The similarity of the temperatures on the bright and dark sides of the visible surface suggests that differential heating is not sufficient but has its effect (such as microwave emissions) at some lower level that is substantially warmer on the bright side than on the dark side, and that the resulting vigorous circulation tends to equalize the temperature around the planet at the visible surface.

The greenhouse model is more widely accepted than the aeolosphere model, and its atmospheric circulation requirements are less severe. The greenhouse model (assuming water clouds) requires sufficient convection to maintain a permanent cloud cover, but not enough convection to dissipate high surface temperatures through vertical transport of heat. Mintz (refs. 123 and 128) stressed the latter requirement in his rejection of the greenhouse theory. He felt that small-scale vertical convection and the planetary meridional circulation would place a limit much less than 300° K on the greenhouse effect. Sagan (ref. 83), on the other hand, stated that most of the solar radiation absorbed by Venus heats the massive atmosphere; therefore, convection would be weaker than on Earth, and surface winds should be mild breezes.

If the clouds of Venus are like terrestrial convective clouds, they should be discontinuous. There is inconclusive evidence from Earth-based observations that breaks do occur, perhaps over less than 10 percent of the surface. Mariner II, however, performed several scans in two infrared frequencies, and, according to Sonett (ref. 129), discovered no breaks within the limits of the experiment. Sonett concludes that heat must be transported in an efficient manner from the sunlit hemisphere to the dark side without an obvious pattern of convection at the uppermost cloud level.

Any theoretical study of the atmospheric circulation of Venus must take into account the planet's peculiar rotation (see ch. 4). It was once thought that Venus was nearly in synchronous rotation, but recent observations indicate retrograde rotation about an axis inclined approximately 87° from the plane of the orbit, with a sidereal period of 247 ± 5 days. In either case, the Rossby number for Venus is so large that the Coriolis force can be neglected for most purposes when the dynamics of the atmosphere of Venus are considered. The solar heating function, however, is more complicated because, as figure 13–1 shows, any given point on the surface of Venus has nearly 60 terrestrial days of continuous illumination and an equivalent period of darkness.

Since this period is long compared with the characteristic duration of terrestrial synoptic disturbances, a first approximation might consider Venus to be in synchronous rotation with a particular hemisphere continuously heated by the Sun. Such studies have been made by Mintz (ref. 130) and Mahoney (ref. 131).

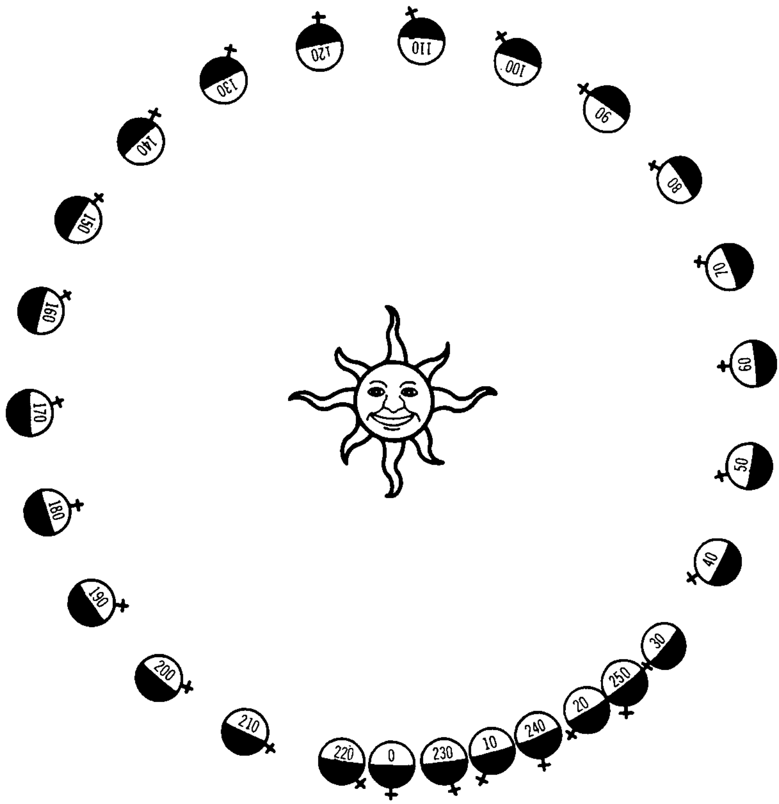

FIGURE 13–1.—Consequences of retrograde rotation of Venus. (The orbital position of the planet is shown at 10-day intervals from 0 to 250 days. The position of the point on the surface that was the antisolar point at day zero is indicated by a cross.)

Mahoney, using a specified temperature distribution (but with too low a surface temperature) and steady-state equations of motion, showed an inflow toward the subsolar point below 10 kilometers with maximum speed on the order of 35 m sec^{-1} and an outflow of equal strength above 10 kilometers. The vertical component of wind was upward throughout the sunlit hemisphere, with a maximum of 10 cm sec^{-1} near 20 kilometers. Advection of the cloud to the dark side was suggested, with the possibility of cloud-free areas on the dark side, though such areas are difficult to reconcile with radiometric temperature measurements that show almost the same temperature in both hemispheres. Mintz showed that, if the greenhouse model prevails and there is high surface pressure, winds are very light (on the order of 0.1 m sec^{-1}).

In an earlier paper, Mintz (ref. 128) considered, in some detail, the atmosphere of a rotating planet. Two regimes are possible, depending on the rate of rotation and the amount of differential heating between equator and pole. The symmetric regime, shown in figure 13–2, is characterized by ascent in all longitudes at the equator, poleward flow aloft, descent at the poles, and equatorward flow near the surface. The flow is symmetric about the poles

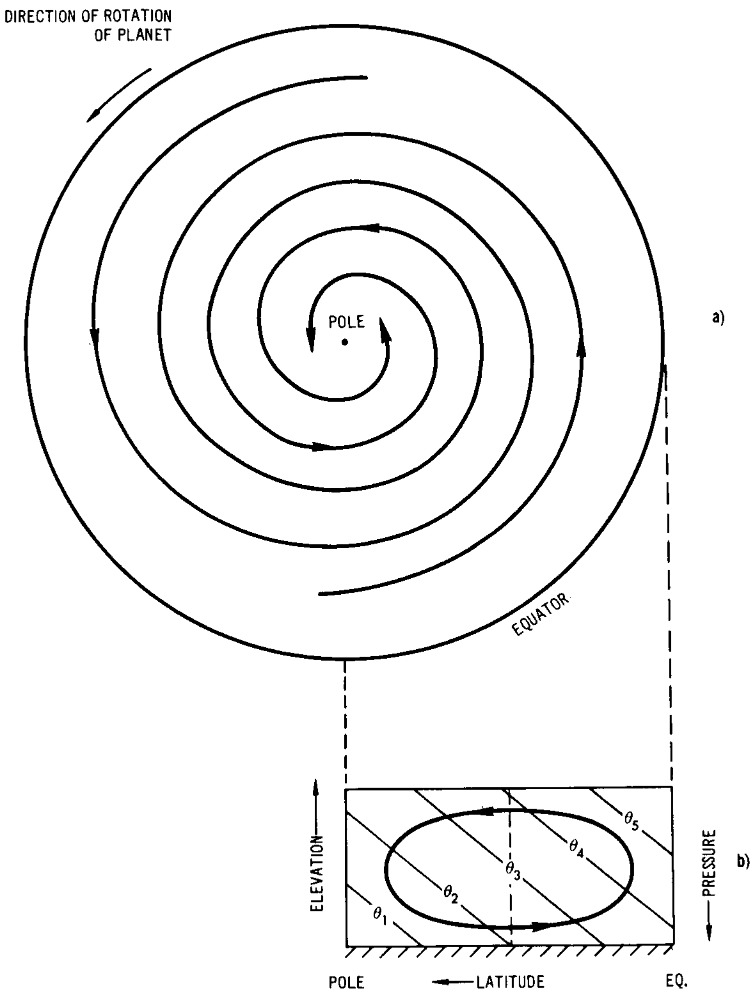

FIGURE 13–2.—Symmetric regime of general circulation. (a) Streamlines of the flow at the upper levels; (b) Cross-section showing the meridional projection of the circulation and isotherms of potential temperature θ. (After ref. 128.)

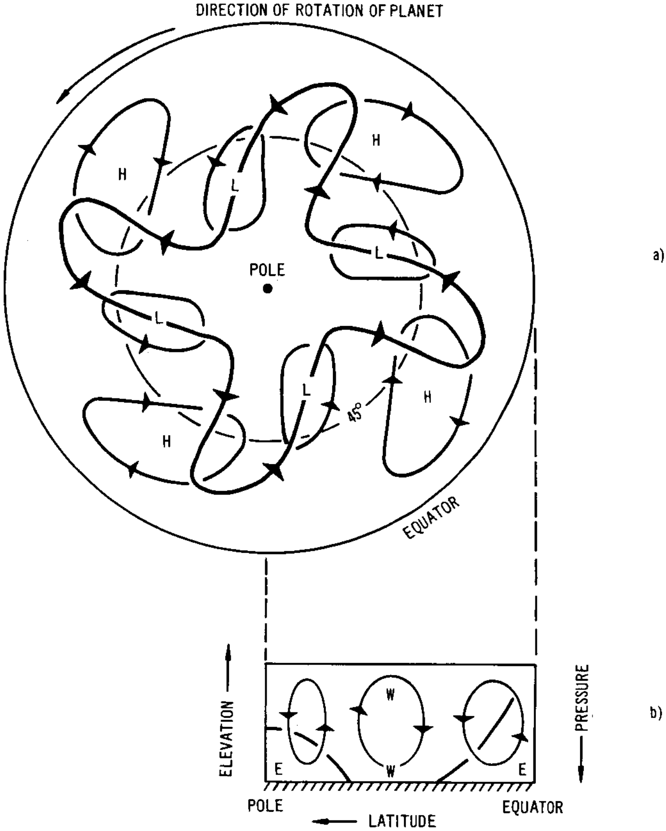

FIGURE 13–3.—Wave regime of general circulation. (a) Streamlines of the flow at the middle and upper levels (heavy line) and near ground (thin line). L=low pressure, H=high pressure; (b) Cross-section showing the zonally averaged meridional circulation, and the zonally-averaged zonal wind, where W=westerly wind, E=easterly wind. (After ref. 128.)

and can produce a net poleward transport of heat only when the lapse rate is subadiabatic.

The wave regime, illustrated in figure 13–3, is characterized by horizontal waves of large amplitude in the middle and upper levels and large eddies in the lower levels. Heat is transported poleward by the action of tongues of warm air extending away from the equator and tongues of cold air extending away from the poles. The study of the dynamic stability of the flow shows that the wave regime is characteristic of large meridional temperature gradients and fast rotation. For extremely slow rotation, where the geostrophic approximation is not valid, the analysis by Mintz is not quite applicable; however, it is reasonable that some variation of the symmetric regime prevails on Venus.

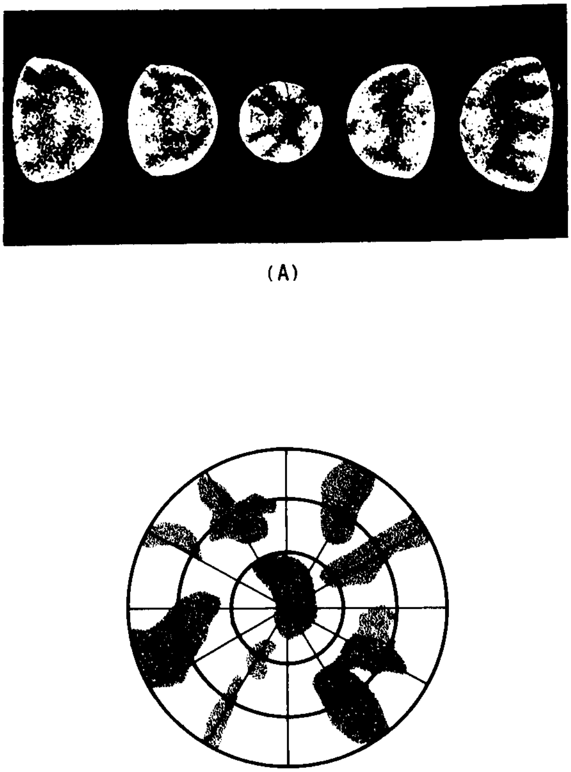

(A)

(B)

FIGURE 13–4.—Composite map centered on the subpolar point. (A) Composite observations of the visible surface of Venus at different phases. (B) Planisphere. (From ref. 34.)

Mintz (ref. 123) found evidence for a symmetric circulation in some results obtained by Dollfus (ref. 34). By superimposing several images of Venus photographed through a yellow filter, Dollfus found quasi-permanent markings that enabled him to produce a composite map centered on the subsolar point (see fig. 13–4). This suggested a cellular circulation centered on the subsolar point with bands of low-level convergence and rising air separating cells of low-level divergence and subsiding air. Mintz tied his theory to a structure based on a global oil field with relatively low surface temperature and hydrocarbon clouds, but it should be equally applicable to the more likely hot, dry surface with water or ice clouds. At higher levels, Mintz suggested that there is the ordinary type of symmetric flow (symmetric about the poles) in line with straight markings perpendicular to the

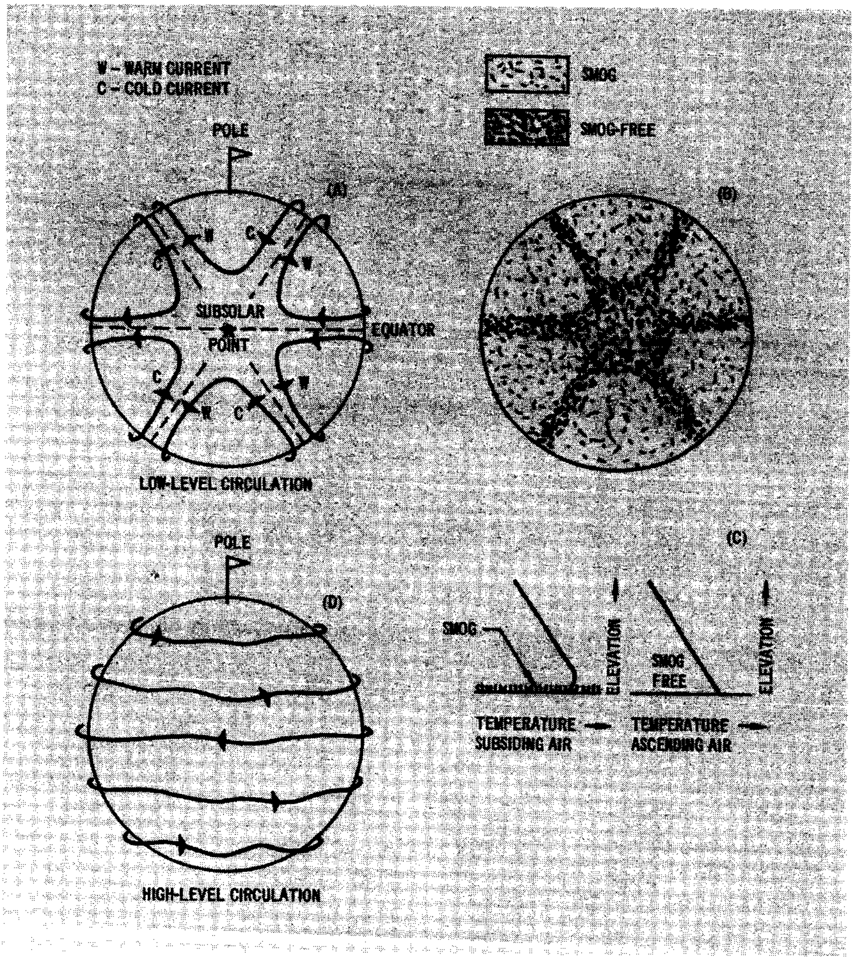

FIGURE 13–5.—Mintz model of the atmospheric circulation of Venus. (A) Low-level cellular circulation; (B) and (C) Distribution of the surface smog; (D) High-level zonal circulation. (After ref. 123.)

terminator, which have been seen by many observers in the ultraviolet. His model is illustrated schematically in figure 13–5. Mintz cautions, however, that such a circulation drifting with the subsolar point over a slowly rotating planet has not been shown to be dynamically possible.

A vertical section from subsolar to antisolar points for circulation symmetric about these points has been given by Sagan and Kellogg (ref. 132). The model shown in figure 13–6 is almost the same as one given by Mintz (ref. 130) differing mainly in its more complicated wind profile. Sagan and Kellogg suggested that

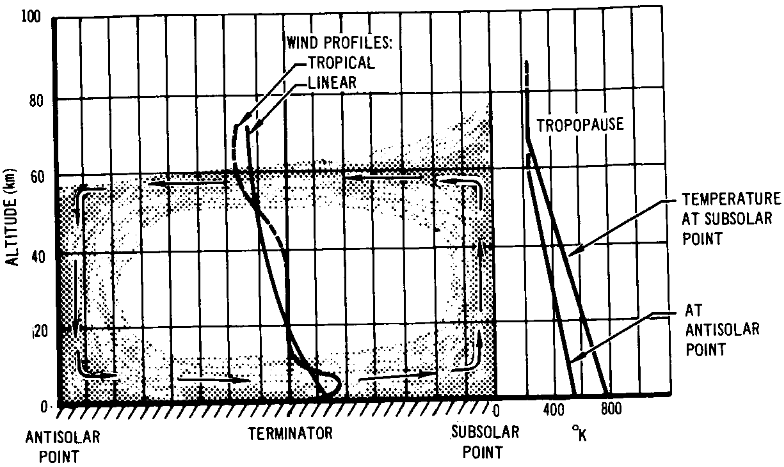

FIGURE 13–6.—Suggested circulation in the atmosphere of Venus. (After ref. 132, modified from ref. 130.)

the column of rising air could lift enough dust (which would then be spread into the dark hemisphere by the outflowing air) to produce a thin layer covering the planet. This dust layer would be the visible clouds.

14

Clouds

APPEARANCE

THE SURFACE FEATURES OF VENUS are obscured by an opaque cloudy mask that appears light yellow. Generally, Venus is featureless when viewed or photographed in near-infrared or red light, but in the shorter wavelengths, markings that apparently represent a cloud cover become visible. Large, diffuse, and more or less parallel bands are nearly always found in photographs taken in ultraviolet light. The bands are usually parallel to the equator (perpendicular to the line that joins the cusps) and favor the equatorial regions. These shadow bands, as they are sometimes called, indicate the existence of active meteorological processes on the planet, because they rapidly and frequently change shape. Such changes may occur within 24 hours; at other times, only slight change is observed from one day (Earth day) to the next.

Certain low-contrast markings, seen primarily in yellow light, appear to be quasi-permanent. It has been thought these features indicate that the surface of the planet occasionally becomes visible; however, it is more likely the markings are caused by clouds associated either with some surface anomaly (clouds on Earth are frequently rooted to mountain chains), or they are caused by diurnal heating effects. The former interpretation is supported by radar evidence of particularly rough areas on the planet that could be interpreted as mountains (see ch. 17). Bright clouds are often seen near the cusp of the planet (refs. 34, 9, 7, and 133).

Visual dichotomy or half phase occurs later than the theoretical time of occurrence when Venus approaches Earth and earlier when it moves away from Earth. The difference between theoretical and visual dichotomy ranges between about 4 and 12 days, and therefore the phase angle discrepancy is about 4° to 5°. Edson (ref. 134) has discussed this phenomenon and suggested several possible explanations including the effect of possible differences between the cusps and the midpoint of the terminator in the effective depth to which one may observe the scattering layer, or the possibility that the opaque cloud deck has a downward slope of about 5° from the center of the disk toward the cusps. In the latter case, the altitude of the cloud summit would decrease about 40 kilometers in this distance and in view of the essentially constant radiometric temperature of the cloud, this explanation seems unlikely.

STRUCTURE

The true structure and chemical composition of the clouds of Venus are subjects of conjecture and are related to the overall structure of the atmosphere (see ch. 12). Attempts have even been made to develop a case for a semi-infinite atmosphere in which no clouds are present, and the high albedo of the planet is accounted for by molecular scattering.

The photographic evidence is more easily interpreted if it is assumed that there are multiple cloud layers in the atmosphere of Venus. This assumption is supported by Kaplan's analysis of the infrared (IR) spectrum of Venus (ref. 126). Mintz (ref. 123) interpreted photographs of Venus taken in different light wavelengths as indicating two different types of planetary circulation. This interpretation also suggests these are low and high cloud layers (see ch. 13).

In this discussion, the word cloud denotes a region in the atmosphere in which there is a higher than average concentration of particulate matter. To present the data on the clouds of Venus with reasonable clarity, it is assumed in the following discussion that there is more than one cloud layer; since this may not be true, however, the data discussed may refer to a single cloud layer or to a cloudless atmosphere, although the latter condition is unlikely. The division of the clouds by location in the atmosphere is, of course, speculative.

STRATOSPHERIC CLOUD LAYER

Photographic evidence of features shown in ultraviolet light is often interpreted to indicate that a relatively thin, nonuniform cloud layer exists in the upper atmosphere. The opacity of this layer to ultraviolet light varies, but the layer is essentially transparent to visible and near-infrared solar radiation. Therefore, the structure of this cloud can be observed in ultraviolet light, but solar emissions of longer wavelengths pass through it and are reflected from a featureless lower cloud layer. The clouds that appear darkest in ultraviolet light should be the highest in the atmosphere if the cloud particles absorb radiation and the atmospheric molecules do not, as is often assumed (ref. 112). The uniform planetary emission in the 8- to 13-micron region of infrared radiation may or may not be associated with this upper cloud layer. Thus, the upper cloud layer may be at a level where the temperature is approximately 235° K, or it may be higher in the atmosphere. Commonly, it is believed that the 8- to 13-micron infrared emissions, used to establish the 235° K cloud summit temperature, are not associated with the uppermost cloud layer but arise from a lower cloud system (ref. 83). A single cloud layer, however, could possibly satisfy all observational requirements (ref. 86).

Various substances, from water to organic materials, have been suggested as the material that composes the clouds seen in ultraviolet light. Colored materials have often been suggested to explain the yellow coloration of the planet, but it has been argued that these are not required because Rayleigh scattering in a thick, molecular atmosphere above a white cloud will result in yellow tinting of the reflected light (see ch. 10). By analogy with Earth, it is reasonable to assume that if the clouds seen in ultraviolet light are a stratospheric phenomenon, they are either sulfur-bearing (ref. 135) or aqueous (similar to noctilucent clouds). Suggested compositions other than water of the upper cloud layer of Venus are listed in table 14–1 (refs. 83, 87, 112, 136, 137).

TABLE 14–1.—*Suggested Composition (Other Than Water) of Upper Cloud Layer of Venus*

Author	Substance	Comment
Dauvillier (ref. 136)	Ammonium nitride	Reaction assumed to occur in lightning discharges on planet.
Robbins (ref. 137)	Hydrocarbonamide type polymers	Reaction occurring with solar hydrogen.
Harteck and Groth, discussed by Harteck et al. (ref. 87)	Carbon suboxide	Later, Harteck et al. (ref. (87) cast doubt on this.
Wildt, discussed by Kuiper (ref. 112)	Formaldehyde	Proposed by Wildt in 1937 but rejected in 1942 for lack of evidence for CH_2O.
Heyden et al., discussed by Sagan (ref. 83)	Nitrogen dioxide	

UPPER TROPOSPHERIC CLOUDS

This discussion assumes that a separate stratospheric cloud is responsible for ultraviolet markings on Venus; a lower cloud, then, gives rise to the 8- to 13-micron emissions. If interpreted as arising from blackbody radiators, these emissions indicate a cloud-summit temperature near 235° K (ref. 119). Goody (ref. 138) and Chamberlain (ref. 139) have proposed gray-body corrections that suggest that the true temperature is approximately 255° K. The summit temperature is remarkably constant on both the sunlit and dark hemispheres. Infrared limb darkening indicates that an essentially isothermal region exists above the cloud summit (King, quoted by Sagan, ref. 86). This suggests that the cloud summit is near the tropopause.

Sinton (ref. 140) attempted to measure emissions from the dark side of Venus at 3.5 and 3.75 microns. In this region, water and carbon dioxide do not absorb radiation. Although the instrumentation was sensitive to energy equivalent to a blackbody of 230° K, Sinton was unable to detect emission from the dark side of Venus. He concluded that a cloud layer blocked ground emission in the 3- to 4-micron region and that the layer was continuous, with less than 0.1 percent gap; otherwise, emissions from the hot, lower surface would have been detected. He suggested that the absorbing layer was at a level where 8- to 13-micron emissions indicate a temperature of about 235° K. Mariner II data also suggest that the cloud layer at 235° K is essentially uniform and continuous (ref. 141).

Detailed mapping of Venus in the infrared radiation region between 8 and 14 microns with the 200-inch Hale telescope has recently revealed general bilateral symmetry and small asymmetries and anomalies, particularly near the southern cusp. Day-to-day differences were noticeable. The highest brightness temperatures were found at the antisolar point (see fig. 14–1; and refs. 142 and 143). These infrared data indicate there is a restless atmosphere with some anomaly near the southern pole; the data are consistent with visual data reported by Ross (ref. 97).

By extrapolation of occultation data, Sagan (ref. 86) has concluded that the most probable pressure at the summit of the cloud on the dark side is approximately 90 millibars, with an uncertainty of at least a factor of 3. His best estimate for the cloudtop pressure on the sunlit side, which was derived from infrared data, is 600 millibars. Dollfus (ref. 94) interpreted polarimeter data as indicating the cloudtop pressure in the sunlit hemisphere is 90 millibars.

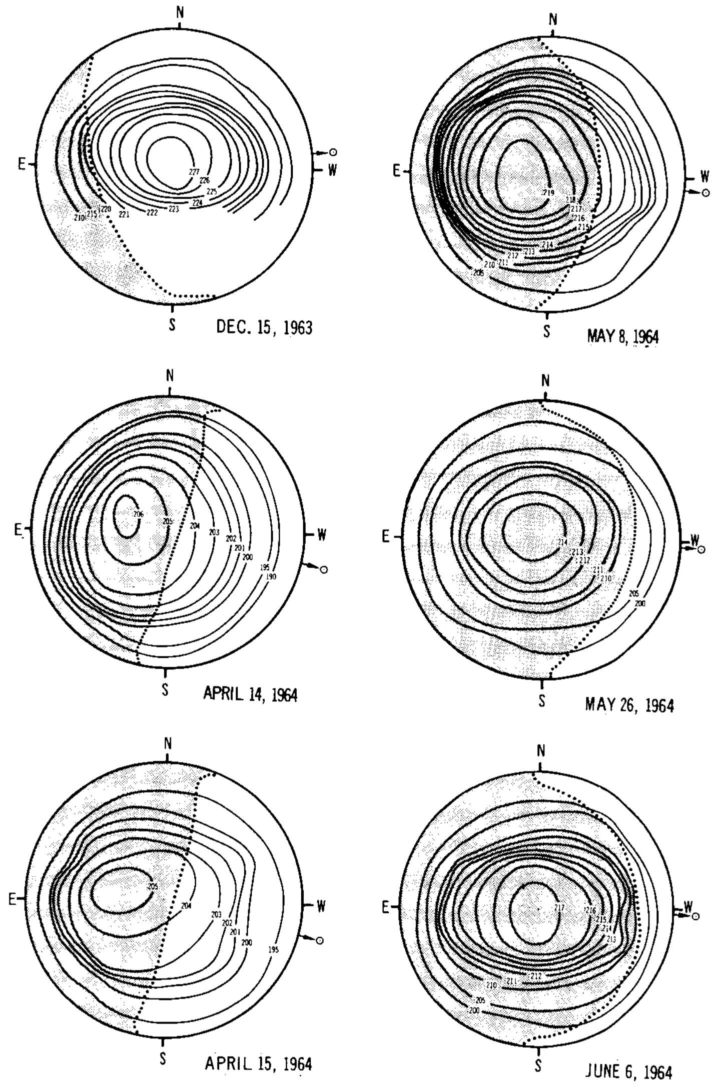

FIGURE 14–1.—Brightness contour maps of Venus. (Ref. 142.)

The cloud is variously described as a thick, precipitating, aqueous cloud (ref. 60) ; a reasonably thick cloud of unspecified composition (ref. 86) ; a thin hydrocarbon droplet cloud lying near the surface (ref. 123) ; and a dust cloud (ref. 84). (The possibility of hydrocarbon and dust-cloud layers is discussed in the next section of this chapter.) The more recent data on Venus suggest that the major reflecting surface is a water cloud with a summit temperature of approximately 235° K (blackbody equivalent temperature). This hypothesis is supported by the reflection spectrum of Venus (fig. 14–2) obtained by Bottema et al. (ref. 104) with balloon-borne spectroscopy, the evidence of water vapor on Venus obtained by Bottema et al. (ref. 107), and the geological expectation of large amounts of water. The polarization curve of Venus (fig. 10–4) obtained by Lyot and discussed by Dollfus (ref. 94) is duplicated roughly by small water droplets; however, other materials also provide agreement.

Barrett and Staelin (ref. 62) tend to favor a water cloud on the basis of analysis of microwave spectral data. However, Spinrad (ref. 124) searched for water vapor by a Doppler-shift method using water lines near λ 8180 Å and was unable to detect it to a pressure of 8 atmospheres. He deduced pressures from carbon dioxide rotational spectra at λ 7820 Å. Chamberlain (ref. 139) suggests that, because of multiple scattering effects on the absorption line spectra, Spinrad's measurements should correspond to a pressure of approximately 4 atmospheres. Chamberlain concludes that there is not enough water vapor to permit condensation of water droplets or ice crystals at cloud-summit temperatures and pressures estimated from infrared data, although he believes serious errors of interpretation or measurement may have been made in arriving at these estimates.

Deirmendjian (ref. 60) questions Spinrad's results because scattering was not considered. Deirmendjian postulates a thick,

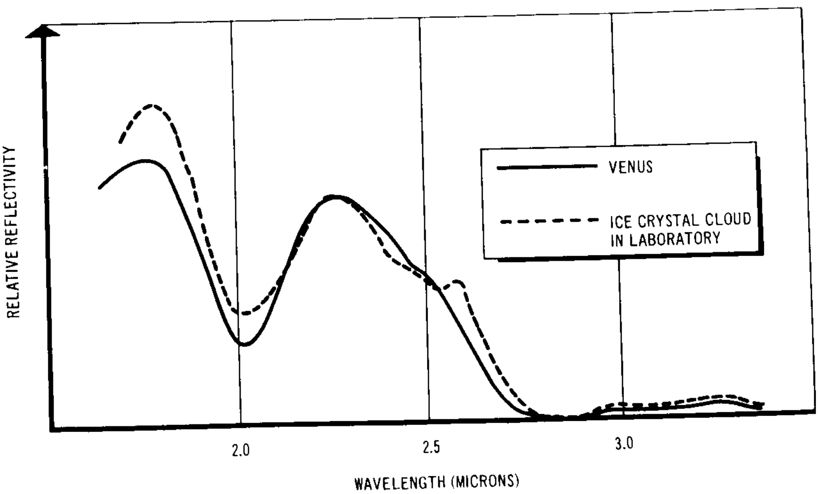

FIGURE 14–2.—Reflection spectrum of Venus clouds observed from high-altitude balloon. (After ref. 104.)

opaque, precipitating aqueous cloud deck to explain the spectrum of microwave emissions. A 10-kilometer-thick cloud of water drops with 100 drops cm^{-3} and 0.5 kilometer of rain appears to provide attenuation to reasonably fit microwave data from Venus to a blackbody at 600° K. Such a cloud would be similar to some occurring on Earth, and electrical discharges within the cloud could contribute nonthermal energy in the microwave frequencies. If so, the planetary surface temperature may be lower than it is now assumed to be (see ch. 9).

LOWER TROPOSPHERIC CLOUDS

It is generally believed that the main cloud system is high in the troposphere, but the presence of a lower cloud layer has been claimed by Kaplan (ref. 126) on the basis of two separate Boltzmann rotational maxima in the infrared spectrum of Venus. These maxima may be interpreted to indicate the existence of two distinct cloud layers from which the infrared emissions originate. Kaplan suggested that the summit of one cloud layer (the upper tropospheric cloud) is at a level where the temperature is near 235° K and the lower layer is at a level corresponding to approximately 400° K. Various atmospheric models that reject the greenhouse model also predicate a cloud near the surface of the planet. These clouds are considered in the following discussion.

Kaplan's evidence of a cloud layer at approximately 400° K suggests the existence of nonaqueous (hydrocarbon or dust) clouds. If a dust cloud exists, its particles will consist of surface mineral matter (see ch. 17). Because of the high albedo of the planet, either the minerals must be highly reflective or the major reflecting level must be above the dust cloud. Quartz (SiO_2) particles may be sufficiently reflective, and similarities between the polarization of Venus and the polarization of a cloud of quartz particles can be demonstrated (Lyot, discussed by Dollfus, ref. 94). But the consensus opposes the dust-cloud aeolosphere model proposed by Öpik (ref. 84), in which thick dust is carried to a great height in the troposphere. This however, is a situation which could contribute to a nonthermal source for the microwave emissions upon which high planetary temperatures are based (see ch. 9).

The oil, or smog, cloud hypothesis of Hoyle (ref. 144) and Mintz (ref. 123) has found little acceptance as an explanation of the major reflecting surface; however, Kaplan (ref. 126) interprets his data to support a low-level, hot hydrocarbon cloud, which he feels is necessary to complete the atmospheric greenhouse effect.

TABLE 14–2.—*Venus Cloud Models*

Authority	Source of data	Structure	Layer I	Layer II	Atmospheric model
Sagan (ref. 86)	Interpretation of large quantities of data	Single layer	Temp. = 234° K Pressure $\simeq$ 0.6 atm, Height = 80 km } bright side Pressure = 90 mb {+180, −60 mb} dark side Height = 80 km	Higher clouds possible, but not necessary	Greenhouse
Bottema et al. (ref. 104)	Comparison of laboratory and planetary reflectance data	....	....	Ice crystals	....
Kaplan (ref. 126)	Infrared rotational temperatures from spectrogram analysis	Multiple layers	Temp. = 220° K 2- to 3-km-deep minimum	Temp. = 400° K organic material to provide C-H bonds to complete greenhouse	Greenhouse
Deirmendjian (ref. 60)	Analysis of microwave data on basis of scattering and absorption in clouds	....	Aqueous clouds, continuous, thick, optically deep; rain topped by cloud drops and ice crystals		Internal heat source, no greenhouse because solar energy cannot reach surface

Öpik (ref. 84)	Analysis of data	Multiple layers	Haze Pressure = 0.08 atm Temp. = 234° K D_{av} of haze = 0.5 μ	Dust of calcium and magnesium carbonates Temp. = 340° K to 570° K Pressure = 0.6 atm Top, D_{av} = 5 μ Bottom, D_{av} = 5 to 10 μ approximately 200 particles cm^{-3}	Aeolosphere, where wind and particle friction causes high surface temperature
Chase et al. (ref. 141)	Mariner II radiometric data	Continuous cover			
Mintz (ref. 123)	Analysis of thermal and dynamic properties; rejects high surface temperature	Low-level haze	Hydrocarbon smog		Universal ocean theory
Hoyle (ref. 144)		Low-level haze	Hydrocarbon smog		
Menzel and Whipple (ref. 145)	General analysis	Cumuliform aqueous clouds			
Barrett and Staelin (ref. 62)	Analysis of microwave data	Complex	Not specified		

SUMMARY

Table 14–2 summarizes various cloud models (ref. 145). The composition and nature of the cloud system of Venus are conjectural. Barrett and Staelin (ref. 62), who computed microwave spectra corresponding to a variety of simple cloud models, conclude that no single model, of those tested, could adequately explain observations; therefore, they tend to favor a complex cloud atmosphere, such as that discussed in this chapter. However, they point out that no unique combination is possible until further data are obtained.

15

Ashen Light

VARIOUS OBSERVERS HAVE REPORTED that the dark side of Venus is at times dimly illuminated by what they describe as an "ashen light." Considerable doubt has been expressed as to whether this phenomenon really exists. Explanations, as might be expected, usually draw on apparently similar phenomena for parallels.

In its crescent phase, the moon's dark side is also faintly visible in earth-shine, the sunlight reflected from Earth to the moon. Venus, however, has no known satellite or other nearby body to act as a similar reflector.

The upper atmosphere of Earth continuously exhibits a faint but distinct luminescence called airglow which is caused by the emission of photons during the reradiation of energy involved in photochemical reactions that occur in this region. It is relatively constant in intensity, as distinguished from the highly variable aurora which is associated with the influx of solar particles into the magnetic field of the upper atmosphere. In the past, both these phenomena, airglow and aurora, have been used to explain ashen light. There is no reason to doubt the existence of airglow on Venus. It now appears, however, that Venus has at best a very weak magnetic field, so that it is doubtful whether ashen light can be an auroral phenomenon (ref. 129).

After assessing the results of attempts by many observers to see the ashen light during the 1934 and 1935 inferior conjunctions, Barbier (refs. 146 and 147) concluded that it was not real. Danjon (ref. 148) also rejected the phenomenon, and many observers have been of the opinion that it is either an Earth-atmosphere phenomenon or an instrument aberration.

More recently, however, Kozyrev (ref. 149), through use of a 50-inch reflector at the Crimean Observatory, and Newkirk (ref. 150) through use of a low-dispersion, high-speed instrument, obtained marginal spectrograms of the night side of Venus in which emission lines of N^{+}_{2} were tentatively identified. Warner (ref. 151) further analyzed the data published by Kozyrev and found evidence of oxygen in the spectra. Kozyrev used an observing system considerably larger than those used by the observers who had rejected the reality of ashen light. The absence from his data of the prominent oxygen line at 5577 Å, found in terrestrial airglow, supports the interpretation that the spectra represent light from Venus and not simply terrestrial airglow.

The energies in the spectra obtained by Kozyrev and Newkirk indicated that the nightglow of Venus was approximately 50 (Kozyrev) to 80 (Newkirk) times brighter than terrestrial airglow. If the light were caused solely by photochemical reactions in the upper atmosphere, a well-developed ionosphere would be indicated. This would agree with ionospheric explanations for the microwave emission from the planet. However, as a result of observations of limb-darkening effects by Mariner II (ref. 73), the ionospheric model is no longer tenable as an explanation of that microwave emission. Further, both radar observations and calculations based on photochemical equilibrium (ref. 117) indicate that Venus has an ionosphere no more dense than that of Earth. Thus, it is doubtful that the energies observed radiating from the dark side of Venus could be solely an ionospheric phenomenon.

Other unlikely mechanisms have been proposed to explain the ashen light including earthshine and the incandescent glow of meteors entering the atmosphere of Venus. Weinberg and Newkirk (ref. 152) were unable to identify any emission lines on 20 spectrograms taken of the unilluminated portion of Venus in 1959. But their failure in 1959 and Newkirk's success in 1958 are consistent with independent visual searches during these two periods.

However, Weinberg and Newkirk are not convinced of the reality of the ashen light phenomenon and, at present, it must be concluded that there is neither a satisfactory explanation nor definite proof of its existence.

16

Mariner II Mission

IN 1961, NASA WAS PLANNING two interplanetary missions, Mariner A and Mariner B, both to be launched by an Atlas booster and a Centaur second stage which was then under development. The Mariner program had two targets: Mariner A was to travel to Venus, and Mariner B was scheduled for Mars. The Jet Propulsion Laboratory (JPL) of the California Institute of Technology (CIT) was given the management responsibility for both programs by NASA. The 1000- to 1250-pound space vehicles were to be launched at appropriate times during 1962 through 1967. However, by late summer of 1961, it became evident that the Centaur second stage would not be available to launch Mariner A in time for the 1962 inferior conjunction of Venus. JPL advised NASA that a lightweight ($\sim$460 lb) hybrid spacecraft, combining features of Ranger III (a lunar spacecraft) and Mariner A, could be sent to Venus in 1962 using an Atlas/Agena-B launch vehicle. As a result, Mariner A was cancelled and JPL was assigned the management of the Mariner B project in which two spacecraft (Mariner I and II) were to encounter Venus during the 1962 inferior conjunction. Scientists and engineers had approximately 11 months to design, develop, assemble, test, and launch Mariner I and Mariner II. The stringent schedule was met and the program was climaxed by the successful flight of Mariner II to Venus.

OVERVIEW OF THE MISSION

Mariner II was launched from Cape Canaveral, Florida, on August 27, 1962. On December 14, 1962, the Mariner II spacecraft at some 36 million miles from Earth, climaxed its 180-million mile, 109-day journey through interplanetary space between Earth and Venus and passed within 21 598 miles of the center of Venus. Scientific and engineering information were radioed to the Goldstone Tracking Station in California. These data were the first ever received from a man-made vehicle in the vicinity of another planet. Figure 16–1 illustrates the trajectory of Mariner II; the spacecraft is shown in figure 16–2.

During the trip, scientific information such as magnetic fields along flight path, positive charged components of the solar winds, microcosmic dust particles, and cosmic rays was monitored continuously and telemetered back to Earth. Additional scientific data on the microwave and infrared electromagnetic radiation emission from Venus were obtained during the 35 minutes of closest encounter with the planet.

The Mariner II project required the launching of a 447-pound spacecraft from Earth (which is moving around the Sun at 66 600 mph) with sufficiently precise aiming so that the spacecraft would intercept Venus (which is moving at 78 300 mph) at a point in space and time some 180.2 million miles and 109 days away with only one opportunity to correct the trajectory by a midcourse maneuver.

The trajectory was chosen to be a near-miss because more data could be gathered that way than by an impact encounter. The space vehicle was to pass between 8000 and 40 000 miles from Venus, with the chance of impact not to exceed 1 in 1000. Mariner II was not sterilized and contamination of Venus might result if a landing were made. At encounter, the spacecraft had to be positioned so that it could simultaneously telemeter data back to Earth, see the Sun with its solar panels, and scan the disk of Venus.

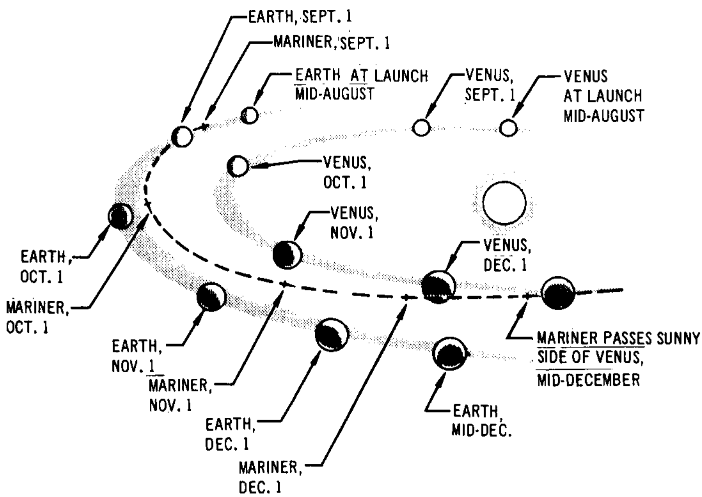

FIGURE 16–1.—Mariner II trajectory.

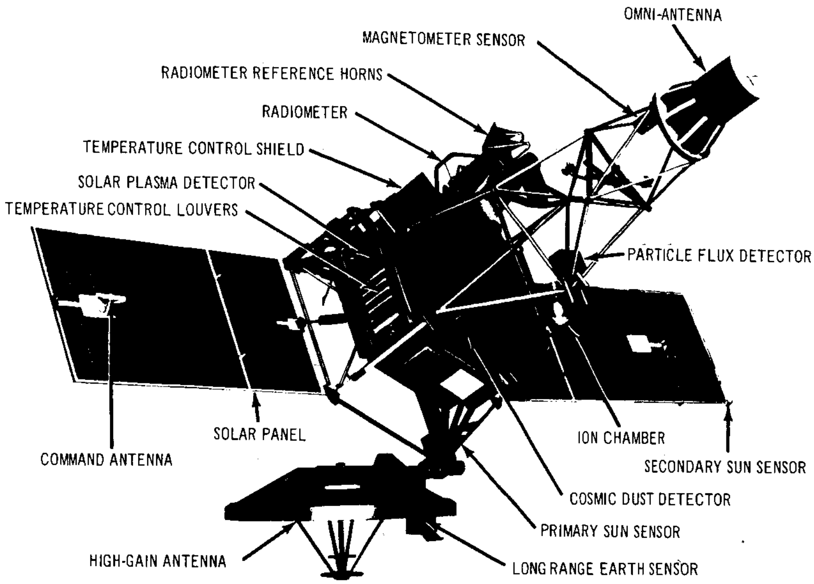

FIGURE 16–2.—Mariner II spacecraft.

ONBOARD EXPERIMENTS AND RESULTS

The following is a brief description of the results derived from each of the experiments.

MICROWAVE RADIOMETER

A microwave radiometer is an instrument that measures electromagnetic radiation fluxes at selected wavelengths. These measurements then can be assigned brightness temperatures by assuming that the radiation is of thermal origin and by adopting the Rayleigh-Jeans Law.

The microwave radiometer aboard Mariner II was designed to scan Venus at wavelengths of 13.5 and 19.0 millimeters. The 13.5-millimeter wavelength corresponds to the center of the main water vapor absorption line in the microwave region, while the 19.0-millimeter wavelength lies on the wing of this line. The absorption of radiation at wavelengths near 13.5 millimeters is mainly caused by the dipole moment of the water vapor molecule.

The 19.0-millimeter wavelength radiation was chosen because it would be substantially unaffected by atmospheric water vapor and would originate deep in the atmosphere, possibly from or near the surface. However, the 13.5-millimeter radiation would be affected by the water vapor in the atmosphere; consequently, it would be some function of the high and low temperatures in the atmosphere. Differences in temperature between the 19.0- and 13.5-millimeter readings would be indicative of the relative amounts of water vapor in the atmosphere.

The microwave experiment was intended to help resolve some of the controversies about the origin and numerical values of the temperatures detected on Venus from Earth-based measurements. Prior to Mariner II, scientists had proposed two main theories for these measurements. The ionospheric model proposed an extensive, hot, highly charged ionosphere; the free/free transitions of electrons in the dense ionosphere were supposed to produce the electro-magnetic radiative fluxes observed. According to the ionospheric theory, as the radiometer scans the planet, a limb brightening should occur since the radiometer would observe more of the ionosphere near the limb than at the center of the disk. On the other hand, the greenhouse theory envisioned a hot surface with a cloudy atmosphere. The atmospheric temperature is supposed to decrease with increasing height above the surface. According to this theory, limb darkening should be observed as the radiometer scans from the center of the disk to the limb, because the cold atmosphere would increasingly contribute to the radiative flux.

The microwave observations made from Mariner II are summarized in tables 16–1 and 16–2 (refs. 153 and 154). Three scans were made during the encounter, the first, up the planet on the dark side; the second, approximately down the terminator (which was near the center of the planet); and the third, up the sunlit side of the planet. The observations showed no significant differences between the light and dark sides of Venus, and higher temperatures were found along the terminator. Since the edges were cooler than the center of the planet, the results indicate a definite limb-darkening effect.

INFRARED RADIOMETER

The selected wavelengths for measurement in the infrared regions were 8.4 and 10.4 microns. Both wavelengths penetrate water vapor but not clouds. The 10-micron region is subject to absorption by carbon dioxide; if there were any cloud breaks, radiation from the 8-micron region would originate at a much lower point in the atmosphere than the 10-micron radiation and, therefore, differences should be observed. At the center of Venus, the radiometer recorded a thicker, hotter part of the cloud layer; while at the limbs, it could not see as deeply, and the colder upper layers were visible. In other words, a definite limb darkening was observed in both wavelengths (8.4 and 10.4 μ) ; the radiation indicated a decrease of approximately 20° K between the central region and the limbs. The central regions were estimated to have been approximately 240° K (−33° C) (ref. 141). Also, the temperatures along the cloud tops were approximately equally distributed, indicating dense clouds opaque to infrared radiation. The temperatures observed by the 8- and 10-micron wavelengths were approximately equal, indicating there was not much carbon dioxide absorption, or that there were no cloud breaks (see ch. 14).

MAGNETOMETER EXPERIMENT

Mariner's magnetometers attempted to verify the existence and the nature of a magnetic field in interplanetary space between Venus and Earth. A relatively quiet magnetic field was found with a strength of less than 10 gamma (1 gamma $= 10^{-5}$ oersted). Fluctuations over periods of 1 second to 1 minute were noted.

During the encounter with Venus, no changes in field strength over that recorded in interplanetary space were apparent. On the basis that Mariner II did not enter the Venus magnetosphere, the upper boundary of the field strength can be estimated (ref. 58) between ½ and ⅙ that of Earth. However, the absence of field fluctuations near Venus may be due to a shell of disordered fields similar to that which has been detected outside the Earth's magnetosphere by satellites and space probes. The field of Venus is lower than that of Earth, probably by a factor of 1/10 to 1/20 (refs. 46 and 58). There was no indication of trapped particles or modification in the flow of solar plasma.

COSMIC-DUST DETECTOR

Analysis of the cosmic-dust detector data indicated that, in the interplanetary space between Earth and Venus, the concentration of microdust particles was 1/10,000 that observed by space probes near Earth. During the mission, the data showed only one dust particle impact, which occurred in deep space and not near Venus. Equivalent experiments near Earth have yielded 3700 such impacts within approximately 500 hours.

SOLAR-PLASMA EXPERIMENT

It has long been believed that a plasma flow, or so-called solar wind, streams from the Sun. A plasma is a gas containing an electrically neutral mixture of ionized atoms (positively charged) and free electrons (negatively charged). Plasma moving at high

TABLE 16-1.—*Mariner II Experiments*

Mission objectives	Experiment	Objectives	Exact quantities measured
To obtain basic data about Venus, in particular, magnetic fields, radiation belts, temperature, composition of clouds, and temperature and conditions on the surface of Venus	Microwave radiometer	Ascertain the origin of high temperatures and details concerning the atmosphere	Measurements of microwave electromagnetic flux at wavelengths 19.0 and 13.5 mm from points on Venus disk and cold space as a reference
	Infrared radiometer	Determine the structure of the cloud layer and temperature distributions at cloud altitudes	Infrared, electromagnetic radiation flux between 8.1 to 8.7 μ and 10.2 to 10.5 μ from points on Venus disk and cold space as a reference. Central wavelengths of bands 8.4 and 10.4 μ; 10.4 is center of CO_2 band
To investigate interplanetary space between Earth and Venus by measuring such phenomena as cosmic dust, positive charged particles coming from the Sun (solar wind), high-energy cosmic rays from outer space, and magnetic fields of interplanetary space	Magnetometer	Measure planetary and interplanetary magnetic fields	Three mutually perpendicular components of magnetic fields along Mariner's interplanetary trajectory
	High-energy radiation experiment ion chamber and matched Geiger-Müller tubes	Measure high-energy cosmic radiation	Measure flux density of protons, helium nuclei, nuclei of heavier atoms, and electrons. Specifically, cosmic rays coming from outside the solar system, solar-flare particles, and particles trapped in radiation belts around Venus
	Cosmic dust detector	Measure flux of cosmic dust	Measure the flux density and approximate direction of high- and low-momentum dust particles
	Solar-plasma spectrometer	Measure the intensity of low-energy positive charged particles from Sun	Measurements of flux density and energy spectrum of positive charged particles of solar wind, between 240 and 8400 eV

TABLE 16–2.—*Summary of Results of Experiments*

Experiment	Results	Implications of observations
Microwave radiometer	First contact made with planet 18:59 Greenwich mean time, December 14, 1962, 35 min encounter. Three scans across planetary disk obtained, represented by 18 digital data points. Telemetered digital data represented by voltages as a function of time. Approximate angular extent of each scan and distance from center of planet at mid-scan. Scan 1 10° 46 800 km Scan 2 15° 44 350 km Scan 3 10° 42 500 km Preliminary estimates of brightness temperatures (After ref. 154): 19 mm channel: Scan 1 460° K±15%; Scan 2 570° K±15%; Scan 3 400° K±15% Final estimates of temperatures (After ref. 73): 19 mm channel: Scan 1 480° K±5% dark side; Scan 2 590° K±5% terminator; Scan 3 460° K±5% sunlit side 13.5 mm channel: Scan 1 393° K±25%; Scan 2 400° K±25%; Scan 3 396° K±25%	(1) No significant differences in microwave temperatures on light and dark side of planet (2) Results suggest a limb-darkening, that is, edges were cooler than center of disk (3) Confirmation of high near-surface or surface temperatures (4) Because of large uncertainty in 13.5-mm data, it is difficult to draw conclusions concerning presence of water vapor, except that very little water vapor appears to be in the atmosphere.
Infrared radiometer	Operation mode similar to microwave radiometer, three scans across planetary disk with 18 data points. Data showed equality between 8- and 10-μ radiation temperatures measured. About 20° K decrease between limbs and center of disk with central radiation temperatures on the order of 240° K. One anomaly on the southern part of the terminator scan which was 10° K cooler than the surrounding layers.	The equality of the 10.4 and 8.4 μ measurement suggests that there was very little CO_2 absorption in the light path. This implies that the measured temperatures were cloud temperatures, that the clouds were thick, and essentially no radiation was transmitted from the surface.

TABLE 16–1.—*Mariner II Experiments*—Concluded

Mode	Description of instrumentation	
Encounter	*Crystal video-type radiometer* Wavelengths, 19 mm, 13.5 mm Frequency,[a] 15.8 GHz, 22.2 GHz Bandwidth, 1.5 GHz, 2.0 GHz Sensitivity, 15° K, 15° K Time constant, 40 sec, 40 sec Beamwidth, $2^\circ.5$, $2^\circ.2$ Weight, 20 lb Average power, 4w Parabolic antenna, 48.5 cm	Angular scan of $123^\circ.5$ extent at 1 deg sec^{-1} or 0.1 deg sec^{-1} rate Radiometer activated 6½ hr before 35-min encounter 23 noise calibrations during 109-day flight to Venus Venus orientated
Encounter	*Infrared radiometer* Wavelengths, 8.4 μ, 10.4 μ Beamwidth, $0^\circ.9 \times 0^\circ.9$ Time constant, 3 sec between 10 and 90% points Temperature limits, 200° K to 600° K Weight, 2.88 lb	Power, 2.4 w Planetary radiation chopped against cold space Infrared radiometer attached to microwave radiometer so mode of operation is the same Venus orientated
Cruise and encounter	*Fluxgate magnetometer* Three mutual perpendicular field components by three magnetic core sensors Sensitivity, 4γ[b] change on any axis Continuous measurements for 129 days. Readings made every 20 sec during encounter	
Cruise and encounter	*High-energy detectors* Ionization chamber—particle energies required >10 MeV protons Geiger-Müller tubes—particle energies required <0.5 MeV electrons Geiger-Müller tubes—particle energies required 40.0 MeV helium nuclei *Low-energy detector* Anton 213 Geiger-Müller tube—particle energies { >40 keV electrons; >0.5 MeV protons } Counting rate continuously monitored	
Cruise	*Sounding board or acoustical detector plate* Size, 55 $in.^2$ Weight, 1.8 lb Power, 0.8 w	1700 hrs of dust data over a 219-day period including postencounter
Cruise	*Positive ion spectrometer* Components: electrostatic deflector plates collector cup electrometer sweep amplifier programer Measures energy fluxes at 10 different energy levels between 240 and 8400 eV Power=1 w	Sun-orientated 104 days of sampling with 40 000 spectra obtained

[a] 1 GHz (gigahertz)=10^9 cycles sec^{-1}.
[b] 1γ (oersted)=10^{-5} gauss.

Magnetometer	During encounter, magnetometer data gave no evidence of a magnetic field different from the average value of the interplanetary magnetic field along the trajectory. Interplanetary field strengths were less than 10γ with 1-sec to 1-min fluctuations.	(1) The magnetic field of Venus does not extend to Mariner II trajectory, for which the minimum distance to the center of Venus was approximately 41 000 km. (2) The results do not mean that Venus has no magnetic field, for the solar wind could confine a weak field to a limited region; results are consistent with the possibility that Venus has no magnetic field.
High-energy experiment	Low-energy experiment: Anton type 213 Geiger-Müller tube. Average counting rate during encounter 1.125 particles sec^{-1}. Background counting rate due to galactic cosmic rays, 0.6 particles sec^{-1}. High-energy experiment: Average proton flux 3 cm^{-2} sec^{-1}. A clear increase in high-energy particles was noted only once, during solar flare on Oct. 23. The Geiger counter flux rose from a background of 3 to a peak of 16 particles cm^{-2} sec^{-1}. No protons found in 10- to 800-MeV range except during solar flare. Protons in range of 0.5 to 10 MeV were not numerous.	(1) No radiation belts around Venus similar to Van Allen radiation belts around Earth. (2) The magnetosphere of Venus, if it exists, does not extend to Mariner II trajectory.
Cosmic dust	Of the 129 days monitored, only one dust particle impact was recorded in deep space and not near Venus. Analyses of some 1700 hrs of cosmic dust detector data seem to indicate that between Earth and Venus the concentration of microdust particles is some 10^4 times less than that observed near Earth.	A very low concentration of dust particles exists between Earth and Venus.
Solar plasma	*Quiet Sun* / *Flare activity* Energies .... few 100 eV / few 1000 eV Velocity of solar winds....... less than 250 Mps / about 500 Mps Electron and proton densities...... 10 to 20 cm^{-3}	(1) Definite confirmation of the existence of plasma streams emitted by the Sun (2) Variation of this solar wind with solar activity.

velocities is capable of carrying lines of magnetic force with it; therefore, corpuscular emission streaming from the Sun would be capable of altering the shape of the Sun's external magnetic field, as well as the size and shape of the magnetic field of a planet.

Mariner II observations confirmed the existence of a continuous flow of plasma from the Sun. The solar wind was observed to move between 200 and 500 miles sec^{-1}. The energies of the particles in the winds were from a few hundred to a few thousand electron volts, with particle densities of approximately 10 to 20 protons and electrons cm^{-3}. The lower values of these quantities are for a relatively inactive Sun, while the upper values correspond to flare activity.

The experiment showed that the plasma velocity undergoes frequent fluctuations apparently associated with flare activity. On 20 occasions, the velocity increased by 20 to 100 percent within a day or two. These fluctuations seem well correlated with magnetic storms observed on Earth.

HIGH-ENERGY RADIATION EXPERIMENT

The high-energy particle detectors aboard Mariner II were designed to detect particles originating from outside the solar system (galactic space), solar-flare particles, and radiation that might be trapped around Venus in belts similar to Earth's radiation belts.

The Anton type 213 Geiger-Müller tube was used to detect low-energy particles. This tube can measure protons with energies greater than 500 kiloelectron volts and electrons with energies greater than 40 kiloelectron volts. This detector continuously monitored the energy particle flux between Earth and Venus during encounter. Little variation in particle flux during the trip was noted and no apparent increase, from magnetically trapped particles or radiation belts, occurred during flyby. The average counting rate was 1.125 particles sec^{-1}. High-energy cosmic rays caused a background rate of 0.6 particle sec^{-1} (ref. 120).

The ionization chamber measurements of high-energy protons (greater than 10 MeV) were rather uniform throughout the flight. The high-energy proton flux was approximately 3 particles cm^{-2} sec^{-1}. On October 23 and 24, 1961, an increase in high-energy particles as a result of solar flare activity was noted.

The accumulated radiation inside the counters was approximately 3 roentgens for the entire 4-month journey; and during the solar storm of October 23, the dosage was approximately $\frac{1}{4}$ roentgen. This amounts to approximately 1/1000 of the usually accepted half-lethal dosage, or that level at which half of the persons exposed would die (ref. 153).

These observations imply that there are no radiation belts around Venus such as the Van Allen radiation belts around Earth. Also, if Venus has a magnetosphere, it did not extend to the Mariner II during encounter.

DETERMINATION OF MASS FROM TRAJECTORY

Detailed analysis of the trajectory of the Mariner II spacecraft has made possible the most precise determination to date of the mass of Venus. The mass of the planet was 0.81585 times that of Earth, or 4.869×10^{27} grams.

17

Surface Properties

SINCE VENUS IS SHROUDED with clouds that are opaque to visible radiation, the surface cannot be seen with ordinary telescopes. Radio telescopes using microwave radiation can penetrate the clouds and atmosphere, and by correctly interpreting active (radar) and passive (radiometry) microwave radiation, knowledge of the surface properties of the planet can be obtained. Calculations of chemical thermodynamic equilibria postulated between the atmosphere and the lithosphere may also provide information concerning surface materials.

TOPOGRAPHY

Estimates of surface relief can be made from knowledge of how microwave radiation is scattered from the planet's surface. The degree of depolarization of polarized radar waves reflected from the surface, the analysis of scattering behavior as a function of angle of incidence, and the polarization of emitted radiation all may be used to gain knowledge of surface characteristics.

For a perfectly reflective surface, implying a perfectly smooth surface, total reflection back to the source occurs at zero angle, and at any other angle of incidence no reflections return to the source. If the surface were rough and diffusely scattering (Lambert surface), the reflection would be proportional to the square of the cosine of the angle of incidence.

Interpretations of scattering laws by Muhleman (ref. 39) and Carpenter (ref. 37), in which the power of the radar return echo is analyzed as a function of angle of incidence, are in agreement that the echo is qualitatively similar to that from the Moon. The backscattering function determined by Carpenter is shown in figure 17–1. In that figure, the higher and lower frequency data refer to Doppler shifts in the continuous-wave radar caused by the rotation of the planet, and the theoretical curve has the same function form as one proposed by Evans and Pettengill (ref. 155) for the Moon. It is given by

$$\sigma(\phi) + \frac{208}{209}e^{-16.5\sin\phi} + \frac{1}{209}\cos^2\phi$$

The backscattering function for Venus has a steep quasi-specular component for incident angles less than 25° and a diffuse component for larger angles. The specular component is more angle-dependent than that of the Moon, which suggests that the surface of Venus is smoother than that of the Moon. On the basis of radar cross-section (reflectivity) data at wavelengths ranging from 12.5 centimeters to 7.84 meters, Evans et al. (ref. 156) have concluded that the surface of Venus is more compacted than that of the Moon and that surface elements about 5 to 50 meters across have a mean slope of about 8°.

James and Ingalls (ref. 157) carried out extensive radar measurements of Venus at 38 megacycles per second (7.84 m) during November and December 1962. Their average value for the radar cross-section was 1.9×10^{13} m^2, or approximately 15 percent of the projected geometrical area. Large variations were observed from day to day as shown in figure 17–2. Variations at shorter wavelengths are not so large as those at 38 megacycles per second. According to James and Ingalls, these variations could possibly be explained as follows:

(1) An ionosphere which in certain regions may become critically dense, perhaps two orders of magnitude greater (2×10^7 electrons cm^{-3}) than the density of Earth's ionosphere.

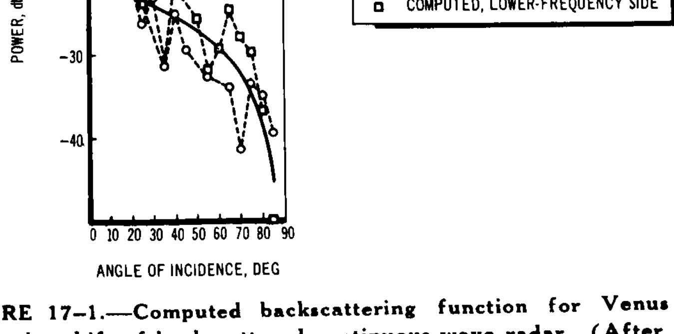

FIGURE 17–1.—Computed backscattering function for Venus based on Doppler shift of backscattered continuous-wave radar. (After ref. 37.)

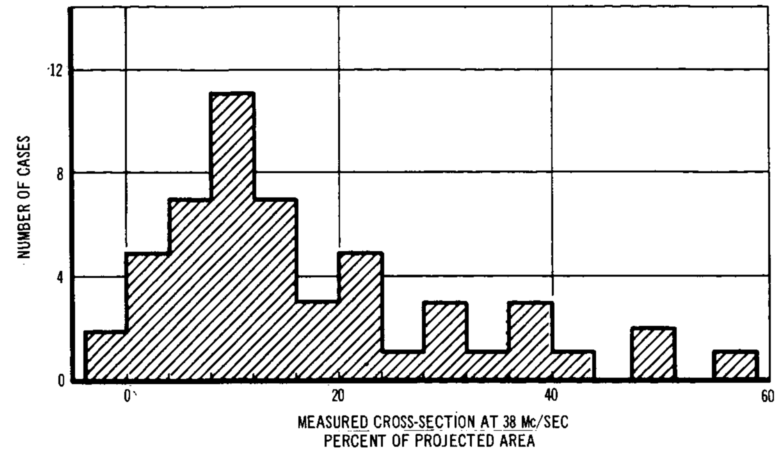

FIGURE 17–2.—Distribution of measured radar cross sections for Venus. (After ref. 157.)

(2) An unusual surface material or feature that is not uniform over the planet, i.e., a layer of material having a larger dielectric constant than the surface. The depth of the top layer would be large compared with 0.68 meter, but small compared with 7.8 meters.

(3) Variation in the effect of solar plasma, which will depend on the intensity of emissions from the Sun during observation and on phase angle.

Barrett and Staelin (ref. 62) have computed the microwave emission of Venus for several model atmospheres. According to their analyses, the absorptivity of the atmosphere of the planet for short wavelengths of microwave radiation is not negligible. They believe absorption of radar signals in the atmosphere of Venus caused the failure of the attempt by Lincoln Laboratory, MIT, to make radar observations at 3.6 centimeters during the inferior conjunction of 1962.

Karp, Morrow, and Smith (ref. 158) of Lincoln Laboratory have since made successful radar observations at the 3.6-centimeter wavelength. They obtained a reflectivity value of 1 percent, which is less than 1/10 that usually obtained at longer wavelengths. They suggested that the low reflectivity resulted from variable absorption in the Venusian atmosphere. On the basis of the X-band (3.5 cm) Doppler spread, they inferred extremely rough surface features of dimensions comparable to the wavelength.

Pollack and Sagan (ref. 61) have attempted to explain variations in reflectivity with wavelength on the basis of either an anomalously opaque cold spot but a very low disk-integrated opacity, or a variation in surface porosity with depth. The shorter radiation would be reflected from near-surface material, with high porosity (approximately 75 percent voids), and the longer radiation would be reflected from deeper surface material having less porosity and therefore a higher dielectric constant. They believe low radar reflectivities at 3.6 centimeters are not the result of general atmospheric absorption.

Goldstein (ref. 159) has interpreted polarized radar spectrograms to indicate that there are at least two particularly rough areas on Venus (see fig. 17–3). The rough areas rotate with the planet and perhaps are indicative of mountainous regions, although this need not be the case, for roughness, as measured by radar, is related to the properties of matter with dimensions approximating the radar wavelength.

SURFACE MATERIALS

The radar cross-section of the planet, a measure of its reflectivity, can provide a clue to the dielectric constant of the surface material. Evans et al. (ref. 156) have noted that radar cross-sections of Venus at wavelengths ranging from 12.5 centimeters (2.4 gigacycles/sec) to 7.84 meters (38.4 Mc/sec) vary only between 10 and 15 percent of the geometric cross-section. They interpret this to exclude reflection from the ionosphere and, consequently, to be indicative of the response of the radiation to surface materials. This low reflectivity rules out the presence of extensive bodies of liquid water at the surface, for the reflectivity

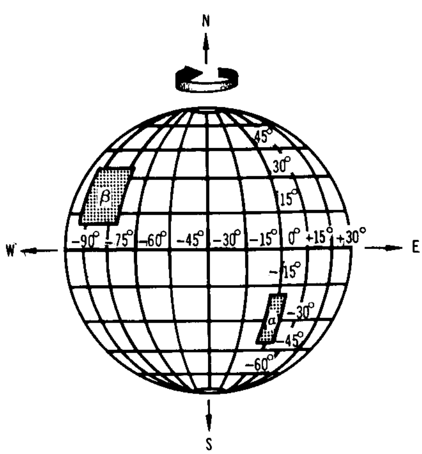

FIGURE 17–3. — Venus-centered coordinate system showing areas of exceptional roughness. Prime meridian was chosen to go through roughest area. (After ref. 159.)

of oceans at microwave frequencies is about 0.5. Pettengill (ref. 160), assuming the conductivity of the surface to be low, has found the dielectric constant of the surface material to be 4.1 (+1.9, −0.9), based on reflectivity of 0.114 (+0.062, −0.035) at a wavelength of 68 centimeters. Using 12.5 centimeter radar, Carpenter (ref. 37) found the dielectric constant to be 3.75 (+0.55, −0.25), based on reflectivity of 0.0975 (+0.026, −0.020).

Dielectric constants in this range are consistent with the interpretation that dry, rocky, or sandy conditions exist at the surface. This is in agreement with the high surface temperatures implied by passive microwave radiometry (see ch. 9). However, oceans of hydrocarbons are not excluded (see ref. 144).

Mueller (ref. 161) has considered a number of possible reactions near, and at the surface of, the planet. On the basis of thermodynamic equilibrium and the assumption of surface temperatures of 700° K, surface partial pressure of carbon dioxide of 10 atmospheres and of water 0.001 atmosphere or less, he concludes that metallic iron, free carbon, and hydrocarbons are not stable on the surface. Also, if there were free silica (quartz) at the surface, magnesite (magnesium carbonate) and dolomite (calcium magnesium carbonate) would be unstable, and no substantial deposits of carbonate sediments should exist. The latter conclusions are based on the failure of the so-called Urey equilibrium (ref. 162):

$$MgCO_3 \text{ (magnesite)} + SiO_2 \text{ (quartz)} \rightleftharpoons MgSiO_3 \text{ (enstatite)} + CO_2 \text{ (carbon dioxide)}$$

$$CaMgC_2O_6 \text{ (dolomite)} + 2\ SiO_2 \text{ (quartz)} \rightleftharpoons CaMgSi_2O_6 \text{ (diopside)} + 2\ CO_2 \text{ (carbon dioxide)}$$

$$CaCO_3 \text{ (calcite)} + SiO_2 \text{ (quartz)} \rightleftharpoons CaSiO_3 \text{ (wollastonite)} + CO_2 \text{ (carbon dioxide)}$$

These reactions are shifted far to the right in the absence of liquid water. The failure of these equilibrium reactions is believed to be the cause of the high carbon dioxide content in the atmosphere of Venus.

If there is little SiO_2 at the surface, calcite, dolomite, and magnesite may be present but are probably well-mixed with silicates. Mueller also concludes, under the conditions assumed for *T* and

$p_{CO}/p_{CO_2} = 0.001$ or less, that mica and phlogopite ($KMg_3AlSi_3O_{10}(OH)_2$) may be stable on Venus and that the reactions

$$2Fe_3O_4 \text{ (magnetite)} + 6MgSiO_3 \text{ (pyroxene)}$$
$$\rightleftarrows 3Fe_2SiO_4 \text{ (olivine)} + 3Mg_2SiO_4 \text{ (olivine)} + 1O_2 \text{ (oxygen)}$$

$$3Fe_2O_3 \text{ (hematite)} \rightleftarrows 2Fe_3O_4 \text{ (magnetite)} + \tfrac{1}{2}O_2 \text{ (oxygen)}$$

may be buffered so that a complex system of iron-bearing materials may be expected.

On the basis of the electromagnetic properties of the planet, the thermal and electrical properties of various materials, and Mueller's chemical equilibria study, Pollack and Sagan (ref. 61) have concluded that possible surface materials are quartz (SiO_2), aluminum oxide (Al_2O_3), wollastonite ($CaSiO_3$), periclase (MgO), enstatite ($MgSiO_3$), and limonite ($2Fe_2O_3 \cdot 3H_2O$). Granite. ferromagnetic materials, and polycyclic aromatic hydrocarbons if present, should be minor constituents.

References

1. NEWCOMB, S.: Tables of the Heliocentric Motion of Venus. Tables of the Four Inner Planets, pt. III. Astronomical Papers Prepared for the Use of The American Ephemeris and Nautical Almanac, vol. 6, 1895, pp. 271–382.
2. DUNCOMBE, R.L.: The Motion of Venus 1750–1949. Astron. J., vol. 61, 1956, pp. 266–268.
3. DUNCOMBE, R.L.: The Motion of Venus 1750–1949. Astronomical Papers Prepared for the Use of the American Ephemeris and Nautical Almanac, vol. 16, pt. 1, 1958, pp. 1–258.
4. MUHLEMAN, D.O.: Relationship Between the System of Astronomical Constants and the Radar Determination of the Astronomical Unit. JPL Tech. Rept. No. 32–477, Jan. 15, 1964, 17 pp.
5. CLEMENCE, G.M.: The Relativity Effect in Planetary Motions. Rev. Mod. Phys., vol. 19, no. 4, Oct. 1947, pp. 361–364.
6. BLANCO, V.M.; AND MCCUSKEY, S.W.: Celestial Dynamics II: Three- and n-Body Problems. Basic Physics of the Solar System, ch. 5. Addison-Wesley Publishing Co. (Reading, Mass.), 1961, pp. 169–221.
7. HERGET, P.: Solar Coordinates 1800–2000. Astronomical Papers Prepared for the Use of The American Ephemeris and Nautical Almanac, vol. 14, 1953.
8. HERGET, P.: Coordinates of Venus 1800–2000. Astronomical Papers Prepared for the Use of The American Ephemeris and Nautical Almanac, vol. 15, pt. 3, 1955, pp. 217–523.
9. MOORE, P.: The Planet Venus. The Macmillan Co., 1960, 151 pp. (See Appendix 3, Phenomena of Venus 1959–2000.)
10. KUIPER, G.P.: Limits of Completeness. Planets and Satellites, ch. 18. The Solar System, vol. III, G. P. Kuiper and M. B. Middlehurst, eds. University of Chicago Press, 1961, pp. 575–591.
11. CLEMENCE, G.M.: Theory of Mars—Completion. Astronomical Papers Prepared for the Use of The American Ephemeris and Nautical Almanac, vol. 16, pt. 2, 1961, pp. 261–333.
12. RABE, E.: Derivation of Fundamental Astronomical Constants from the Observations of Eros During 1926–1945. Astron. J., vol. 55, no. 4, 1950, pp. 112–126.
13. NEWCOMB, S.: The Elements of the Four Inner Planets and The Fundamental Constants of Astronomy. Suppl. American Ephemeris for 1897, Government Printing Office (Washington, D. C.), 1895, 202 pp.
14. BROUWER, D.; AND CLEMENCE, G.M.: Orbits and Masses of Planets and Satellites. Planets and Satellites, ch. 3. The Solar System, vol. III, G.P. Kuiper and B.M. Middlehurst, eds. University of Chicago Press, 1961, pp. 31–94.

15. ANDERSON, J.D.; NULL, G.W.; AND THORNTON, C.T.: The Evaluation of Certain Astronomical Constants from the Radio Tracking of Mariner II. Prog. in Astronaut. Aeron., vol. 14, 1964, pp. 131–155. Or: JPL Tech. Rept. No. 32-476, Mar. 1, 1965, 25 pp.
16. ROSS, F.E.: New Elements of Mars and Tables for Correcting the Heliocentric Positions Derived from Astronomical Papers, vol. VI, pt. IV. Astronomical Papers Prepared for the Use of The American Ephemeris and Nautical Almanac, vol. 9, pt. 2, 1917, pp. 251–274.
17. FOTHERINGHAM, J.K.: Note on the Mass of Venus. Monthly Notices Roy. Astron. Soc., vol. 86, no. 5, 1926, pp. 296–300. Or: The Mass of Venus and the Obliquity of the Ecliptic. Astron. Nachr., Bd. 256, no. 6121, 1935, cols. 1–18.
18. SPENCER-JONES, H.: Discussion on the Greenwich Observations of the Sun, 1836–1923. Monthly Notices Roy. Astron. Soc., vol. 86, no. 6, 1926, pp. 426–438.
19. DE SITTER, W.; AND BROUWER, D.: On the System of Astronomical Constants. Bull. Astron. Inst. Neth., vol. 8, no. 307, July 8, 1938, pp. 213–231.
20. MORGAN, H.R.; AND SCOTT, F.P.: Observations of the Sun 1900–1937 Compared with Newcomb's Tables. Astron. J., vol. 47, no. 22, Feb. 27, 1939, pp. 193–198.
21. CLEMENCE, G.M.: The Motion of Mercury, 1765–1937. Astronomical Papers Prepared for the Use of The American Ephemeris and Nautical Almanac, vol. 11, pt. 1, 1943, p. 46.
22. BROUWER D.: A New Determination of the Solar Parallax from the Parallatic Inequality in the Moon's Longitude; Comments of the Masses of the Inner Planets; Notes on Investigations in Progress. Bull. Astron., New Series, vol. 15, no. 3, 1950, pp. 165–180.
23. MAKEMSON, M.W.; BAKER, R.M.L., JR.; AND WESTROM, G.B.: Analysis and Standardization of Astrodynamic Constants. J. Astron. Sci., vol. 8, no. 1, 1961, pp. 1–13.
24. ALLEN, C.W.: Astrophysical Quantities. Second ed., University of London, Athlone Press (London), 1963, 291 pp. (First ed., 1955.)
25. DE VAUCOULEURS, G.: Geometric and Photometric Parameters of the Terrestrial Planets. Icarus, vol. 3, no. 3, 1964, pp. 187–235.
26. MENZEL, D.H.; AND DE VAUCOULEURS, G.: Final Report on the Occultation of Regulus by Venus, July 7, 1959. Air Force Cambridge Res. Lab. Rept. No. 227, 1961.
27. TAYLOR, G.E.: Occultation of Regulus by Venus in 1959, July 7. Royal Obs. Bull. (Greenwich), series E, no. 72, 1963. pp. 355–366.
28. MUHLEMAN, D.O.; HOLDRIDGE, D.B.; AND BLOCK, N.: Astronomical Unit Determined by Radar Reflections from Venus. Astron. J., vol. 67, 1962, pp. 191–203.
29. RICHARDSON, R.S.: Spectroscopic Observations of Venus for Rotation Made at Mount Wilson, Publ. Astron. Soc. Pacific, vol. 70, no. 6, 1958, pp. 251–260.
30. SLIPHER, V.M.: A Spectrographic Investigation of the Rotation Velocity of Venus. Lowell Obs. Bull., vol. 1, bull. no. 3, 1903, 9 pp.
31. LOWELL, P.: On the Spectrographic Investigation of the Rotation Period of the Planet Venus. Astron. Nachr., Bd. 163, no. 3891–3892, 1903, cols. 33–36.

32. SCHIAPARELLI, G.V.: Considérations sur le mouvement de rotation de la planète Vénus. Ciel Terre, vol. 11, 1890, pp. 49–62, 125–143, 183–190, 214–222, and 259–269. Translated from: Rendiconti del R. Instituto Lombardo, vol. 23, 1890.
33. PERROTIN, X.: Observations de la Planète Vénus à l'Observatoire de Nice. Compt. Rend. Acad. Sci., vol. 111, 1890, pp. 587-591.
34. DOLLFUS, A.: Étude Visuelle et Photographique de l'Atmosphère de Vénus. L'Astronomie, vol. 69, 1955, pp. 413–425.
35. GOLDSTEIN, R.M.: Venus Characteristics by Earth-Based Radar. Astron. J., vol. 69, no. 1, 1964, pp. 12–18.
36. SHAPIRO, I.I.: Quoted in Astronomical Notes from Hamburg—1. Sky and Telescope, vol. 28, no. 6, Dec. 1964, p. 341.
37. CARPENTER, R.L.: Studies of Venus by CW Radar. Astron. J., vol. 69, no. 1, 1964, pp. 2–11.
38. KLEMPERER, W.K.; OCHS, G.R.; AND BOWLES, K.L.: Radar Echoes from Venus at 50 Mc/sec. Astron. J., vol. 69, no. 1, 1964, pp. 22–28.
39. MUHLEMAN, D.O.: Radar Scattering from Venus and the Moon. Astron. J., vol. 69, no. 1, 1964, pp. 34–41.
40. DRAKE, F.D.: Microwave Observations of Venus, 1962–1963. Astron. J., vol. 69, no. 1, 1964, pp. 62–64.
41. RZHIGA, O.N.: Radar Observations of Venus in the Soviet Union in 1962. Part III.8, Life Sciences and Space Research II, M. Florkin and A. Dollfus, eds. North-Holland Publ. Co. (Amsterdam), 1964, pp. 178–189.
42. PONSONBY, J.E.; THOMSON, J.H.; AND IMRIE, K.S.: Rotation Rate of Venus Measured by Radar Observations, 1964. Nature, vol. 204, no. 4953, Oct. 3, 1964, pp. 63–64.
43. DE VAUCOULEURS, G.: Geometric and Photometric Parameters of the Terrestrial Planets. Rand Corp. Memo. RM-4000-NASA, 1964, 121 pp.
44. COWLING, T.G.: Magnetohydrodynamics. Interscience Tracts on Physics and Astronomy, no. 4, 1957, pp. 77–98.
45. JACOBS, J.A.: The Earth's Core and Geomagnetism. Pergamon Press, 1963, pp. 24–34, 63–91.
46. SMITH, E.J.; DAVIS, L., JR.; COLEMAN, P.J., JR.; AND SONNET, C.P.: Mariner II: Preliminary Reports on Measurements on Venus. Science, vol. 139, 1963, pp. 909–910.
47. JEFFREYS, H.: The Density Distributions in the Inner Planets. Monthly Notices Roy. Astron. Soc., Geophysical Suppl., vol. 4, 1937, pp. 62–71.
48. BULLEN, K.E.: On the Constitution of Venus. Monthly Notices Roy. Astron. Soc., vol. 109, 1949, pp. 457–461.
49. BULLEN, K.E.: Introduction to Theory of Seismology. University of Cambridge Press (Cambridge), 1963, p. 232.
50. GILVARRY, J.J.: Temperatures in the Earth's Interior. J. Atmospheric Terrest. Phys., vol. 10, 1957, pp. 84–95.
51. RAMSEY, W.H.: On the Constitution of the Terrestrial Planets. Monthly Notices Roy. Astron. Soc., vol. 108, 1948, pp. 406–413.
52. MACDONALD, G.J.F.: On the Internal Constitution of the Inner Planets. J. Geophys. Res., vol. 67, 1962, no. 7, pp. 2945–2974.
53. MACDONALD, G.J.F.: The Internal Constitutions of the Inner Planets and the Moon. Space Sci. Rev., vol. 2, No. 4, Oct. 1963, pp. 473–557.

54. LYTTLETON, R.A.: On the Internal Constitution of the Terrestrial Planets. JPL Tech. Rept. No. 32–522, 1963.
55. MACDONALD, G.J.F.: Calculations of the Thermal History of the Earth. J. Geophys. Res., vol. 64, 1959, pp. 1967–2000.
56. HOUTGAST, J.: Indication of a Magnetic Field of the Planet Venus. Nature, vol. 175 (4459), Apr. 16, 1955, pp. 678–679.
57. HOUTGAST, J.; AND VAN SLUITERS, A.: A New Estimate of the Strength of the Magnetic Field of Venus. Nature, vol. 196 (4853), Nov. 3, 1962, pp. 462–463.
58. SMITH, E.J.; DAVIS, L., JR.; COLEMAN, P.J., JR.; AND SONNET, C.P.: Magnetic Measurements Near Venus. J. Geophys. Res., vol. 70, no. 7, 1965, pp. 1571–1586.
59. NEUGEBAUER, M.; AND SNYDER, C.W.: Solar-Wind Measurements near Venus. J. Geophys. Res., vol. 70, no. 7, 1965, pp. 1587–1591.
60. DEIRMENDJIAN, D.: A Water-Cloud Interpretation of Venus' Microwave Continuum. Icarus, vol. 3, 1964, pp. 109–120; or Rand Corp. Memo. RM-4060-PR, 1964, 31 pp.
61. POLLACK, J.B.; AND SAGAN, C.: The Microwave Phase Effect of Venus. Icarus, vol. 4, 1965, pp. 62–103.
62. BARRETT, A.H.; AND STAELIN, D.H.: Radio Observations of Venus and the Interpretations. Space Sci. Rev., vol. 3, no. 1, 1964, pp. 109–135.
63. TOLBERT, C.W.; AND STRAITON, A.W.: An Investigation of 35 Gc, 70 Gc, and 94 Gc Cytherian Radiation. Nature, vol. 204, 1964, pp. 1242–1245.
64. KISLYAKOV, A.G.; KUZMIN, A.D.; AND SALOMONOVICH, A.E.: 4-mm Radio Emissions from Venus. Astron. Zh., vol. 39, 1962, pp. 410–417; or translation, Soviet Astron.—AJ, vol. 6, 1962, pp. 328–332.
65. GRANT, C.R.; CORBETT, H.H.; AND GIBSON, J.E.: Measurements of the 4.3-mm Radiation of Venus. Astrophys. J., vol. 137, 1963, pp. 620–627.
66. KUZ'MIN, A.D.; AND SALOMONOVICH, A.E.: Observations of Radio Emission from Venus and Jupiter at 8-mm Wavelength. Astron. Zh., vol. 39, 1962, pp. 660–668; or translation, Soviet Astron.—AJ, vol. 6, 1963, pp. 518–524.
67. THORNTON, D.D.; AND WELCH, W.J.: Radio Emission from Venus at 8.35-mm. Astron. J., vol. 69, 1964, pp. 71–72.
68. LYNN, V.L.; MEEKS, M.L.; AND SOHIGIAN, M.D.: Observations of Venus, the Region of Taurus A, and the Moon at 8.5-Millimeter Wavelength. Astron. J., vol. 69, 1964, pp. 65–67.
69. COPELAND, J.; AND TYLER, W.C.: Preliminary Results from Measurements of 8.6-mm Radiation from Venus. Astrophys. J., vol. 139, 1964, pp. 409–412.
70. GIBSON, J.E.: The Brightness Temperature of Venus at 8.6-mm. Astrophys. J., vol. 137, 1963, pp. 611–619.
71. STAELIN, D.H.; BARRETT, A.H.; AND KUSSE, B.R.: Observations of Venus, the Sun, Moon, and Tau A at 1.18-cm Wavelength. Astron. J., vol. 69, 1964, pp. 69–70.
72. GIBSON, J.E.; AND CORBETT, H.H: The Brightness Temperature of Venus at 1.35 cm. Astron. J., vol. 68, 1963, p. 74; or Naval Res. Lab. Rept. 5937, Apr. 11, 1963.
73. BARATH, E.T.; BARRETT, A.H.; COPELAND, J.; JONES, D.E.; AND LILLEY, A.E.: Mariner II Microwave Radiometer Experiment and Results. Astron. J., vol. 69, no. 1, 1964, pp. 49–58.

74. McCullough, T.P.; and Boland, J.W.: Observations of Venus at 2.07 cm. Astron. J., vol. 69, 1964, p. 68.
75. Mayer, C.H.; McCullough, T.P.; and Sloanaker, R.M.: 3.15-cm Observations of Venus in 1961. Mem. Soc. Roy. Sci. Liege, serie 5, vol. 7, 1962, pp. 357–363.
76. Bibinova, V.P.; Kuz'min, A.D.; Salomonovich, A.E.; and Shavlovskii, I.V.: Observations of the Radio Emission from Venus and Jupiter on a Wavelength of 3.3 cm. Astron. Zh., vol. 39, 1962, pp. 1083–1088; or translation, Soviet Astron.—AJ, vol. 6, 1963, pp. 840–844.
77. Mayer, C.H.: Radio Emission of the Moon and Planets. Planets and Satellites, ch. 12. The Solar System, vol. III, G.P. Kuiper and B.M. Middlehurst, eds. University of Chicago Press, 1961, pp. 442–472.
78. Kuz'min, A.D.; and Salomonovich, A.E.: Some Conclusions about Physicial Conditions of Venus According to Radio Astronomical Observations at P.N. Lebedev Physical Institute. Mem. Soc. Roy. Sci. Liege, series 5, vol. 7, 1962b, pp. 344–356.
79. Mayer, C.H.; McCullough, T.P.; and Sloanaker, R.M.: Observations of Venus at 10.2-cm Wavelength. Astron. J., vol. 65, 1960, pp. 349–350 (abstract).
80. Clark, B.G.; and Spencer, C.L.: Some Decimeter Observations of Venus During the 1962 Conjunction. Astron. J., vol. 69, 1964, pp. 59–61.
81. Lilley, A.E.: The Temperature of Venus. Astron. J., vol. 66, 1961, p. 290 (abstract).
82. Drake, F.D.: Microwave Observations of Venus, 1962–1963. Astron. J., vol. 69, 1964, pp. 62–64.
83. Sagan, C.: The Planet Venus. Science, vol. 133, 1961, pp. 849–858.
84. Öpik, E.J.: The Aeolosphere and Atmosphere of Venus. J. Geophys. Res., vol. 66, 1961, pp. 2807–2819.
85. Owen, R.B.: Theoretical Model Atmospheres of Venus. NASA TN D–2527, Jan. 1965, 41 pp.
86. Sagan, C.: Structure of the Lower Atmosphere of Venus. Icarus, vol. 1, 1962, pp. 151–169.
87. Harteck, P.; Reeves, R.R., Jr.; and Thompson, B.A.: Photochemical Problems of the Venus Atmosphere. NASA TN D–1984, 1963, 39 pp.
88. Tolbert, C.W.; and Straiton, A.W.: A Consideration of Microwave Radiation Associated with Particles in the Atmosphere of Venus. J. Geophys. Res., vol. 67, 1962, pp. 1741–1744.
89. Coulson, K.L.: Characteristics of the Radiation Emerging from the Top of a Rayleigh Atmosphere—I. Intensity and Polarization. Planetary and Space Science, vol. 1, 1959, pp. 265–276.
90. Sekera, Z.; and Viezee, W.: Distribution of the Intensity and Polarization of the Diffusely Reflected Light Over a Planetary Disk. Rand Corp., R–389–PR, 1961, 45 pp.
91. Harris, D.: Photometry and Colorimetry of Planets and Satellites. Planets and Satellites, ch. 8. Vol. III of The Solar System, G.P. Kuiper and B.M. Middlehurst, eds. University of Chicago Press, 1961, pp. 272–342.
92. Van De Hulst, H.C.: Scattering in the Atmospheres of the Earth and the Planets. The Atmospheres of the Earth and Planets, ch. 3, G.P. Kuiper, ed. University of Chicago Press, Revised ed., 1952, pp. 49–111.

93. KNUCKLES, C.F.; SINTON, M.K.; AND SINTON, W.M.: UBV Photometry of Venus. Lowell Obs. Bull. vol. 5, no. 115, 1961, pp. 153–156.
94. DOLLFUS, A.: Polarization Studies of Planets. Planets and Satellites, ch. 9. Vol. III of The Solar System, G.P. Kuiper and B.M. Middlehurst, eds. University of Chicago Press, 1961, pp. 343–399.
95. COULSON, K.L.; AND LOTMAN, M.: Molecular Optical Thickness of the Atmospheres of Mars and Venus. Technical Information Series, No. R625D71, General Electric Space Sciences Laboratory (AD283055), 1962, 56 pp.
96. COULSON, K.L.; DAVE, J.V.; AND SEKERA, Z.: Tables Related to Radiation Emerging from a Planetary Atmosphere with Rayleigh Scattering. University of California Press, 1960, 548 pp.
97. ROSS, F.E.: Photographs of Venus. Astron. J., vol. 67, 1928, pp. 57–92.
98. YEZERSKII, V.I.: Photographic Photometry of Venus. Transactions of A.M. Gorki Astronomical Observatory, Kharkov State University, vol. 12, 1957, pp. 73–165, Translation by Jakubski, Z.: STL–TR–61–5110–40, Advanced Research Group, Space Tech. Lab., Los Angeles, 1961, 114 pp.
99. BROWN, H.: Rare Gases and the Formation of the Earth's Atmosphere. The Atmospheres of the Earth and Planets, G.P. Kuiper, ed. The University of Chicago Press, 1952, pp. 258–266.
100. SUESS, H.E.: Remarks Concerning the Chemical Composition of the Atmosphere of Venus. Z. Naturforschung (Section A), vol. 19, 1964, pp. 84–87.
101. ADAMS, W.S.; AND DUNHAM, T., JR.: Absorption Bands in the Infrared Spectrum of Venus. Publ. Astron. Soc. Pacific, vol. 44, 1932, pp. 243–247.
102. PROKOFYEV, V.K.; AND PETROVA, N.N.: On the Presence of Oxygen in the Atmosphere of Venus. Proc. 11th Intern. Astrophys. Symp., Liège, July 9–12, 1962. Mem. Soc. Roy. Sci. Liege, serie 5, vol. 8, 1963, pp. 311–321.
103. PROKOFYEV, V.K.: On the Presence of Oxygen in the Atmosphere II. Izv. Krymsk. Astrofiz. Obs., Akad. Nauk SSSR, vol. 31, 1964, pp. 276–380.
104. BOTTEMA, M.; PLUMMER, W.; STRONG, J.; AND ZANDER, R.: Composition of the Clouds of Venus. Astrophys. J., vol. 140, 1964, pp. 1640–1641.
105. STRONG, J.: Infrared Astronomy by Balloon. Sci. Am., vol. 212, 1965, pp. 28–37.
106. DOLLFUS, A.: Mesure de la Vapeur d'Eau dans les Atmosphères de Mars et de Vénus. Proc. 12th Intern. Astrophys. Symp., Liège, June 24–26, 1963, Mem. Soc. Roy. Sci. Liege, serie 5, vol. 9, 1964, pp. 392–395.
107. BOTTEMA, M.; PLUMMER, W.; AND STRONG, J.: A Quantitative Measurement of Water Vapor in the Atmosphere of Venus. Ann. Astrophys., vol. 28, 1965, pp. 225–228.
108. SINTON, W.M.: Infrared Observations of Venus. Proc. 11th Intern. Astrophys. Symp., Liège, July 9–12, 1962, Mem. Soc. Roy. Sci. Liege, serie 5, vol. 7, 1963, pp. 300–310.
109. KUIPER, G.P.: Photometry of the Infrared Spectrum of Venus. Proc. 11th Intern. Astrophys. Symp., Liège, July 9–12, 1962, Mem. Soc. Roy. Sci. Liege, serie 5, vol. 7, 1963, pp. 269–299.
110. DE VAUCOULEURS, G.; AND MENZEL, D.H.: Results of the Occultation of Regulus by Venus, July 7, 1959. Nature, vol. 188, 1960, pp. 28–33.

111. SPINRAD, H.: Spectroscopic Temperature and Pressure Measurements in the Venus Atmosphere. Publ. Astron. Soc. Pacific, vol. 74, 1962, pp. 187–201.
112. KUIPER, G.P.: Planetary Atmospheres and Their Origin. The Atmospheres of the Earth and Planets, ch. 12, G.P. Kuiper, ed. The University of Chicago Press, 1952, pp. 306–416.
113. SPINRAD, H.; AND RICHARDSON, E.H.: An Upper Limit to the Molecular Oxygen Content of the Venus Atmosphere. Astrophys. J., vol. 141, 1964, pp. 282–286.
114. MOROZ, V.I.: The Infrared Spectrum of Venus (1–2.5 microns). Soviet Astron., vol. 7, 1963, pp. 109–115.
115. SHIMIZU, M.: Vertical Distribution of Neutral Gases on Venus. Planetary and Space Science, vol. 11, 1963, pp. 269, 273.
116. KELLOGG, W.W.; AND SAGAN, C.: The Atmospheres of Mars and Venus. National Academy of Sciences—National Research Council (Washington, D.C.), 1961, p. 151.
117. DANILOV, A.D.: Models for the Ionosphere of Venus and Mars. Proc. 3rd Intern. Space Sci. Symp., Washington, D.C., May 2–8, 1962, W. Priester, ed. North-Holland Publ. Co. (Amsterdam, Holland), 1963, pp. 1026–1035.
118. DANILOV, A.D.; AND YATSENKO, S.P.: The Ionospheric Interpretation of the Results of Radar Observations of Venus. Geomagnetism and Aeronomy, vol. 3, 1963, pp. 475–483.
119. SINTON, W.M.; AND STRONG, J.: Radiometric Observations of Venus. Astron. J., vol. 131, 1960, pp. 470–490.
120. FRANK, L.A.; VAN ALLEN, J.A.; AND HILLS, H.K.: Mariner II: Preliminary Reports on Measurements of Venus; Charged Particles. Science, vol. 139, 1963, pp. 905–907.
121. KAPLAN, L.D.: A Preliminary Model of the Venus Atmosphere. JPL Tech. Rept. No. 32–379, Dec. 12, 1962, 5 pp.
122. RASOOL, S.I.: Structure of Planetary Atmospheres. J. Am. Inst. Astronaut. and Aeron., vol. 1, 1963, pp. 6–19.
123. MINTZ, Y.: Temperature and Circulation of the Venus Atmosphere. Planetary and Space Science, vol. 5, 1961, pp. 141–152.
124. SPINRAD, H.: A Search for Water Vapor and Trace Constituents in the Venus Atmosphere. Icarus, vol. 1, 1962, pp. 266–270.
125. ANDERSON, C.E.; AND EVANS, D.C.: The Nature of the Venus Cloud System. Paper presented to the Institute of Aerospace Sciences, Los Angeles, June 1962.
126. KAPLAN, L.D.: Spectroscopic Investigation of Venus. J. Quant. Spectr. & Radiative Transfer, vol. 3, 1963, pp. 537–539.
127. HANEL, R.A.; AND BARTKO, F.: Radiative Equilibrium in Planetary Atmospheres, I. Application of the Strong Line Absorption Law to the Atmosphere of Venus. NASA TN D-2397, Aug. 1964, 23 pp.
128. MINTZ, Y.: The General Circulation of Planetary Atmospheres. The Atmospheres of Mars and Venus, app. 8, W.W. Kellogg and C. Sagan, eds. Publication 944, National Academy of Sciences—National Research Council, 1961, pp. 107–146.
129. SONETT, C.P.: A Summary Review of the Scientific Findings of the Mariner Venus Mission. Space Sci. Rev., vol. 2, 1963, pp. 751–777.
130. MINTZ, Y.: The Energy Budget and Atmospheric Circulation in a Synchronously Rotating Planet. Icarus, vol. 1, 1962, pp. 172–173.

131. MAHONEY, J.R.: A Dynamical Study of the Venus Atmosphere. Space Tech. Lab. Rept. 9990-6332-KU-000, 1962, 8 pp.

132. SAGAN, C.; AND KELLOGG, W.W.: The Terrestrial Planets. Ann. Rev. Astron. and Astrophys., vol. I, Annual Reviews, Inc. (Palo Alto), 1963, pp. 235–266.

133. TOMBAUGH, C.W.: Visual and Photographic Observations of Venus and Mars. The Atmospheres of Mars and Venus, app. 2. Publication 944, National Academy of Sciences—National Research Council (Washington, D.C.), 1961.

134. EDSON, J.B.: The Twilight Zone of Venus. Adv. Astron. and Astrophys., vol. 2, Z. Kopal, ed. Academic Press (New York), 1963, pp. 1–42.

135. JUNGE, C.E.; CHAGNON, C.W.; AND MANSON, J.E.: Stratospheric Aerosols. J. Meteorol., vol. 18, 1961, pp. 81–108.

136. DAUVILLIER, A.: Sur la nature des Nuages de Vénus. Compt. Rend. Acad. Sci., vol. 243, 1956, pp. 1257–1258.

137. ROBBINS, R.C.: The Reaction Products of Solar Hydrogen and Components of the High Atmosphere of Venus—A Possible Source of the Venusian Clouds. Planetary and Space Science, vol. 12, 1964, pp. 1143–1146.

138. GOODY, R.: Limb-Darkening of Thermal Emission From Venus. Icarus, vol. 3, no. 2, 1964, pp. 98–102.

139. CHAMBERLAIN, J.W.: The Atmosphere of Venus Near Her Cloud Tops. Astron. J., vol. 141, no. 3, 1965, pp. 1184–1205.

140. SINTON, W.M.: Recent Infrared Spectra of Mars and Venus. J. Quant. Spectr. & Radiative Transfer, vol. 3, 1963, pp. 551–558.

141. CHASE, S.C.; KAPLAN, L.D.; AND NEUGEBAUER, G.: The Mariner II Infrared Radiometer Experiment. J. Geophys. Res., vol. 68, no. 22, 1963, pp. 6157–6169.

142. WESTPHAL, J.A.; WILDEY, R.L.; AND MURRAY, B.C.: The 8–14 Micron Appearance of Venus Before the 1964 Conjunction. Contribution No. 1318 of the Division of Geological Sciences, California Institute of Technology (Pasadena), 1965, 8 pp. Astrophys. J., vol. 142, no. 2, Aug. 1965, pp. 799–802.

143. MURRAY, B.C.; WILDEY, R.L.; AND WESTPHAL, J.A.: Infrared Photometric Mapping of Venus Through the 8- to 14-Micron Atmospheric Window. J. Geophys. Res., vol. 68, no. 15, 1963, pp. 4813–4818.

144. HOYLE, F.: Frontiers of Astronomy. Harper and Co. (New York), 1955, 350 pp.

145. MENZEL, D.H.; AND WHIPPLE, F.L.: The Case of H_2O Clouds on Venus. Publ. Astron. Soc. Pacific, vol. 67, 1955, pp. 161–168.

146. BARBIER, D.: La Lumière cendrée de Vénus. L'Astronomie, vol. 48, 1934, pp. 289–296.

147. BARBIER, D.: Recherche de la Lumière cendrée de Vénus pendant la Conjunction inférieure de 1935. L'Astronomie, vol. 50, 1936, pp. 27–32.

148. DANJON, A.: Sur la Prétendue Lumière cendrée de Vénus. L'Astronomie, vol. 48, 1934, pp. 370–372.

149. KOZYREV, H.A.: The Luminosity of the Night Sky of Venus. Izv. Krymsk. Astrofiz. Observ., Akad. Nauk SSSR, vol. 12, 1954, pp. 169–176.

150. NEWKIRK, G., JR.: The Airglow of Venus. Planetary and Space Science, vol. 1, 1959, pp. 32–36.

151. WARNER, B.: The Emission Spectrum of the Night Side of Venus. Monthly Notices Roy. Astron. Soc., vol. 121, 1960, pp. 279–283.

152. WEINBERG, J.L.; AND NEWKIRK, G., JR.: Airglow of Venus: a Re-Examination. Planetary and Space Science, vol. 5, 1963, pp. 163–167.

153. STAFF, JET PROPULSION LABORATORY: Mariner: Mission to Venus. McGraw-Hill Book Co., Inc., 1963.

154. BARATH, F.T.; BARRETT, A.H.; COPELAND, J.; JONES, D.C.; AND LILLEY, A.E.: Microwave Radiometers, part of Mariner II: Preliminary Reports on Measurements of Venus. Science, vol. 139, 1963, pp. 908–909.

155. EVANS, J.V.; AND PETTENGILL, G.H.: The Scattering Behavior of the Moon at Wavelengths of 3.6, 68, and 784 Centimeters. J. Geophys. Res., vol. 68, 1963, pp. 423–447.

156. EVANS, J.V.; BROCKELMAN, R.A.; HENRY, J.C.; HYDE, G.M.; KRAFT, L.G.; REID, W.A.; AND SMITH, W.W.: Radio Echo Observations of Venus and Mercury at 23 cm Wavelength. Astron. J., vol. 70, 1965, pp. 486–501.

157. JAMES, J.C.; AND INGALLS, R.P.: Radar Observation of Venus at 38 Mc/Sec. Astron. J., vol. 69, no. 1, 1964, pp. 19–22.

158. KARP, D.; MORROW, W.E., JR.; AND SMITH, W.B.: Radar Observation of Venus at 3.6 Centimeters. Icarus, vol. 3, 1964, pp. 473–475.

159. GOLDSTEIN, R.M.: Preliminary Venus Radar Results. Radio Science, vol. 69D, 1965, pp. 1623–1625.

160. PETTENGILL, G.H.: Radar Measurements of Venus in Space Research III. Proc. of Intern. Space Sci. Symp., Washington, D.C., 1962, W. Priester, ed., North-Holland Publ. Co. (Amsterdam), 1963, pp. 872–885.

161. MUELLER, R.F.: A Chemical Model for the Lower Atmosphere of Venus. Icarus, vol. 3, 1964, pp. 285–298.

162. UREY, H.C.: The Planets: Their Origin and Development. Yale University Press (New Haven, Connecticut), 1952.

Glossary

Adiabatic process—A thermodynamic change of state of a system in which there is no transfer of heat or mass across the system's boundaries.

Albedo—The ratio of electromagnetic radiation reflected by a body to that incident upon it.

Aphelion—The point on a heliocentric elliptical orbit farthest from the Sun.

Ascending node (of an orbit)—That point on an orbit at which a body (planet or satellite) crosses from south to north the reference plane (e.g., the ecliptic for the planets) on the celestial sphere. The opposite point, separated by 180° of longitude, is the descending node.

Astronomical unit (A.U.)—A fundamental unit of length in astronomy. Originally, the astronomical unit was defined as the mean distance of Earth from the Sun. In celestial mechanics, it is defined as the radius of an idealized circular and unperturbed orbit of Earth around the Sun. The recent radar determination of Mühleman (1964) is 1 astronomical unit=149 598 900±600 kilometers.

Bond albedo (or Russell-Bond albedo)—The ratio of the total flux, reflected in all directions by a sphere (planet), to the total flux incident in parallel rays from a distant source (Sun) and expressed as the product, $A=p \cdot q$, of a full-phase albedo factor p (geometrical albedo) and a phase-varying factor q (phase integral).

Brilliancy (of a disk)—A geometrical measure of disk brightness, independent of albedo, that is determined only by phase k, the apparent semidiameter s, and solar distance r according to the defining formula: $L=k\,s^2/r^2$.

Conjunction—The configuration of the Sun, a planet, and Earth when the heliocentric longitudes of the latter two are equal. The three bodies then lie most nearly in a straight line. When the planet is between the Sun and Earth, the planet is said to be in inferior conjunction; when the Sun is between Earth and the planet, the planet is said to be in superior conjunction.

Coriolis force—The deflecting force caused by a planet's rotation that acts on a moving particle on the planet, normal to the particle's relative velocity. The deflection is to the right in the northern hemisphere and to the left in the southern.

Declination (of a celestial point)—The angle between a point and the celestial equator, measured along the hour circle through the point and counted as north (+) or south (−) of the equator.

Day (ephemeris)—Average value of the mean solar day taken over the last three centuries.

Day (sidereal)—Time interval between two successive transits of the vernal equinox over the same meridian.

Day (solar)—Time interval between two consecutive transits of the Sun over a meridian. Since this time interval varies with Earth's orbital motion, a mean solar day was chosen, based on a mean annual motion of Earth (assuming an equivalent circular orbit) or a fictitious mean Sun.

Disk—The flattened appearance of a celestial body as it is observed, or the projection on the celestial sphere of that portion of the observed body which is visible.

Dry adiabatic lapse-rate—The rate of decrease of temperature with height of a parcel of dry air lifted adiabatically through an atmosphere in hydrostatic equilibrium.

Ecliptic—The annual, apparent path of the Sun's center on the celestial sphere, as seen from Earth, or the intersection of Earth's orbital plane with the celestial sphere.

Elongation (of a planet)—The angle between the Sun and a planet and Earth with the vertex at the center of Earth. Elongation is measured east or west of the Sun.

Emissivity—The ratio of the total flux of radiation at all wavelengths emitted by a surface to that emitted by a perfect radiator (the ideal blackbody) at the same temperature and conditions.

Ephemeris (fundamental)—An astronomical table predicting the positions of celestial bodies at regular intervals of time (also called almanac).

Ephemeris time—Uniform or Newtonian time based on the mean rotation of Earth during the year 1900.

Epoch—An arbitrary instance of time at which positions are measured or calculated.

Geometrical albedo—The ratio of the actual brightness of a reflecting body (planet or satellite) at full solar phase to that of a self-luminous body of the same size and position and radiating a flux of light equal to that incident on the first body.

Graybody—A hypothetical body that absorbs, independently of wavelength, some constant fraction between zero and one of all electromagnetic radiation incident upon that body.

Greenhouse effect—The heating of the lower atmosphere by certain gases (e.g., water vapor or carbon dioxide) which transmit shortwave solar radiation to the surface, yet absorb and re-emit portions of the planetary longwave (infrared) radiation back to the surface; thus, a downward counter-radiation is produced.

Gregorian date—A date on the official calendar in use throughout the Christian world. The Gregorian calendar was instituted in 1582 by Pope Gregory XIII to correct errors accumulating in the Julian calendar.

Heliocentric—Sun centered; term derived from helios, the Greek word for sun.

Julian date—The number of mean solar days that have elapsed since the adopted epoch of Greenwich mean noon on January 1, 4713 B.C.

Kepler's laws—Three laws of undisturbed planetary motion formulated by Kepler:

1st law:	The orbits of the planets are ellipses with the sun at one focus.
2nd law:	The radius vector Sun-to-planet sweeps equal areas in equal times.
3rd law:	The squares of the planets' periods of revolution are proportional to the cubes of their mean solar distances (semimajor axes of ellipses).

Limb—Edge of the illuminated part of a disk.

Line of apsides—A straight line infinitely extending the major axis of an elliptical orbit. This line passes through those points closest (periapsis) and farthest (apoapsis) from the dynamical center or forms.

Line of nodes—A straight line that joins the intersection points (nodes) of the two great celestial circles that determine the orbital plane and the reference plane used to describe the motion of a planet or satellite.

Magnitude (stellar)—An inverse logarithmic measure of the brightness of a celestial body such that an increase of five magnitudes represents a hundredfold decrease in the body's brightness.

Mie scattering—That scattering of radiation which is produced by spherical particles of any size (see for comparison "Rayleigh scattering").

Mixing ratio—The ratio of the mass of the gas considered to that of the remaining gases in a given atmospheric mass.

North celestial pole—The northern point of intersection of Earth's rotation axis with the celestial sphere.

Occultation—The obscuring of an observed body by a larger body passing in front of it.

Opposition—The configuration of Sun, Earth, and planet when the heliocentric longitudes of the latter two are equal. The three bodies, with Earth in the middle, are then most nearly in a straight line.

Pericenter (or, perifocus)—That point on an orbit which is closest to the attracting center.

Perihelion—That point on a heliocentric elliptical orbit which is closest to the Sun.

Phase—The illuminated fraction of the disk area.

Phase angle—The angle between the Sun and Earth, as observed from a planet whose center is the vertex.

Phase function—The ratio of the brightness of a planet at any phase angle α to that at full phase ($\alpha=0$), assuming the planet at unit distances from the Sun and Earth.

Phase curve or Law—The plot or mathematical law of the phase function $\phi(\alpha)$ of a planet versus phase angle α.

Phase integral—The phase varying factor that modifies the geometrical albedo (or, full-phase factor) that enters into the definition of the Bond albedo of a planet. It is expressed as the integral:

$$q=\int_0^{2\pi}\phi(\alpha)\,\sin\alpha\,d\alpha$$

of the phase function $\phi(\alpha)$.

Polarization, amount or degree of—The proportion of polarized light to total light; it is defined by:

$$P=\frac{I_1-I_2}{I_1+I_2}$$

where I_1 is the component of intensity perpendicular to the plane of vision (defined by directions of illumination and observation) and I_2 is the intensity component contained in this plane.

Polarization curve—The plot of degree of polarization versus phase angle of a planet.

Precipitable water—The total mass of atmospheric water vapor contained in a vertical column of unit cross-section extending between any two specified levels (usually the total atmospheric height).

Quadrature—The configuration of the Sun, Earth, and a planet when the geocentric longitudes of the Sun and the planet are 90° apart. The three bodies then most nearly form a right angle.

Rayleigh scattering—That scattering of radiation which is produced by spherical particles of radii smaller than about one-tenth the wavelength of the radiation (Rayleigh limit). Also called "molecular scattering."

Retrograde sense—The opposite of direct sense of rotation; that is, clockwise.

Right ascension—The angular arc measured along the celestial equator from the vernal equinox eastward (i.e., counterclockwise) to the intersection with the hour circle of the point (semigreat circle passing through the north celestial pole and the point).

Rotational lines—Spectral lines caused by rotational energy changes in a molecule.

Scale height (of an atmosphere)—The distance in which an isothermal atmosphere decreases in density from 1 to $1/e$.

Synchronous rotation—That rotation of a planet or satellite when the rotation period is equal to the period of revolution around the Sun or primary; thus, the same side of the rotating body always faces the attracting body (for example, the Moon).

Synodic period of revolution (of two planets or satellites)—The time interval between consecutive oppositions or conjunctions of two bodies revolving around the same center.

Terminator—That line which separates the illuminated from the non-illuminated portions of a planet or satellite; one observes a morning or evening terminator on the disk.

Twilight arc—The planetocentric angular arc that measures the displacement, resulting from atmospheric scattering of light on the planet, of the actual terminator from the theoretical terminator.

Vernal equinox—The point at which the Sun in its annual apparent path around Earth appears to cross the celestial equator from south to north at a certain time of the year (presently on Mar. 21), or the ascending node of the ecliptic on the equator.

Year, Julian—The mean length of the year on the Julian calendar; it is equal to 365.25 mean solar days, or $365^d\ 6^h$ exactly.

Year, sidereal—The time interval between two successive returns of the Sun to a fixed celestial point (fixed star); it is the true period of revolution of Earth and is equal to 365.25636 mean solar days, or $365^d\ 6^h\ 9^m\ 10^s$.

Year, tropical—The time interval between two successive returns of the Sun to the vernal equinox. Because of precession, it is shorter than the sidereal or true year. It is equal to 365.24220 mean solar days, or $365^d\ 5^h\ 48^m\ 46^s$.

☆ U.S. GOVERNMENT PRINTING OFFICE: 1967—245-169

8/1/67

"The aeronautical and space activities of the United States shall be conducted so as to contribute . . . to the expansion of human knowledge of phenomena in the atmosphere and space. The Administration shall provide for the widest practicable and appropriate dissemination of information concerning its activities and the results thereof."

—NATIONAL AERONAUTICS AND SPACE ACT OF 1958

NASA SCIENTIFIC AND TECHNICAL PUBLICATIONS

TECHNICAL REPORTS: Scientific and technical information considered important, complete, and a lasting contribution to existing knowledge.

TECHNICAL NOTES: Information less broad in scope but nevertheless of importance as a contribution to existing knowledge.

TECHNICAL MEMORANDUMS: Information receiving limited distribution because of preliminary data, security classification, or other reasons.

CONTRACTOR REPORTS: Scientific and technical information generated under a NASA contract or grant and considered an important contribution to existing knowledge.

TECHNICAL TRANSLATIONS: Information published in a foreign language considered to merit NASA distribution in English.

SPECIAL PUBLICATIONS: Information derived from or of value to NASA activities. Publications include conference proceedings, monographs, data compilations, handbooks, sourcebooks, and special bibliographies.

TECHNOLOGY UTILIZATION PUBLICATIONS: Information on technology used by NASA that may be of particular interest in commercial and other non-aerospace applications. Publications include Tech Briefs, Technology Utilization Reports and Notes, and Technology Surveys.

Details on the availability of these publications may be obtained from:

SCIENTIFIC AND TECHNICAL INFORMATION DIVISION

NATIONAL AERONAUTICS AND SPACE ADMINISTRATION

Washington, D.C. 20546